Dynamic Characterisation of the Head-Media Interface in Hard Disk Drives using Novel Sensor Systems

By

Glen Alan Tunstall

A thesis submitted to the University of Plymouth

in partial fulfilment for the degree of

DOCTOR OF PHILOSOPHY

Department of Communication and Electronic Engineering

Faculty of Technology

UNIVERSITY OF PLYMOUTH
Item No. 9005255515
Date - 3 DEC 2002 T
Class No. YHESIS 004.563TUN
Cont. No. X704509044
PLYMOUTH LIBRARY

LIBRARY STORE

REFERENCE ONLY

September 2002

This copy of the thesis has been supplied on condition that anyone who consults it is understood to recognise that its copyright rests with its author and that no quotation from the thesis and no information derived from it may be published without the author's prior consent.

Abstract

Hard disk drives function perfectly satisfactorily when used in a stable environment, but in certain applications they are subjected to shock and vibration. During the work reported in this thesis it has been found that when typical hard disk drives are subjected to vibration, data transfer failure is found to be significant at frequencies between 440Hz and 700Hz, at an extreme, failing at only 1g of sinusoidal vibration. These failures can largely be attributed to two key components: the suspension arm and the hard disk. At non-critical frequencies of vibration the typical hard disk drive can reliably transfer data whilst subjected to as much as 45g.

When transferring data to the drive controller, the drive's operations are controlled and monitored using BIOS commands. Examining the embedded error signals proved that the drive predominantly failed due to tracking errors.

Novel piezo-electric sensors have been developed to measure unobtrusively suspension arm and disk motion, the results from which show the disk to be the most significant failure mechanism, with its first mode of resonance at around 440Hz. The suspension arm movement has been found to be greatest at 1kHz.

Extensive modelling of the flexure of the disk, clamped and unclamped, has been undertaken using finite element analysis. The theoretical modelling strongly reinforces the empirical results presented in this thesis.

If suspension arm movement is not directly coupled with disk movement then a flying height variation is created. This, together with tracking variations, leads to data transfer corruption. This has been found to occur at 1kHz and 2kHz.

An optical system has been developed and characterised for a novel and inexpensive flying height measurement system using compact disc player technology.

Acknowledgements

My supervisors Prof. Warwick Clegg, Dr. David Jenkins & Dr. Paul Davey, C.R.I.S.T., University of Plymouth, UK.

James, Nick, Chibesa, Xinqun, Lianna, Phil & Amei, my fellow postgraduates in the (C.R.I.S.T.) research group.

Dr. David Grieve, DMME, University of Plymouth, UK.

The Department of Communication and Electronic Engineering's technical staff: John, Bill, Lee, Bob, Sheila and David.

The Department of Marine and Mechanical Engineering's technical staff: Colin and Mike.

The Department's administrative staff: Barbara, Nicole, Sarah, Sue and Shirley.

Technical services staff: Brian and Adrian.

Royal Academy of Engineering for help with attending IMTC2000 conference.

The Engineering & Physical Sciences Research Council (EPSRC), for providing the financial support to make this work possible.

Glossary

AE	Acoustic Emission
Al	Aluminium
b	Bit
B	Byte
BIOS	Basic Input Output System
CD	Compact Disc
CHS	Cylinder Head Sector
CPU	Central Processor Unit
CRC	Cyclic redundancy check
DAQ	Data Acquisition
dB	Decibel
dBm	Decibel milli
DC	Direct Current
DMA	Direct Memory Access
DSP	Digital Signal Processing
ECC	Error correction code
FEA	Finite element analysis
FFT	Fast Fourier Transform
HDD	Hard Disk Drive
ID	Inner Diameter
LDV	Laser Doppler Vibrometer
Mg	Magnesium
MR	Magneto-Resistive
Ni	Nickel
O	Oxygen
P	Phosphorus
PC	Personal computer
PCI	Peripheral Component Interconnect
PES	Position Error Signal
PVC	Poly Vinyl Chloride
PVDF	Poly vinylidene fluoride
PZT	Lead Zirconate Titanate
RAM	Random Access Memory
RMS	Root Mean Square
TA	Thermal Asperity
TMR	Track Mis-Registration
LBA	Logical Block Address

Contents

List of Figures

1. Introduction

2. The Vibration Problem in Hard Disk Drives

3. Flying Height Measurement for Embedded use in Hard Disk Drives

4. Piezo-electric Sensor and Actuator Overview

5. Vibration Testing Equipment

6.Vibration Testing Results

7. Compact Disk Optical System for Disk Vibration Response Characterisation

8. Finite Element Analysis

9. Results and Discussions

11. Further Work

List of Tables

3. Flying Height Measurement for Embedded use in Hard Disk Drives

5. Experimental

8. Finite Element Analysis

9. Results and Discussion

AUTHOR'S DECLARATION

At no time during the registration for the degree of Doctor of Philosophy has the author been registered for any other University award.

This study was financed with the aid of a studentship from the Engineering and Physical Sciences Research Council.

Research was undertaken in one of the Centre of Research for Information Storage Technology laboratories at the University of Plymouth.

Relevant scientific seminars and conferences were regularly attended at which work was presented and several papers were published.

Publications (or presentation of other forms of creative work):

Actuators for tomorrows ruggedised hard disk drives, D F L Jenkins, W W Clegg, C Chilumbu and G A Tunstall, Datatech Vol. 3, 1999, ICG Publishing.

Sensors for Dynamic Characterisation of Magnetic Storage Systems, DFL Jenkins, WW Clegg, L He, J Windmill, G Tunstall, X Liu, C Chilumbu, A Li, Sensors Review, Vol. 20, No. 4, 2000, Page(s): 307-317, invited paper.

Head-media interface instability under hostile operating conditions, Tunstall, G.; Clegg, W.; Jenkins, D.F.L.; Chilumbu, C. , IEEE Transactions on Instrumentation and Measurement, Volume: 5, Issue: 2 , Apr. 2002, Page(s): 293 -298

Using compact disc player optical systems to measure differentially hard disk drive slider and disk motion under hostile conditions, Tunstall, G., Clegg, W., Jenkins, D., Davey, P., Proceedings of the 18th IEEE Instrumentation and Measurement Technology Conference, (IMTC 2001), Vol. 3, 2001, Page(s): 1526 -1528. Under review for publication in IEEE Transactions on Instrumentation and Measurement.

Multi-layer bulk PZT actuators for flying height control in ruggedised hard disk drives, Jenkins, D.F.L., Chilumbu, C., Tunstall, G., Clegg, W.W., Robinson, P., Proceedings of the 12th IEEE International Symposium on Applications of Ferroelectrics, (ISAF 2000), Vol. 1, 2001, Page(s): 293 -296.

Head-media interface instability under hostile operating conditions, Tunstall, G.; Clegg, W.; Jenkins, D.; Chilumbu, C. , Instrumentation and Measurement Technology Conference, 2000. IMTC 2000., Proceedings of the 17th IEEE , 2000, Page(s): 489 - 492 vol.1

Observing Hard Disk Drive Suspension Arm Strain, Glen Tunstall, Warwick Clegg, David Jenkins and Paul Davey, CMMP2000 poster presentation, 2000.

Vibration Testing of Loaded Suspension Arms to Explore the Characteristics of the Head-Medium Interface in Magnetic Disk Drives, W. W. Clegg, G. Tunstall and D. F. L. Jenkins. CMMP 99. 1999.

Hard Disk Drive Vulnerability Under Hostile Operating Conditions, Glen Tunstall, SET for Britain 2000, 2000.

The Effect of Vibration on Transfer Rate of Hard Disk Drives, G Tunstall, EPSRC seminar, Seagate, 1999.

Observing and Controlling Suspension Structures within Hard Disk Drives to Improve Vibration Susceptibility, Glen Tunstall, Physics2000, 2000.

Signed .....

Date ....14/11/02.....

Summary

In Chapter 1 of this thesis, the importance of the hard disk drive in personal computers is highlighted, and the very steep rate of growth in their data storage capabilities is graphically presented. The operation and construction of the drive is then detailed, indicating key elements of its design that are fundamental to further improvements in data storage densities, data transfer speed and reliability.

Chapter 2 delves more deeply into failure mechanisms of the hard disk drive when operating in a hostile environment of shocks and vibration. Primitive and known methods of suppressing the drive from failing to transfer data are acknowledged. An explanation of the non-trivial problem of data miss-interpretation is given, reinforcing the significance of the mechanical failings of the drive.

An overview of current flying height measurements is given in Chapter 3. Each method is reviewed for its positive and negative attributes, for consideration as an embedded, unobtrusive, flying height measuring method.

Piezo-electric sensors have been used as a means of unobtrusively measuring suspension arm and disk edge deflections. A background explanation of how they function is given in Chapter 4. The definition of the common notation for defining the piezo-electric sensor-actuator's performance is given and explained. The chapter then goes on to explain how to optimise a piezo-electric actuator's operation for the specific task of flying height variation by actuating the suspension arm.

In Chapter 5 a complete overview of the equipment, tasks and experiments of the work reported in this thesis is given. A thorough description of the physical vibration test station is given, along with an account of how the system was optimised. An explanation of the software used to aid the gathering of results is given,

with LabView for Windows construction of a real-time FFT virtual instrument and the C++ BIOS commands for data selection on the hard disk drive. The design, construction and application of the novel piezo-electric sensors for flying height and disk edge displacement measurement is methodically reported throughout Chapter 5.

Chapter 6 presents the results from all the experiments described throughout this thesis. These results start by detailing how hard disk drives perform whilst subjected to vibration, showing their inherent weakness to sinusoidal vibration at around 440Hz to 700Hz. Subsequent results presented provide insight into how the disk performs whilst subjected to vibration from different methods of observation. The results from the novel piezo-electric suspension arm sensor are given over different frequency ranges.

A novel optical system for measuring flying height variations and the phase relationship between disk and slider motion using a pair of compact disc reader optical units has been developed and documented in Chapter 7. Details of the underlying principles of operation are given, and the sensor's performances are observed and reported. This chapter also reports the design and construction of the frame mounting for the dual sensor optical system, allowing independent and complete freedom in all three planes. Finally, the results from experimentation using this novel optical system are given and the system is appraised.

Chapter 8 presents finite element analysis modelling work undertaken to determine the disk's resonant frequencies. This chapter explains the logical model progressions made and the effects made to the frequency response of disk.

An analysis of the results is given in Chapter 9, along with a thorough discussion of all the presented results. The modes of resonance for both the disk and

suspension arm are examined, compared to other research discoveries, and correlated to reinforce the findings.

Conclusions are drawn in Chapter 10 with all the relevant discoveries and significant results highlighted.

Chapter 11 is devoted to further work the author would like to direct future research in this area towards.

Chapter 1. Introduction

1.1 Development of Personal Computers

Personal computers (PC's) operate using digital information, data. All their processing involves either 1's or 0's, and a central processor unit (CPU) manipulates data for each task that it is required. In order for the CPU to operate it requires instructions to follow a program, this is stored in memory. This memory tends to be short term only memory, ie all the memory is lost on power down. Often random access memory (RAM) has been used, which is very highly integrated discrete logic based memory. The program, throughout the history of computing, has been entered into the RAM in numerous ways such as manually using the keyboard, or loaded in from punched tape. In later years magnetic tapes were used to load the data into the computers RAM.

Typing a program is obviously very time consuming and possibly erroneous. Magnetic tape was a huge step forward and is still considered a favourable method of storing data. Early tape systems though lacked speed and presented restrictions when trying to store multiple programs and files onto one tape. Due mainly to speed, reliability, space and cost, hard disk drives have become the dominant means of storing data.

Computer data is of a binary form. The CPU and memory process this data in a parallel manner to aid in processing speed and manipulation. When data is processed serially, one after another, a single piece of data is called a bit. When data is processed in a parallel form, the number of parallel bits processed is given a name to aid representation. 4 bit structures are known as NIBBLES, this is not a

common unit for the storage industry. 8 bit structures are BYTES. This is a typically used notation for data storage. Therefore 8 bits (or 8b) is the same as 1 byte (or 1B).

1.2 Hard Disk Drives – An Overview

A hard disk drive, shown in Figure 1 with its case removed revealing the internal components, stores data magnetically on a disk, unlike RAM that stores data electronically in complex matrices of capacitor and transistor cells. The magnetic 'cells' in hard disk drives retain their data because the magnetic medium is non-volatile, unlike conventional RAM. Non-volatile RAM is available but at greater cost. The problem with RAM is that it provides inherently small quantities of memory. At the time of writing 1GB of RAM represents the same costs as a 20GB hard disk drive. Battery backed non-volatile RAM is even more expensive. Currently, in environments requiring memory robust enough to withstand shock and vibration whilst operating, solid state battery backed RAM is used, at great expense and physical space. Alternatively, hard disk drives are installed in bulky spring-suspended cages or encapsulated in 'gel' to suppress the vibrations experienced by the drive. This adds bulk and weight and does not entirely eliminate the problem of maintaining operation in adverse physical environments.

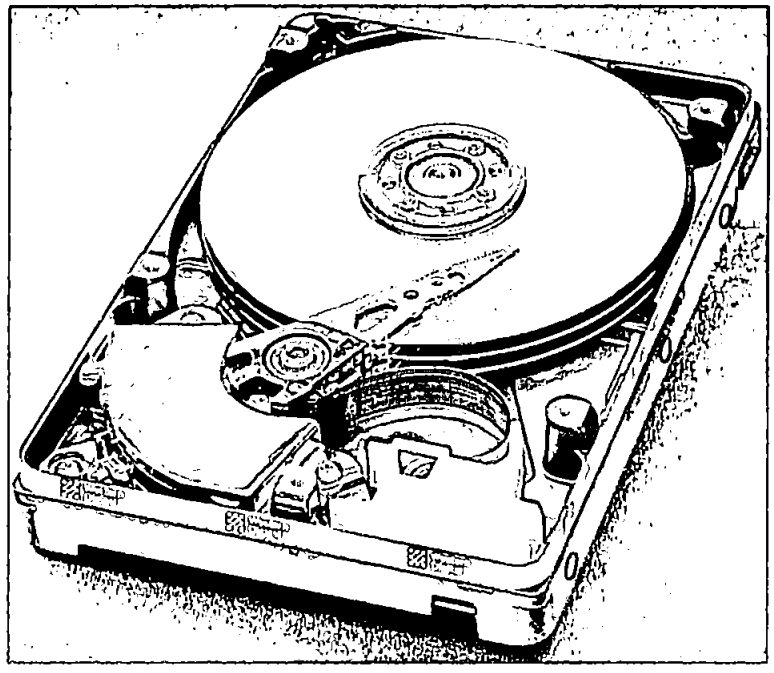

Fig. 1. Picture of a Western Digital hard disk drive. This drive has had its lid removed revealing the internal components. This drive has a three disk stack.

The data is magnetically stored as bits on the disk. A read-write head is used to read, write and re-write the data bits. The read-write head, operating close to the disk, can be simplistically described as having a small electromagnetic coil to switch or sense the magnetic bit orientation beneath the head on the disk. A change in magnetic domain orientation beneath the head induces a positive or negative current spike from the coil. These spikes are very small in magnitude and require highly sensitive, high gain, integrated circuits, for amplification, signal processing and error correction. A recent development has been magneto-resistive (MR) read heads, which IBM pioneered in 1991 to produce the 1GB 3.5- inch 0663-E12 drive [1]. MR heads are sensitive directly to the stray field from the written bits, rather than the change in this field, the sensing mechanism of the inductive head.

Further to signal processing, digital processing is conducted to retrieve the data from the raw head signal. A positive signal spike does not simply mean a logical 1 bit. Clocking and encoding data is integrated with the raw data. In order to increase data reliability the data is encoded [2,3]. This reduces data storage densities but allows for some quite powerful error correction. The data is also spliced to allow for a clocking signal to monitor disk rotation speed and servo information to ensure the head is centrally placed over the track. A result of all this additional information is that the signal received by the head bears little relation to the 'real' data stored on the disk. To extract the data much digital signal processing is required.

1.3 Construction and Design of the Storage Media

Hard disk drives are an economical form of mass storage. They are widely used as secondary memory in virtually all computer systems. Their dominance in the personal computer market can be attributed to their large storage capacities, reliability and relatively low cost. Over the years hard disk drives have grown rapidly in storage capacity and speed of data transfer, Figure 2 shows the progress in storage densities.

Figure 3 shows a photograph of a drive modified with the intention of allowing viewing access of the drive. The location of all the key components within the drive are clearly labelled. This drive has three disks, six media surfaces and therefore six data heads.

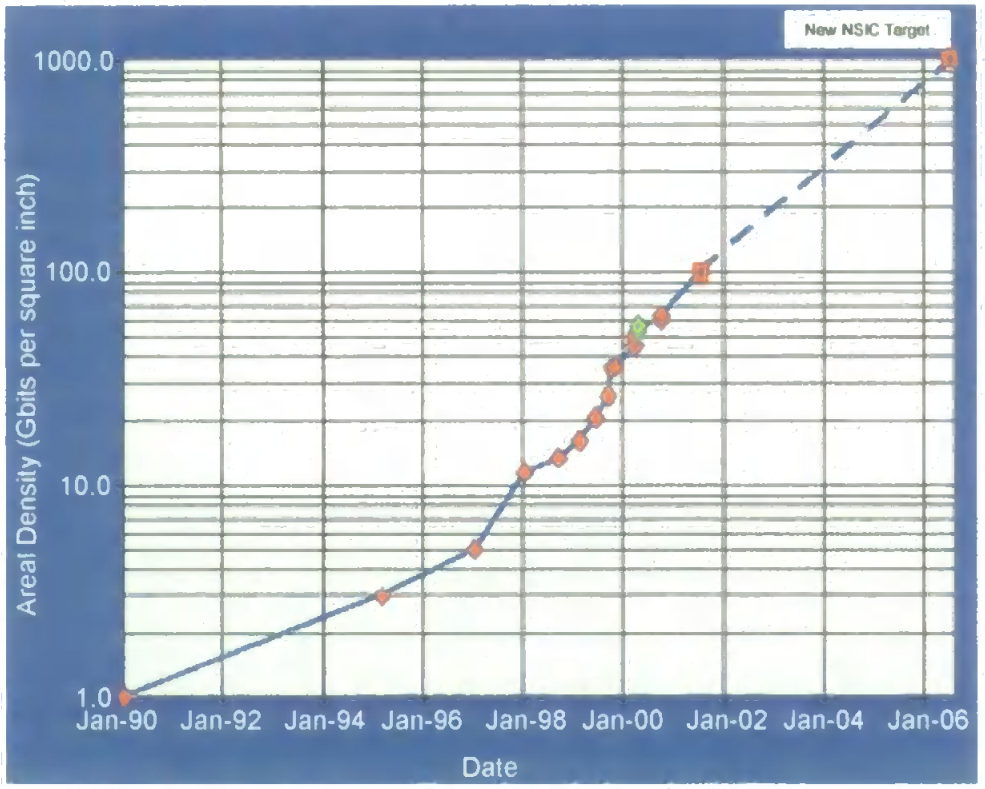

Fig. 2. This graph shows the areal densities demonstrated in research drives since 1990 and the National Storage Industry Consortium (NSIC) target for 2006. NSIC is a consortium of companies involved in the hard disk drive (HDD) industry, [4].

A hard disk drive stores data magnetically in a thin film which is deposited onto a disk. The disk is relatively thick and made of a strong and rigid material, hence it is a hard disk. Data stored on the magnetic disk is divided into different sectors and tracks. Each track is a ring around the disk and a sector is a partition of the disk as shown in Figure 4. There can be multiple stacked disks used within a hard disk drive, each offering two sides for data storage. Increasing the number of disks increases the total storage capacity of the drive at the cost of extra bulk and expense.

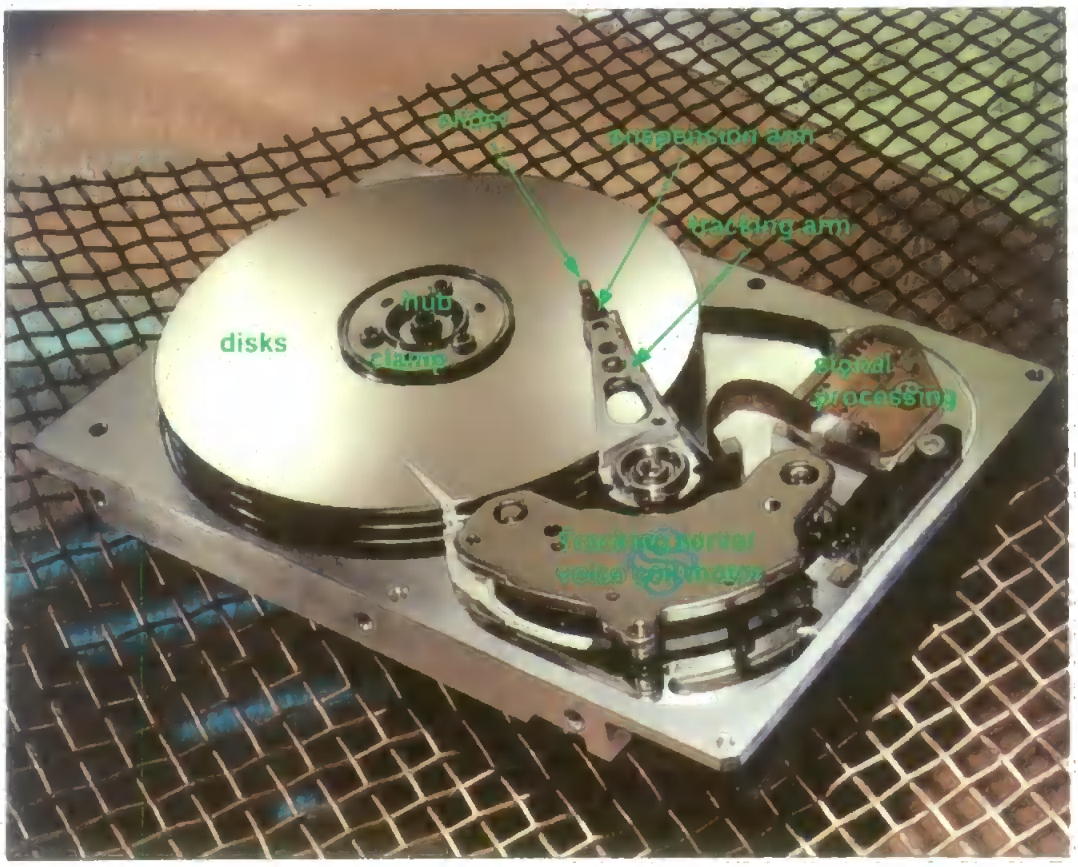

Fig. 3 Photograph of a Seagate drive with modified chassis to display all the internal components of a typical hard disk drive.

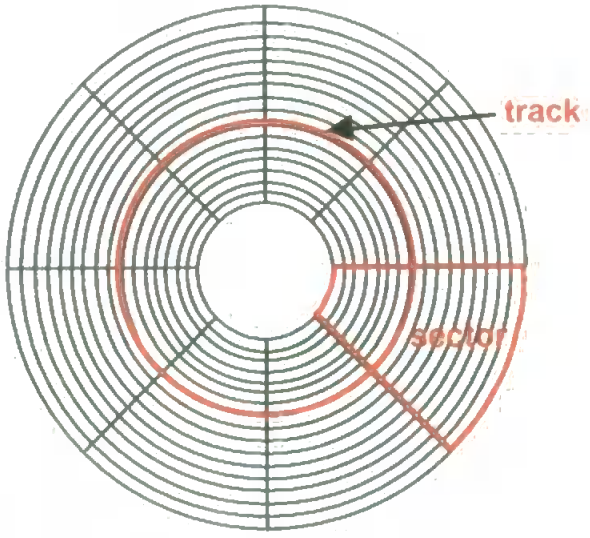

Fig. 4. Schematic diagram showing the segmenting of data on a hard disk. Normally there are many more radial tracks and sectors on the disk.

The disks are generally made from an aluminium/magnesium alloy (AlMg), they used to have a thickness of 1.25mm but now they are typically 0.8mm thick. Today, hard disk drives are typically sold as either 3.5" or 2.5" type drives with the smaller drive suffering slower data transfer rates and reduced storage capacity. Smaller drives are better suited in Laptop computers, where size is a premium. Thicker disks with reduced overall diameter will naturally be stiffer and less prone to bending, making them more suitable in the Laptop environment where the computer is liable to suffer physical mishandling. The trade off for their greater rigidity is greater physical size and reduced storage capacity. Thicker disks will increase the profile of the drive and hence make it larger. Smaller diameter disks reduce the area of data stored so subsequently require more disks for a given storage capacity. Multiple disks enable greater data storage capacities but increase drive space and power consumption. At the time of writing, commercially available drives operate with flying heights of around 5nm. The IBM Ultrastar 146Z10 drive stores 146GB of data with a storage density of 26.3GB per square inch [5].

The disk is constructed with many layers. The disk itself is a 0.8mm thick aluminium magnesium substrate because it favourably combines low density, rigidity and cost. The surface of the disk is required to be extremely smooth to give a uniform read back signal from. the low flying head. However, the aluminium alloy is quite soft and cannot be polished to the required finish. The substrate, therefore, must be modified to provide a surface capable of being polished to a high degree of smoothness and to provide a structural support for the thin magnetic film that stores the data. A soft disk is not desirable as it can be damaged should a read-write head 'crash' occur [6]. For this reason the aluminium

alloy is nickel-phosphorus (Ni-P) plated, which provides a surface hardness of approximately 550 kg/mm^2 on the Brinell scale. The Ni-P surface is abrasively polished and textured to give a 1.0nm root-mean-square (RMS) finish with circumferential grooves. These grooves both minimise head stiction to the disk and provide uniform magnetic read-back signals [7,8].

The thin film magnetic layer requires an underlayer to help nucleate and grow microstructures with appropriate magnetic properties. A chromium underlayer is often used as it provides a good epitaxial match with cobalt-based magnetic alloys, which are commonly used for the thin film magnetic layer. Furthermore, chromium reduces the potential for corrosion.

The magnetic layer needs to be a ferromagnetic material and cobalt-based binary and ternary materials are often used because of their high coercivity [9,10].

The thin film magnetic layer can easily be damaged by the head coming into contact with it. When the drive receives a large shock the read-write head can hit the disk. This can occur when the drive is in operation or not, with the disk spinning or stationary. Without any protection the magnetic layer would be permanently damaged, producing a hard error. To protect the magnetic layer an amorphous carbon overcoat 10 - 15nm thick is sputtered on to the disk. As disk development continues, this overcoat is gradually being reduced in thickness to allow the heads to fly closer to the magnetic layer.

To prevent the head being damaged by the disk spinning underneath it, and to reduce friction, the disk's top layer is a lubricating layer. The lubricating layer is a perfluoropolyether organic polymer of about 1nm thickness [11].

Texturing of the disk surface will create friction between it and the head, which will cause the head to wear. This creates micro-contamination, which

naturally further damages the head and slider [12,13,14], accelerating the process of attrition. Friction, which heats the head, will reduce the signal to noise ratio [15]. When the head parks against the disk, when the disk has stopped rotating, a vacuum can be created between the smooth surface of the disk and the underside of the slider (stiction) [16]. This reduces the drives reliability, hence some texturing is required to prevent stiction.

When the drive is in non-operation it is necessary to 'park' the head, this requires resting the delicate head in a safe manner that minimises damage. When the drive is powered down the disk naturally stops spinning, removing the protective air bearing that the head relies on. The head's flying height is reduced as the disk slows down, eventually leading to the head making contact with the disk. This can cause damage. To prevent permanent damage to the stored data the suspension arm control system pulls the suspension arm, and head, across the disk to its inner circumference, which is a dedicated landing zone where no data is stored. A development of this idea is to have dual texturing. The landing zone has a deeper texture to reduce stiction and prevent a vacuum formation. This allows an extremely smooth disk surface throughout the rest of the disk, resulting in the potential for lower head flying heights. Another means of parking the head is to locate physical ramps at the inner perimeter of the disk. The ramps are profiled such that when the suspension arm swings towards the centre of the disk, the ramp unloads the suspension arm that pretensions the head against the disk. The ramps also provides a gentle means of placing the head on the rotating disk. By waiting for the disk to spin at normal operating speed before arcing the arm across, and gently lowering the head against the disk on its air bearing, the head need never make contact with the disk. This reduces, but does not eliminate, particulate

contamination. The suspension arm loading/unloading against the ramp can generate some contamination [17]. One clear advantage of this method of parking the head is that the head is not in contact with the disk in non-operation, and is held in position so that no head or disk damage can occur.

AlMg disks are not the only ones to be used. Glass disks are gaining popularity as a glass substrate disk offers a far smoother disk surface than its aluminium alloy counterpart, enabling a lower head flying height without the risk of the head hitting high spots, or asperities, on the disk surface. As well as physical damage, such asperities can cause data errors due to their heating offset on magneto-resistive sensors [12,18,19]. Glass disks also behave to vibration differently. They resonate at slightly different frequencies, ie they have a different modal response. This is due to their different mechanical properties such as Young's modulus.

One of the key ways to generate faster data transfer speeds and higher data storage densities is to reduce the flying height of the head above the disk. When magnetic data is stored at greater densities on the disk it becomes more difficult for the head to detect the data bit directly beneath it. This is because the magnetic bits are smaller, a graph showing storage data densities is shown in Figure 2 with current data bits being 0.5μm by 0.05μm [20], and have less accompanying magnetic field. Part of the solution is to reduce the flying height, and Figure 5 shows the trend for flying height reduction. Heads must maintain a flying height, within a specified tolerance, and this tolerance reduces with lowered flying heights. However, when the flying height is reduced it becomes more critical to maintain the required separation or else head-disk contact can occur. The reduced

flying height also poses severe problems in the experimental measurement of the head-disk separation.

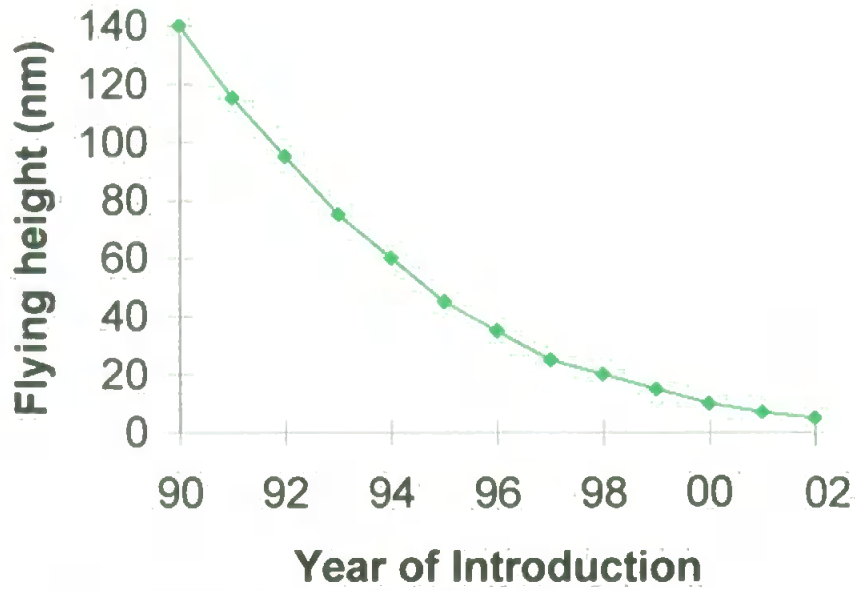

Fig. 5. Graph showing reductions in flying height over the last 12 years. These flying heights were achieved in research drives, and not for commercially - available drives.

The disk is mounted on a hub that is driven by an electric motor at speeds of up to 10,000rpm on current drives: the faster the disk spins the greater the data transfer rate becomes as the data bits pass underneath the head quicker. As the disk spins it generates turbulence or windage, and because of this the head is mounted in an aerodynamic slider that produces lift from the air stream, as shown in Figure 6, enabling the head to fly above the disk at its predetermined height. The force of the lift is balanced by the force provided by a pre-tensioned sprung cantilever; the suspension arm, and the balance between the two provides the required flying height [21].

The slider is fixed to the suspension arm via a coupling that allows for limited movement of the slider. This fixture is known as a gimbal. The gimbal

serves to ensure that the slider cannot be twisted out of plane with the data tracks beneath it. However, it provides near complete freedom to allow the slider to be manipulated by the aerodynamic forces.

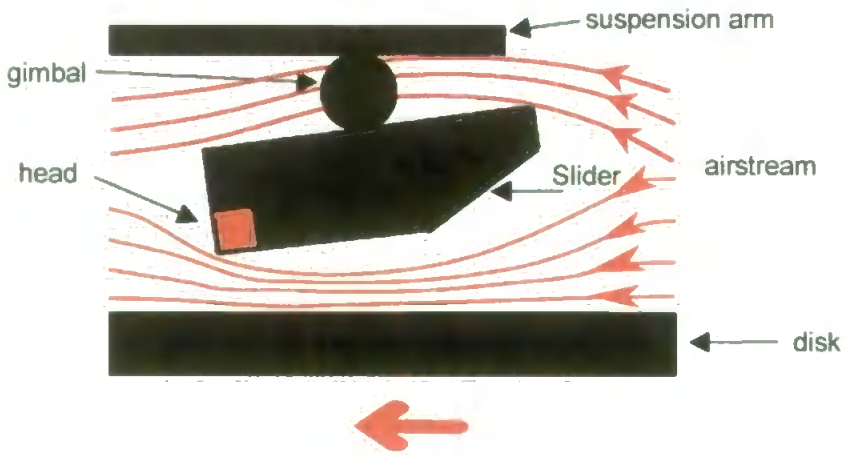

Fig. 6. Schematic diagram representing the head flying over the disk. Airflow is used to orientate the head correctly above the disk.

One type of slider design is the taper flat slider, which has two straight rails on either side of the slider, which are tapered at the leading edge to compress the incoming air to provide lift. Another design is the "self-loading" or negative pressure slider, which differs in as much as its leading edge taper extends across the full width of the slider, with a "crossbar" directly behind the taper connecting the two rails at each side. The front taper provides the compression of the air and hence lift, whereas the recessed pocket behind the "crossbar" creates a sub-ambient pressure, sucking the slider nearer the disk. The recesses cross-sectional area reduces towards the trailing edge of the slider to increase the air speed travelling through it and further improve the negative pressure on the underside of the rear of slider. The downward force generated from the recess results in an air bearing that is stiffer and with a reduced velocity dependence on flying height. Figure 7 shows the difference in the designs.

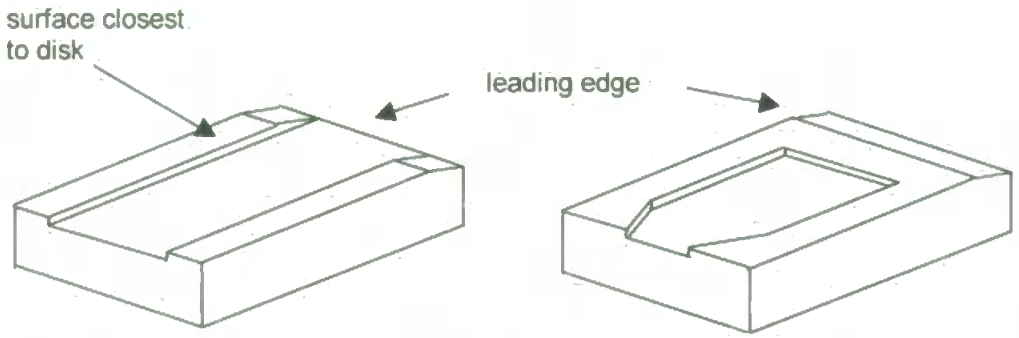

Fig. 7. Schematic diagrams showing the design of the taper flat slider, left, and the "self loading" slider on the right from the underneath.

The head and suspension arm are connected to a rigid arm, as shown in Figure 8, that swings across the disk. This enables data to be transferred from the disk at various radial positions, hence accessing different tracks. The arm is constructed from duralumin, which is an aluminium alloy, that is both light and stiff. The particular alloy used in the hard disk drive industry is 5083, an alloy of 4.4% magnesium, 0.7% manganese and 0.15% chromium, has a density of 2.66g/cm^3 and a Young's modulus of 71Gpa, [22,23]. The lighter the arm the more rapidly it can swing across the disk, allowing for quicker data access rates through improved seek times. The arm pivots on a shaft-mounted bearing and is driven by voice coil motor.

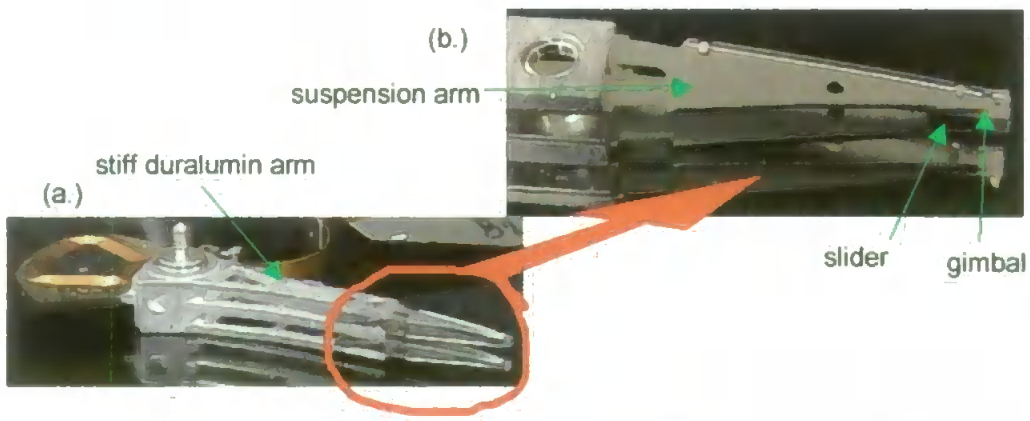

Fig. 8. (a.) Photograph of a suspension arm unit and (b.) shows a close up of the sprung cantilever that pre-tensions the head against the disk.

2. The Vibration Problem in Hard Disk Drives

2.1 Limitations of Hard Disk Drive

Conventional hard drives are very reliable under normal operating conditions, but they can suffer from mechanically-induced failure when operated in hostile conditions. In areas where vibrations exist, hard disk drives can frequently fail catastrophically and can no longer read or write data. At best the data transfer rate becomes vastly inferior.

Environments such as military and aerospace are synonymous with large shocks and vibrations. Ocean going craft can also encounter difficulties with hard drives as the engine and waves transmit vibrations through the hull. Dennis [24] evaluated many proposed solutions, mainly employing large vibration isolation cages and mountings that passively damped the vibrations. However, additional isolation mountings are not the ideal solution. The extra space and weight needed precludes this method from many key areas: adding both weight and bulk to a drive is hardly an improvement. Passive dampers, which are only effective over a limited bandwidth, are all that is used in current 'ruggedised' laptops.

Another approach to passively damp the hard disk drive has been to develop laminate disks constructed from three sections [25,26,27], two normal disks with a damping sandwich layer between them. However, passive damping bandwidth limitations still exist and the disks' thickness increase, again increasing the drive's physical size.

Hard disk drive manufacturers have invested a vast amount of research in how and why drives can become damaged in non-operation. This is primarily not

to provide the end user with a more robust, reliable drive but to reduce failure costs. Drives can experience large shocks during transportation which may cause severe damage and failure during initial usage [6,28,29,30,31]. This is costly for the manufacturer as the drive has to be replaced, and inconvenient for the end user too.

2.2 Susceptible Components within the Hard Disk Drive

It is important to understand precisely what is happening within the drive, and which systems areas are failing under conditions of shock and vibration. When mechanical components are vibrated they bend and distort, and this is further compounded when vibrated at resonant frequencies.

There are two major mechanical components that, when excited at resonance, can result in data-transfer failure. Firstly, there is the suspension arm that pre-tensions the head against the disk to counterbalance its aerodynamic lift. This is designed to control the flying height of the head during normal operating conditions. If the flying height of the head is such that it is outside of its normal operating range, either too high or too low, then the signal degrades ultimately leading to data transfer failure. In severe cases, the head will crash onto the disk, causing irrecoverable damage to the head. Secondly, there is the hard disk (the data storage medium) itself. The disk is often minutely buckled and warped from the way it is clamped to the motor spindle, the clamping area of the disk having a flatness of 5μm or less [32,33]. This is greatly inflated by the very low flying heights used in current and future drives. Additionally, the windage created by the spinning disk [34] and rocking of the disk pack spindle [35,36], due to

manufacturing tolerances, accumulate to provide a disk that flutters sufficiently to cause difficulties during normal operation, a typical Quantum Maverick drive measured 12μm peak-to-peak run-out. During periods when the disk experiences additional vibration, the fluttering is greatly exaggerated, causing track mis-registration and flying height problems. These problems can be compounded by the fact that if the suspension arm is resonating, the disk maybe driven into oscillation due to the slider pushing onto the disk and vice-versa [37,38].

Whilst the head maintains its correct flying height it is still possible for data transfer errors to occur. There are two forms of data recovery error that occur, one called jitter, the other track-mis-registration (TMR).

Jitter is where the head reads the wrong data bit whilst still flying on track, see Figure 9. Instead of the head following the data track, bit by bit in the normal sequence, the data is shuffled forcing the head to reread what it has just detected or jump and miss data bits.

The other form of data error is Track Mis-Registration, where the head is pushed off track, causing loss of signal amplitude, possibly to the point where it is detecting the adjacent track causing cross talk interference, see Figure 10.

The tracking arm arcs across the disk to allow data to be transferred from different tracks on the drive, see Figure11. Therefore the angle at which the head intersects the data track will vary slightly. This has minimal effect on how the head transfers data. However, the angle the suspension arm lays across the disk also varies, albeit through a minimal angle, but it does change the form of data error from induced vibration.

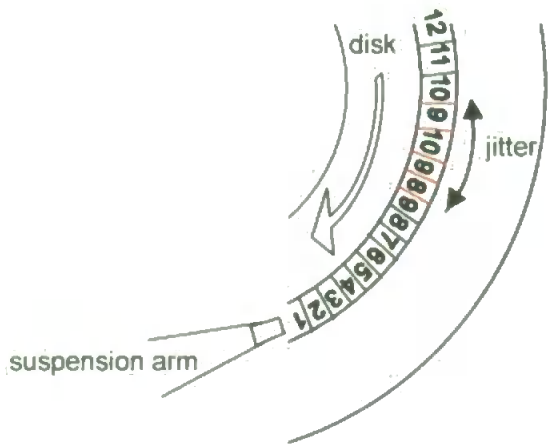

Fig. 9. Depiction of jitter. The bits being read from the disk are observed in an incorrect order due to the head not following the track in a stable manner.

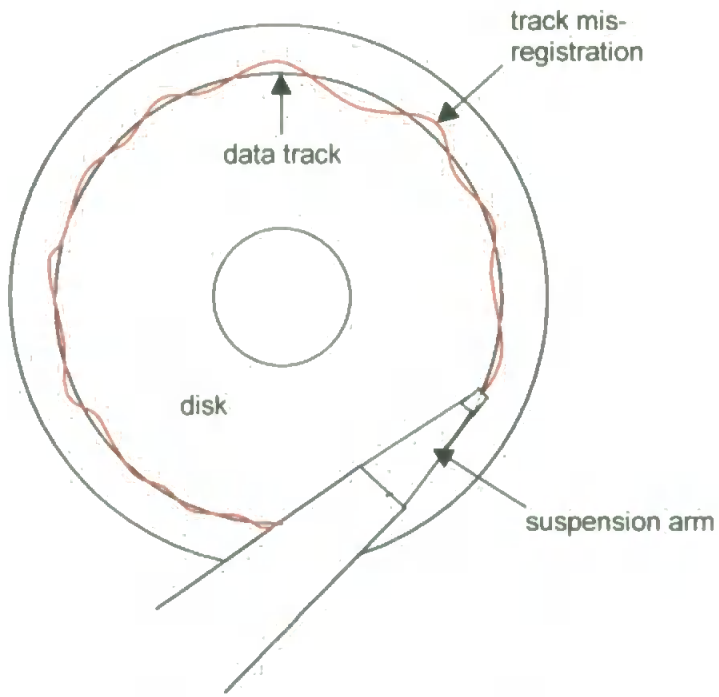

Fig. 10. Diagram showing track mis-registration.

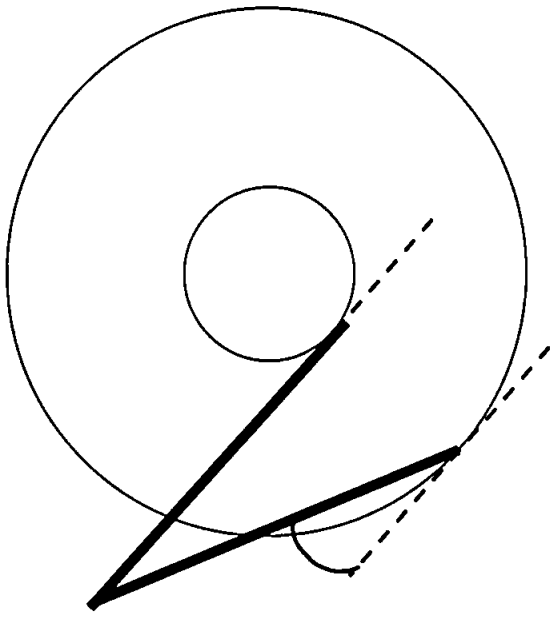

Fig. 11. Diagram depicting the approximate angles reached by a typical suspension arm within a typical hard disk drive.

Hard disk drive manufacturers ensure that the angle variation is minimal through careful design of the tracking arm and pivot position. When the head is located over the centre track, the slider and data track beneath the head will be parallel. When the tracking arm is arced towards the centre or outside of the disk the orientation of the head to the track will become non-parallel. However, because of the careful positioning of the pivot point of the tracking arm this angle change is minimised.

The angle that the head makes with the data track beneath it dictates whether vibration causes jitter or TMR. The jitter and TMR will vary, as one increases the other decreases, depending upon the angle the head makes with the track.

When the disk bends, the head, coupled through its air bearing and sprung suspension arm, should remain at its designed flying height. This causes the

suspension arm to bend to allow the head to follow the disk's movement. A typical sprung suspension arm, shown in Figure 12, is made from 0.2mm thick stainless steel that is typically 15 to 20mm long, this is short in comparison to the 35mm span of the disk. The design includes folded edges throughout most of its length to increases its torsional rigidity along the section, except for a 3 to 4mm part of the suspension arm, where most of the deformation occurs, at the base of the suspension arm. To accommodate the thickness of the slider the suspension arm is parallel to the disk with a gap of the order of 1mm.

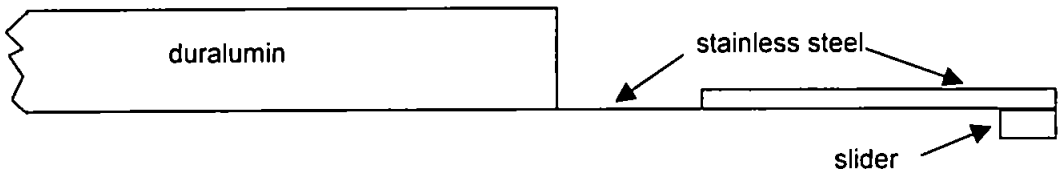

Fig. 12. Diagram depicting suspension arm construction and design. The stainless steel arm flexes at its base where it joins the duralumin section.

Figure 13 illustrates the significance of the suspension arm only bending at its root compared to the disk's bending. When the disk bends away from the head, down, the suspension arm is bending at a greater radius. This, coupled to the fact that the arm's bending is constrained predominantly to the root of the arm, means that the head is pulled back along the disk. When the disk bends upwards, into the suspension arms radius, although the head would be pulled back along the disk due to it bending only at its root, the fact that the arm is bending at a tighter radius than the disk offsets this.

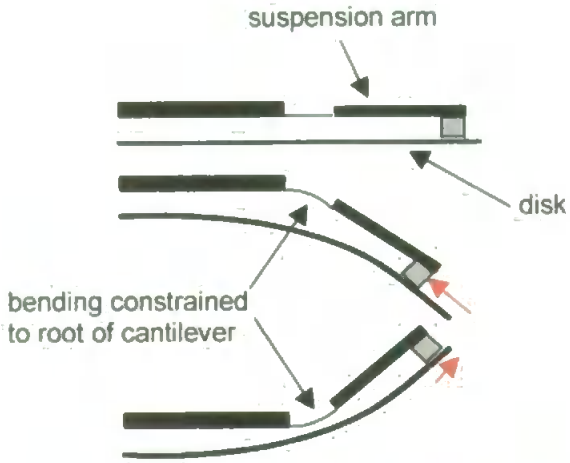

Fig. 13. Diagram representing head position when the disk is bending with the suspension arm at a great angle to the track orientation. This position is not achievable in a real drive.

The other problem associated with the disk bending, and the suspension arm deforming to maintain the required flying height is depicted in Figure 14. Assuming that the suspension arm is at an angle shown in Figure 14, when the disk bends, either up or down, the head is left reading data from a track further from the inner radius of the disk. The example shown in Figure 14 would be the purest form of TMR produced from disk flexure.

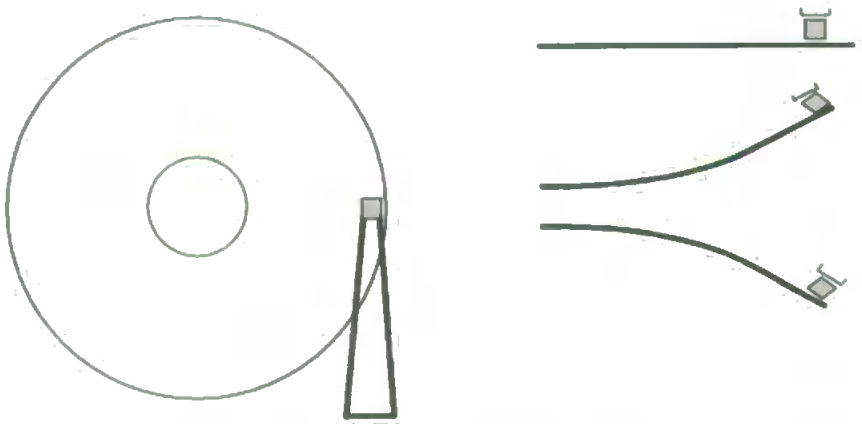

Fig. 14. Diagram depicting the disk and suspension arm motion under bending when the arm is placed straight across the disk. The angle shown is solely for the purpose of demonstration.

Neither of these problems exists in isolation. When the tracking arm moves through its normal arc of operation the suspension arm will cause both jitter, from the arm's bending being confined to one point, and the head to go off track. However, depending on the exact track that the head is flying over, and therefore the angle between the head and the data track, a combination of jitter and TMR is present.

When the head is located at the outer or innermost tracks the angle between the head and the data track is at its greatest. When the slider is at a great angle with the track, as the suspension arm bends and it pulls the head 'back' across the disk, extra TMR is produced. When the head is located above the centre track, jitter is potentially maximised, but track mis-regristration from the disk bending is still present.

The variation of track mis-registration versus jitter created from track position is minimal when compared to the total movement of the disk at each track. At the outside edge of the disk, vibration induced motion is at a maximum, whereas at the centre, next to the rigid hub, disk movement is negligible. Therefore both jitter and TMR peak when the head is located above the outer track of the disk.

Chapter 3. Flying Height Measurement Techniques for Embedded use in Hard Disk Drives

When any system is under observation it is necessary to ensure that the measuring instrument does not effect the system's performance in any way. In practice this can prove to be very difficult. There are several methods currently used to measure the flying height of the head above the disk, varying from being highly obtrusive to almost unobtrusive.

This chapter outlines some of the more common methods of flying height measurement, or hard disk drive observation methods' that can be adapted for head-disk interface observation:

- Acoustic emission detection of head-disk contact
- Thermal detection of head disk contact
- Digital Signal Processing (DSP) measurement of head positioning through raw signal investigation
- Interferometer detection of head-disk spacing
- Laser Doppler vibrometer measurement of head-disk separation
- Glass disk system for head-disk separation and flying height measurement,
- Measuring the flying height via capacitance gauges
- Interrogating the tracking position error signal of the drive to observe head positioning disturbances.

3.1 Acoustic Emissions (AE)

The heads' flying height is extremely small, around 5nm at the time of writing. Stating the head is flying is a slight misnomer, with flying heights this small it is actually intermittently brushing across the surface of the disk. The surface of the disk has undulations, albeit very small, typical runout being less than 8μm and surface roughness peaks of less than 20nm [32,33], but when compared to 5nm flying height they are significant. As a head/slider brushes across the surface of the disk the 'contacts' cause high frequency vibrations [39,40]. The localised pressure fluctuations can be detected through a piezo-electric sensor. These sensors are generally bonded to the tracking arm assembly as near to the head as is practical. The high frequency vibrations are coupled through the tracking arm assembly to the sensor.

The AE signal is in the 200-300MHz region and so the key to such a sensor method is to have a sufficiently high-speed data acquisition system. Through Nyquist theory [41,42] it is known that the sampling rate should be at least twice that of the maximum frequency of signal to be detected, hence requiring data sampling of at least 600M samples/second.

Data acquisition cards are commonly rated at distinct sampling speeds, the most appropriate would be an acquisition card with a sampling speed of 2 Giga samples per second.

A limitation of this system is it is impossible to collate direct information of the flying height should the head not maintain near-contact with the disk. When deliberately vibrating the drive, should the head be 'launched' off the disk due to a

large impulse, flying height determination would be limited to predictive methods through timing the contact separation period of the slider from the disk.

The system is completely unobtrusive. The sensor does not need to be bonded to any mechanically-critical component, and so the slider and air bearing dynamics are unaffected. The sensor would typically measure 5mm squared.

Results from the acoustic emission reveal how the frequency of emission varies with time under certain conditions; some results performed by [43] are shown in Figure 15. The spin-up and spin-down, with contact start-stop head parking mechanism sequences, typically show great acoustic activity. This indicates great activity and contact between the head and the disk before the head takes off and after it lands, as would be expected. It has been proposed that the condition of the drive is correlated to the magnitude of the frequency spike on parking [43]. Considerable ongoing research [44] is concerned with relating spin speed to the frequency of acoustic emissions. It is obvious that the flying height is related to spin speed, due to the slider being unable to fly as high with less windage created by the slower spinning disk [44].

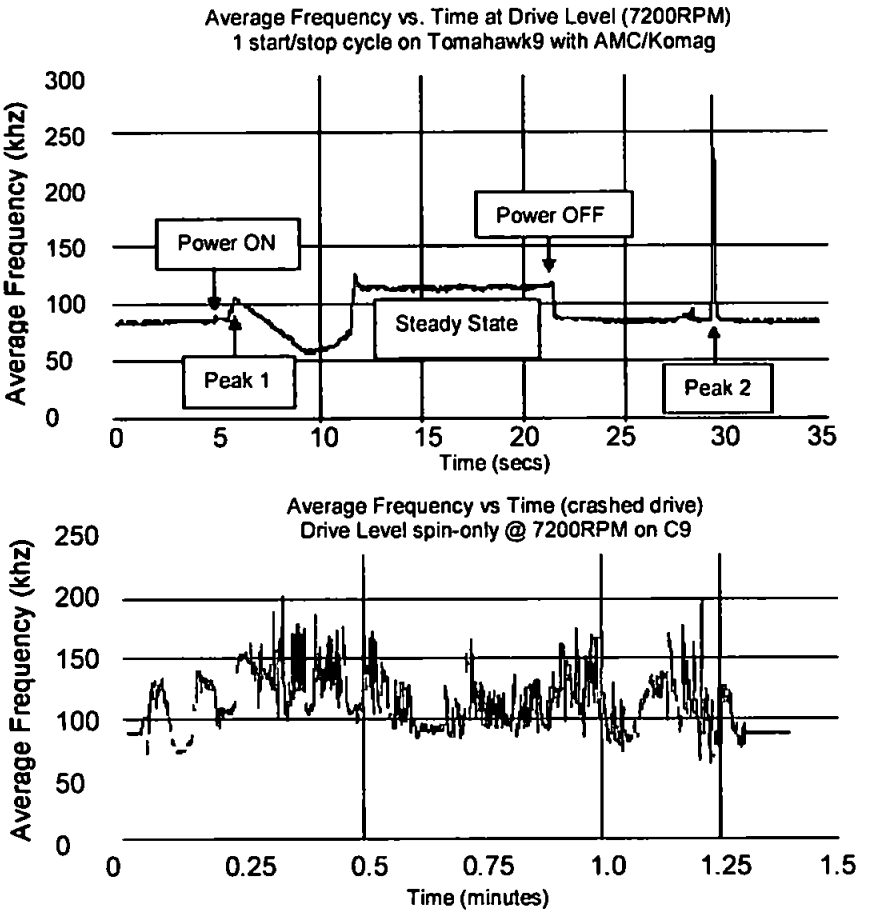

Fig.15. Results from [43] showing acoustic testing on the same drive before (top) and after (bottom) the drive suffered from a 'crashed' head. The graphs show average frequency versus time.

3.2 Thermal Detection

In much the same way that the head produces an acoustic emission when grazing the surface it also generates heat. The heating of the head causes a white noise level to be superimposed onto the read signal from the head. This is generally undesirable; hence manufacturers try to ensure close tolerances on surface roughness to minimise contact, thermal fluctuations and the associated signal-noise reduction.

It is possible to monitor the signal from the head and measure the noise floor. The principle drawback is that the signal is very small, typically the order of 1mV. Although the drive has onboard amplification circuits, these tend to be encapsulated within the encoding circuitry, restricting the ability to measure the raw amplified signal. Therefore the raw signal must be sensed almost straight from the head. This demands sophisticated measuring equipment, for example LeCroy oscilloscopes which are designed for this purpose.

The system also has the same non-contact limitations as the AE system. Furthermore, the system will be subject to ambient temperature variations to a small extent. Should the room temperature change, then the induced noise in the read-back signal will change proportionally to that, although this can be accounted for.

3.3 Readout Signal Analysis

It is known that the head has to be very close to the disk to detect the data with optimal signal-noise ratio. To expand on this: if the head is vertically too far from the disk the high frequency signal response and the signal level from the head diminishes [45], if the head is moved off track, farther from the track centre, then the signal to noise ratio deteriorates. If the head gets too close to the disk signal quality is also impaired due to thermal fluctuations from the head skimming the textured disk.

If the signal from the head is carefully monitored, using real-time Fast Fourier Transform (FFT) techniques, the drives' performance can be assessed.

Ideally distinguishing between off track occurrence and flying height variations, which is a non-trivial feat.

The use of readout signal analysis, from digital signal processing techniques, to identify flying height variations suffers the same limitations as the thermal detection method, in respect of the difficulty to detect the raw signal from the head. One other slight disadvantage is that the FFT transformation requires a finite processing time and therefore induces a minor delay in calculating the flying height, and hence a 'near real-time' system is created.

It does have the distinct advantage that should the head leave contact with the disk, whereas acoustic or thermal emission detection methods are unable to track the heads flying height thereafter, the DSP method can still monitor the height.

3.4 Interferometry

Interferometry is a very sensitive optical technique to absolutely measure the flying height of the head. By reflecting two individual laser beams off of the top side of the slider and the disks' surface it is possible to determine the relative spacing between the two. A reflective surface must be bonded to the top side of the slider in order to gain an efficient reflection of the laser beam. The disk is naturally polished from the manufacturer to the extent that it is sufficiently reflective.

The associated instrumentation to reveal the flying height is both sophisticated, and costly, usually requiring phase-sensitive detection.

The system has some major limitations. There cannot be an opaque lid fitted to the drive, as this would block the optical path, hence the drive is no longer operating in its natural state. Any vibration induced into the system would have to be very small as any optical system would have a small linear operating region. To compound this further, the distance between the object measured and the lens has to be great as the optical system can be large and bulky and space is restrictive within the drive. Another problem is that the point on the disk being measured is not the point directly beneath the head and hence what is measured is not the true flying height. Also, bonding a very small mirror onto the slider affects the system's dynamics. A great problem is that the slider is free to rock and twist to allow the head to follow contours of the disk. The central area of the slider is obscured by part of the suspension arm; hence to measure the slider movement the optical beam must be focused eccentrically onto the slider. Movement detected, therefore, is not purely vertical flying height variation but a mixture of rocking, pitching and flying height movement. For a more accurate measure of flying height change four optical beams would be required, to observe three points on the slider, and one off the disk just in front of the slider, shown in Figure 16. Three points on the slider would enable all the pitching, and rocking as well as the pure flying height change to be monitored. As a next best two points at the back of the slider (and one off the disk), either side of the suspension arm would be able to give the flying height and the rocking of the slider.

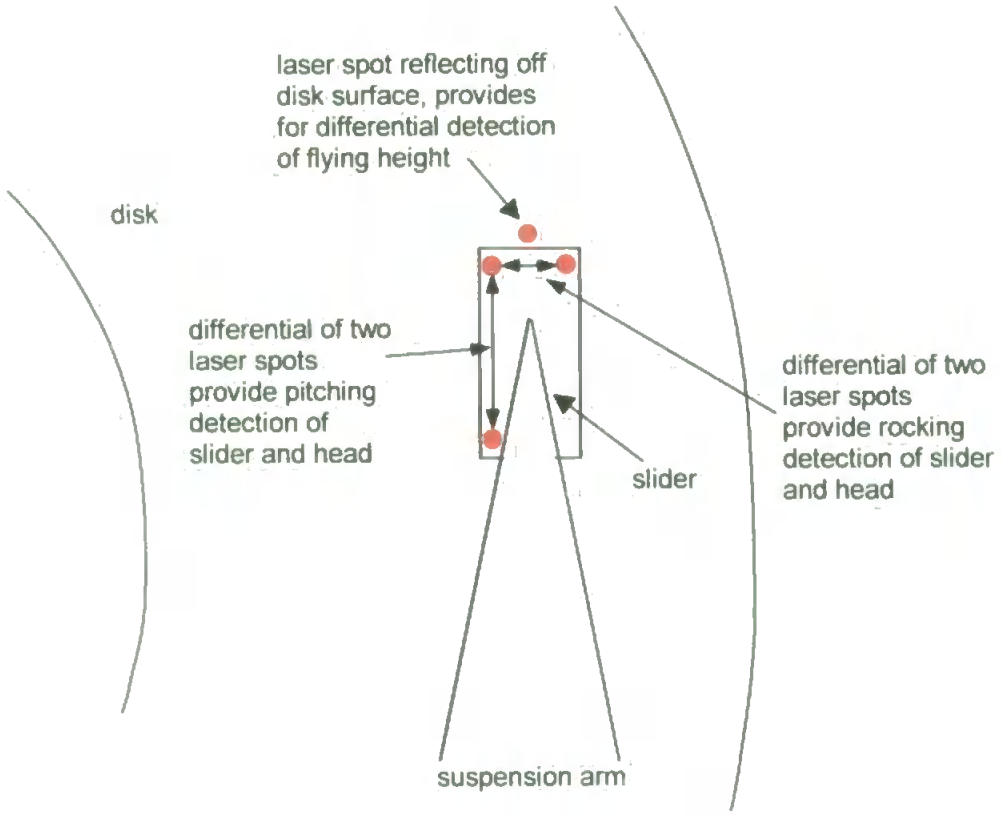

Fig. 16. Diagram showing a possible means of detecting flying height using differential methods. The position of the head requires calculation from both pitch and rock measurements.

3.5 Laser Doppler Vibrometry

The laser Doppler vibrometer (LDV) measures the motion of the object it is focused on through detecting its velocity of movement directly towards and away from the sensor.

A laser beam is focused on an object and the reflected beam monitored. The beam is modulated sinusoidally, for example, and detected by an optical sensor upon reflection from the object. The frequency of this sine wave is dependent of the motion of the object beneath the sensor. If the object is static the

detected frequency of the sine wave should be identical to the input frequency. However, should the object to moving towards or away from the sensor then the frequency will be increased or reduced, the well known Doppler shift [46].

The laser Doppler vibrometer output provides an instantaneous velocity measurement of the disk surface as it rotates under the beam. The signal has very low noise and provides very accurate and repeatable readings. A single integration and a single differential of the signal provide vertical runout, disk buckling from uneven clamping, and acceleration.

This means of measuring disk and slider movement is the most popular method used in the industry. It can therefore be concluded that LDV measuring is a very good method. However, it would still pose limitations for building an integrated measuring system to be embedded with a drive. It is too bulky and costly for this.

Figure 17 shows the results from research conducted by Truong et al. The research used a 50% negative pressure head which was loaded and unloaded by moving a known ramp, which gave an effective vertical velocity of load and unload of approximately 0.3 m/s. Several Load/Unload cycles are shown in Figure 17 with one load and unload event circled. The "Index" pulses at the bottom of the graph represent every revolution of the disk, [47].

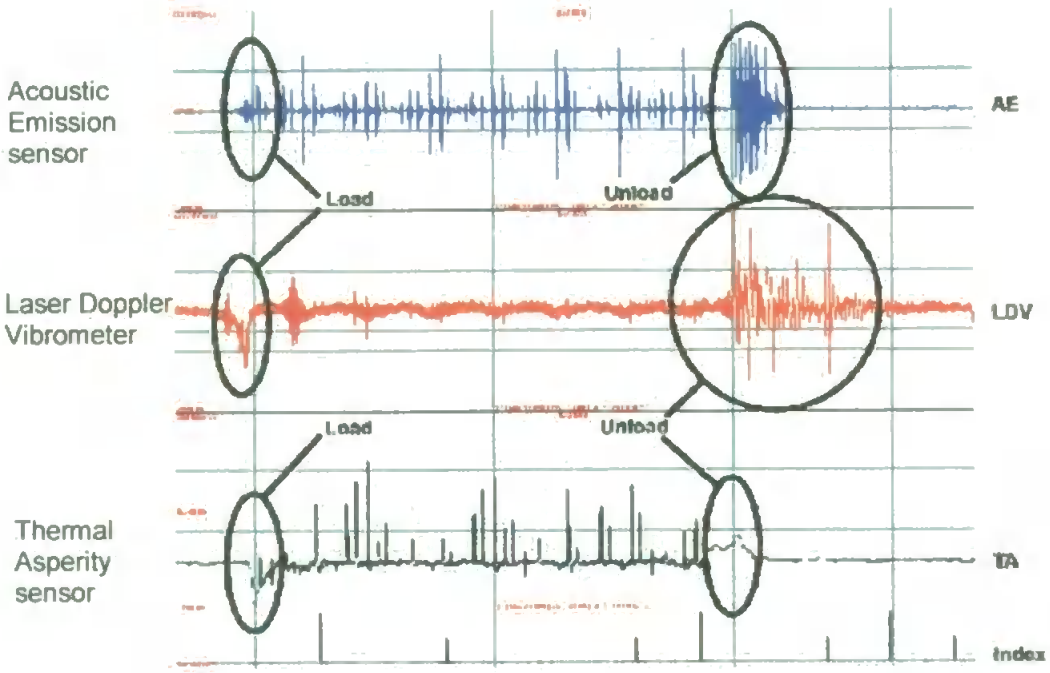

Fig. 17. Actual ramload data using LDV sensors. This experiment studied the transient events of a load/unload cycle. The disk used had known mechanical defects in the load zone, [47].

3.6 Glass Disk Optical Flying Height Measurement

A bespoke hard disk drive is constructed with a glass disk installed in place of the normal AlMg based disk. The glass disk is manufactured to specific properties to try to replicate the original AlMg disk as closely as possible with the exception that it is transparent, allowing optical beams to pass through it to observe the slider and head directly from underneath.

The systems' main drawbacks are that the drive is left unsealed and therefore the air damping effect (attributed to the lid) is lost. Further to this, the glass disk may not have the surface texturing and grain of the AlMg disks, effecting how high the head can fly. The drive will not have a tracking control system as there is no magnetic data stored on the glass disk, affecting the system. The mass and balance of the glass substrate needs to be carefully checked so as

not to affect the hub's inherent bearing rock, known to produce dramatic flying height variations, [35,36].

3.6.1 Dual Beam Interferometer Glass Disk Optical system

This system uses the dual beam interferometer system in a novel manner. The beams are focused, one on the underside of slider by passing through the glass disk relatively unaffected, the other reflected off the disks surface. The second beam that is reflected of the disk's surface to measure the flying height requires the disk to be reflective. Liu [48,49,50,51,52,53] has developed a system using a 3mm thick glass disk with surface roughness of less than 2nm rms, flatness of less than 120nm peak to valley and an anti reflection coating, applied to only one surface, with a residual reflectance of less than 0.1%. Therefore the second beam passes fairly unaffected through the first surface, through the glass substrate, and is then partly reflected off the second surface. This partially reflected beam is then detected to find the reference point for flying height determination, see Figure 18.

Other methods [54,55] for flying height detection using a glass disk rely on using multiple points on the underside of the slider. If two points, one at the front and one at the rear of the slider, are observed optically then the pitch of the slider can be found. The true flying height of the head remains difficult to obtain, as the head position must be predicted from the two, shown in Figure 19, as it is recessed within the slider due to its more vulnerable nature.

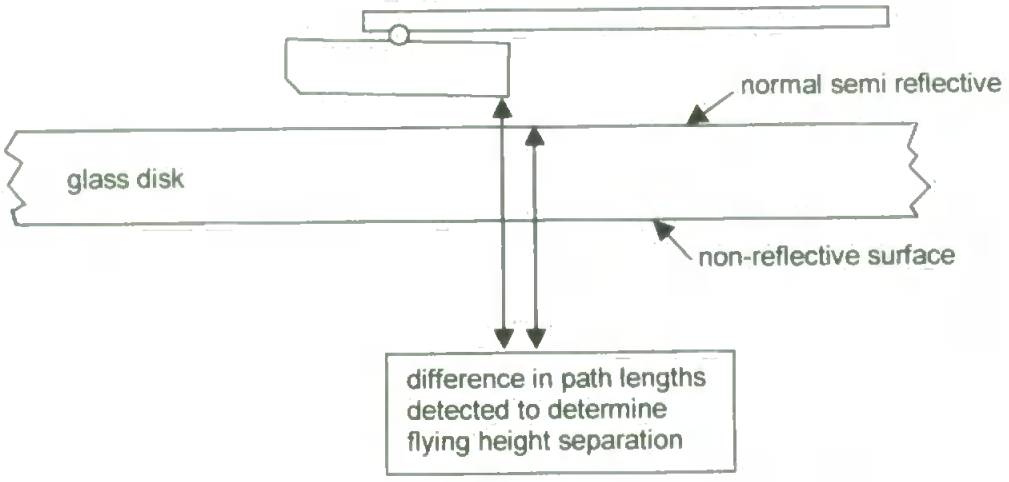

Fig. 18. System overview for differentially measuring the flying height of a glass substrate hard disk drive.

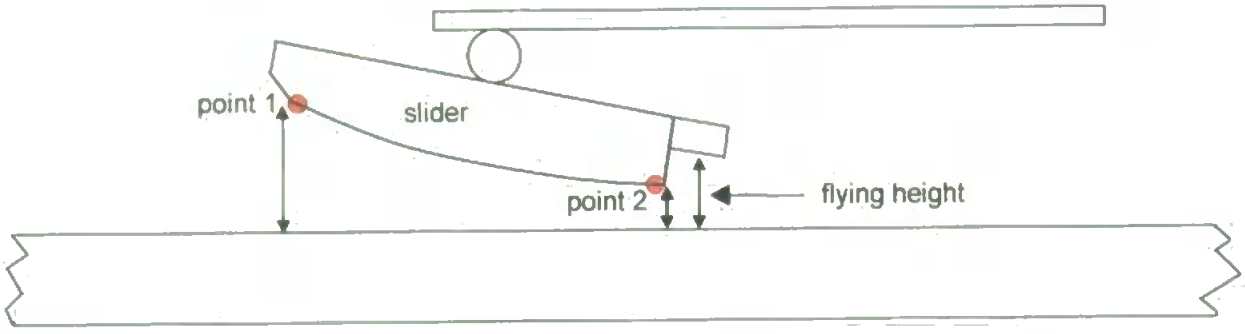

Fig. 19. Diagram showing the typical measuring points used in a conventional, such as a Phase Metrics Flying Height Tester, glass disk flying height measurement system.

It is very difficult to measure directly the head positioning [56]. This is because the head is embedded within a very small aluminium oxide, Al_2O_3, thin film at the rear of the slider. This thin film is of the order 50μm square and house both the read and the write heads, requiring an optical beam smaller than 20μm in diameter to observe it successfully. The thin film is also near transparent, posing further measuring difficulties.

3.7 Capacitance Gauge

A capacitance gauge is a sensor that measures the separation of an object through the change in capacitance due to separation variations between itself and a reference plane. The probe has a shield built around it so that the sensor part of the probe only detects the field directly beneath it. Due to the nature of a capacitor, if the dielectric constant and area of capacitor plate remain constant then the only variable that will effect the capacitance is the distance between the plates. Hence the probe can be used a means of measuring separation, [57].

These probes will be required to be built into the drive's lid in order to measure the disk and its motion. The probes also suffer from pressure fluctuations and instrumentation sensitivity due to temperature changes. Often a Wheatstone bridge arrangement is used with a reference capacitor to help counteract these problems.

3.8 Position Error Signal

The tracking error signal or position error signal (PES) can be observed to detect read/write head disturbances. When either the suspension arm or disk are vibrating the head is going to experience off track motions, as discussed in Chapter 2. This can be detected by tracking the error signal that is fed back into the servo control system, which is ordinarily used predictively to put the head back on track. This signal has been observed and frequency sweeps of vibrating the drive produced to determine areas of activity [25,34]. Certain modes are those

of the tracking system, rocking on its bearings for example, or the lateral mode of the suspension.

Method	Advantages	Disadvantages	Hub Rocking Detection
Acoustic Emissions	Unobtrusive. Real-time.	High freq sampling. Head must be in contact with disk.	No
Thermal Detection	Unobtrusive. Real-time. Inexpensive.	Small signals. Ambient temp changes. Head contact.	No
Readout Signal Analysis	Unobtrusive. Inexpensive.	Small signals.	No
Interferometry	Real-time. Commonly used in industry.	Bulky. Obtrusive. Cannot isolate rocking motion.	Yes
Laser Doppler Vibrometry	Commonly used in industry.	Bulky. Expensive.	Yes
Glass Disk Optical system	Complete slider orientation knowledge.	Bulky. Obtrusive. Artificial conditions.	Yes
Capacitance Gauge	Inexpensive. Real-time.	Temp and pressure sensitive.	Yes
Position Error Signal	Inexpensive.	Very limited direct flying height measurement.	No

Table 1. Table showing the advantages and disadvantages of potential embedded flying height measuring techniques.

Chapter 4. Piezo-Electric Sensor and Actuator Overview

4.1 Sensor and Actuator Principles

In order to measure the small movements involved with the suspension arm bending and disk oscillations, extremely sensitive, light weight, flexible sensor elements must be used. The sensor is required to monitor vibrations unobtrusively, not adversely effecting the dynamics and frequency response of the system being measured.

The piezo-electric sensor-actuator is a very accurate, sensitive form of measuring and controlling. Piezo-electric materials' physical dimensions increase when a voltage is applied to them. Expansion of the structure is proportional to the voltage applied to it [58]. By stretching a piezo-electric material, the voltage potential across it increases.

Natural materials such as quartz, tourmaline, Rochelle salt etc exhibit the piezo-electric effect, however, the effect is limited. Polycrystalline ferroelectric ceramic materials have been developed, such as Lead Zirconate Titanate (PZT), with improved piezo-electric properties.

Ceramic materials consist of many crystals, and dipoles, randomly orientated throughout. Hence, they are naturally isotropic, and yield no piezo-electric effects. The application of a strong d.c. electric field to the ceramic material will have the effect of giving the dipoles parallel alignment with the electric field. This overall alignment gives the material polarisation. When the electric field is removed the unitary alignment of the dipoles is reduced, but

retains enough alignment, whilst below its Curie temperature, to give the material a remnant polarisation and stress, see Figure 20.

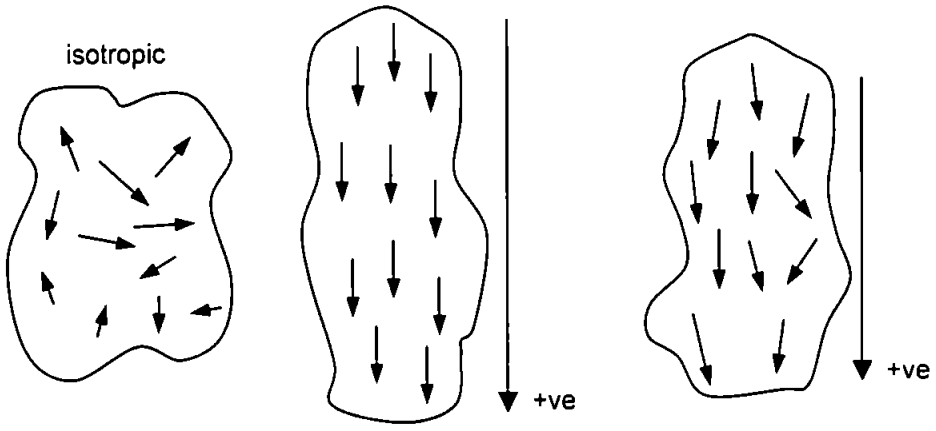

Fig. 20. Diagram indicating dipole orientation in an isotropic material, anisotropic polarised material from an applied electric field and the orientation with the electric field removed.

Piezo-electric elements can work both as sensors and actuators. However different compositions have different sensor-actuator strengths. In general if the piezo-electric has a high 'd' co-efficient it is a good actuator, and if it has a high 'g' co-efficient then it is good sensor. Some consideration must be given to how flexible the element is, and hence its Young's modulus. Any rigid sensing structure will provide an obtrusive presence to a flexible structure, which is undesirable.

The 'd' coefficient is the strain developed (m/m) per electric field applied (V/m), and hence has units of [m/V]. The 'g' coefficient is the open circuit electric field developed (V/m) per applied mechanical stress (N/m^2) giving it units of [Vm/N].

Piezo-electric notation dictates that if the element is electrically driven (or sensed) throughout its *z* plane (3) and its deformation is in its x plane (1) the element is described as d_{ab} where a in this case is 3 and b is 1, hence d_{31}. Figure 21 shows a 3-dimensional representation for piezo-electric notation.

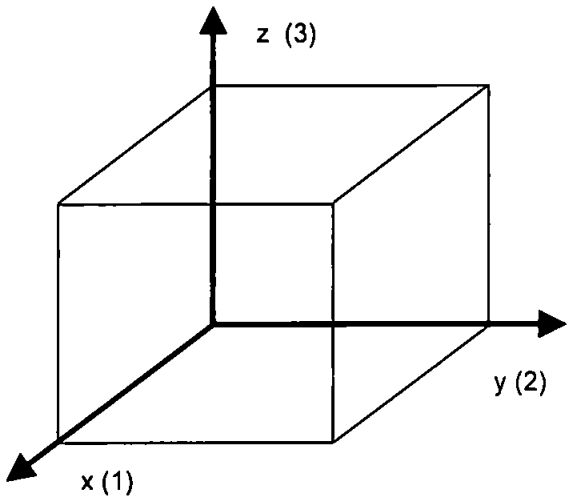

Fig. 21. Diagrammatic representation of piezo-electric structure and orientation of planes.

Piezo-electric elements for sensing and actuating are available in many physical and geometric forms, but only those of 'plate' form are considered here for the use in hard disk drives. Typical dimensions would be 1 - 2mm square. The thickness would be < 0.2mm, depending upon the material itself, ie whether it is ceramic or polymer.

A plate piezo-electric sensor-actuator is extremely thin and therefore not as obtrusive as the other forms of piezo-electric sensors and actuators. It makes for an efficient sensor, being greatly thinner in the *z* plane (3) than its x (1) or y (1) planes. This provides the piezo-electric with good (3,1) and (3,2) characteristics. Hence, if the piezo-electric element is being used as a sensor then deformation throughout its width or length, ie when it is bent, will yield a high

output voltage on its (3) surface, through the sensor measuring the average induced strain. This is perfect for sensing cantilever bending, as the cantilever is deformed the structure will be bent throughout its x or y axis providing a measurable voltage variation. Normally, providing the plate is geometrically symmetrical in form, the plate will have equal $_{31}$ and $_{32}$ properties. Therefore orientation of the sensor is not critical, but it must be parallel to the cantilever and located at the point of maximum strain.

Tubes and cylinders are tuneable in length. The cylinder is extended, by virtue of the electrodes being mounted on the cylinder's circumference. In essence the cylinders' z extension is related to the voltage applied radially. This makes tubes better as actuators then sensors.

Stacks are in essence multilayer structures created from the overlaying of plates together. This creates a 'thicker' structure than a plate. The form of the stacked piezo-electric device is cuboid, to varying extents of 'squareness'. The stack is created from layers of plates to achieve a thicker z dimension. This allows for much superior actuation by virtue of the multiple plates being coupled to multiply their actuation properties. For this reason it is possible to use a stack with a far lower supply voltage then that of a single actuator, of identical proportions, for a given level of actuation. The stack has good d_{31} and d_{32} properties but poor sensing properties compared to the plate, due to the obtrusive nature of the increased stiffness from multiple layers. Actuating the piezo-electric layers proves difficult in practise due to the conductive layers being obscured by the overlapping layer.

Poly vinylidene flouride PVDF* was chosen for the task of sensing suspension arm and disk movement because of its excellent induced voltage to deformation properties, g_{31} and g_{32} which are in excess of twenty times greater than that of ceramic elements and because of its low Young's modulus. The plate configuration, being the optimal sensing structure for cantilever deformation bending, was hence chosen for this task.

4.2 Piezo-Electric Actuation of Suspension Arm

A lead zirconate titanate, PZT, plate was chosen for actuating the suspension arm. PZT plates make good actuators having good d_{31} and d_{32} properties. The PZT plate actuator has a higher Young's modulus than the PVDF plate.

When a voltage is applied to a piezo-electric actuator it deforms in a known way. This can be used to actively distort the suspension arm so as to alter and control the flying height of the read/write head for a hard disk drive. If the suspension arm is vibrating, ideally the actuator can be driven 180° out of phase with the suspension arm motion to suppress the effects of vibration, a form of active damping [59,60]

4.2.1 Actuator Location for Optimal Control

Where the piezo-electric actuator is bonded to the cantilever to be controlled is critical. It has been found by Crawley and Luis [61] that the most

* ATOFINA Chemicals Inc.'s KYNAR® PVDF, http://www.atofinachemicals.com/kynarglobal/

effective location for the piezo-electric actuator is near the root of the cantilever, the first quarter of it. At this point the deflection at the tip becomes optimal, shown in Figure 22.

Fig. 22. Diagram showing how the position of the piezo-electric actuator on the cantilever is critical for maximum head control.

As the actuator bends the arm is deformed in an arc, this causes the tip of the arm to be displaced. The further the actuator is from the tip of the arm the greater the resultant displacement will be. The arm's deformation due to the actuator's growth induces a moment in the arm, such that any force applied to the tip of the arm will create a torque counteracting the actuator's motion. The un-actuated section of the arm acts as a lever, amplifying both the motion of the actuator and the load it is subjected to.

It has also been found [62] that there is an optimal actuator/cantilever thickness ratio. This is related to the Young's modulus of the materials being used. The piezo-electric actuator requires a reasonably rigid base (cantilever) to operate on to provide good purchase for deforming the beam. Experimentation [63] with cantilever thickness has shown that if the cantilever is too thin and flexible, the actuator deforms without pressing the tip of the cantilever down.

The bonding layer between the actuator and the cantilever is also important to the systems performance. It has been found that to optimise the system the bonding layer needs to be as thin and as rigid as possible [64].

To put all of this into a practical context, the suspension arms fitted as standard to most hard disk drives, and used in this research, are constructed to be rigid throughout their entire length except the first quarter. This is near to perfect in the respect for applying a piezo-electric actuator to it. The suspension arm used was constructed from 0.1mm thick sprung stainless steel. Stainless steel cantilevers have been found to work best, with single sided piezo-electric actuators, when the actuator's thickness is 80% of the cantilever's. This dictates that an optimal actuator would be 0.08mm thick. In practise, [63], it has been found that having an actuator with greater cross sectional area is far more efficient than one too thin. Hence an actuator 0.08mm or greater will be useable. Figure 20 shows a diagram of a typical suspension and tracking arms. It can be seen that the flexible root of the suspension arm is 0.1mm thick, 2.35mm long and about 4mm wide. The rigid part of the suspension arm is a further 13.7mm long with a 0.4mm lip at either edge. This creates a cantilever with a total length of about 15mm with the first 2.35mm being flexible. This means that the piezo-electric actuator must be mounted on the first 2.35mm. This is not quite at the quarter of the cantilever's length, but is a good approximation.

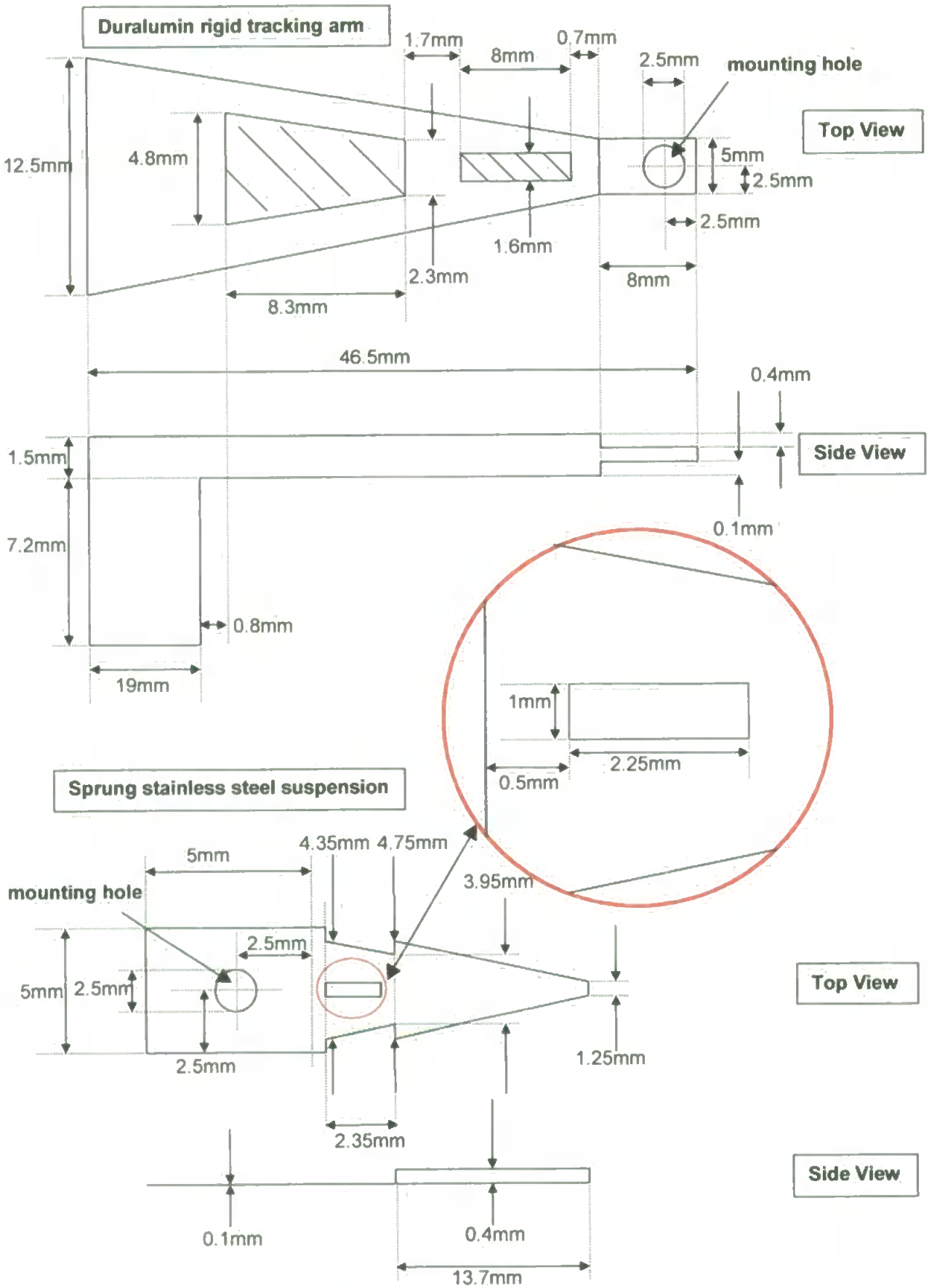

Fig. 23. Diagram showing the dimensions of typical tracking and suspension arms for a 3.5" disk drive. The suspension arm is attached to the servo via a rivet through the mounting hole.

Chapter 5. Vibration Testing Equipment

5.1 The Electrodynamic Shaker

A test facility has been constructed by previous students to allow the hard disk drive to be vibrated over a 10kHz bandwidth at accelerations of up to 50g (where g is the unit for acceleration due to gravity, $9.81ms^{-2}$) [65,66,67], this is depicted in Figure 24. The hard disk drive is rigidly clamped to an aluminium plate and is vibrated by an electro-dynamic shaker, Environmental Equipments Ltd type 1501. The axis of vibration is arranged to be through the spindle of the drive so as to resemble, closely, a drive mounted in a desktop PC experiencing vibration, and to exaggerate the suspension arm's and disk's fundamental modes of resonance. A piezo-electric accelerometer sensor mounted to the plate, see Figure 25, monitors vibrations experienced by the drive, and also provides a feedback signal, which is amplified. It is therefore critical to ensure that the disk drive is solidly mounted to the plate, and in turn the plate to the shaker. It is also extremely important for meaningful results that vibrations detected by the accelerometer match closely with those experienced by the drive. For this reason an improved design of plate and mountings were constructed, since it was suspected that the previous design was not optimum in this respect.

The shaker drives the plate from the centre with the accelerometer mounted at one of the edges and the drive in the centre. With the initial design of plate and mounting, the signal from the accelerometer proved difficult to recover due to the large amount of noise. The noise was reduced somewhat by damping the plate with an adhesive visco-elastic damping sheet and a low pressure gas

damper, which significantly improved the signal-to-noise ratio. It was found that additional noise was induced into the system due to deformation of the mounting plate. The accelerometer was re-mounted closer to the drive and this was found to improve significantly the signal-to-noise ratio. Therefore it was deduced that the accelerometer was experiencing a different displacement to that of the drive, due to the plate flexing, depending on the positioning of the accelerometer.

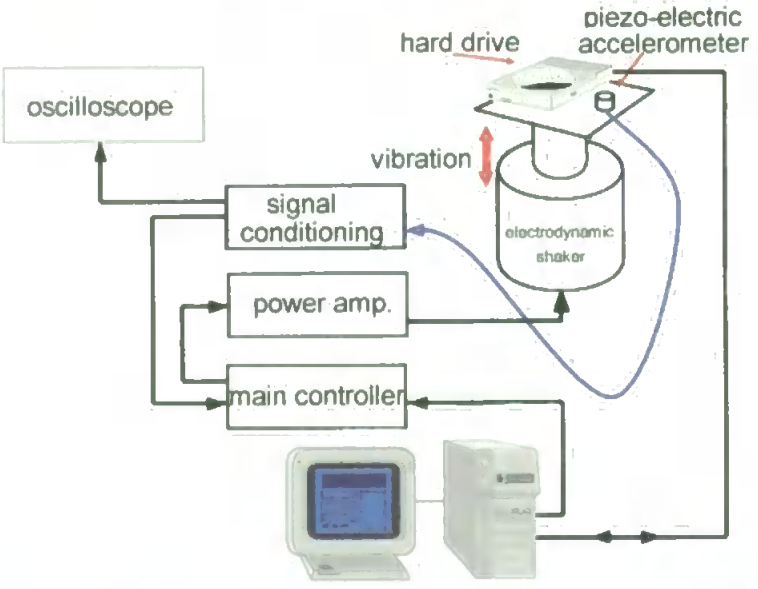

Fig. 24. Block diagram depicting the overall system used to test disk drive performance whilst subjecting the drive to various schedules of vibration.

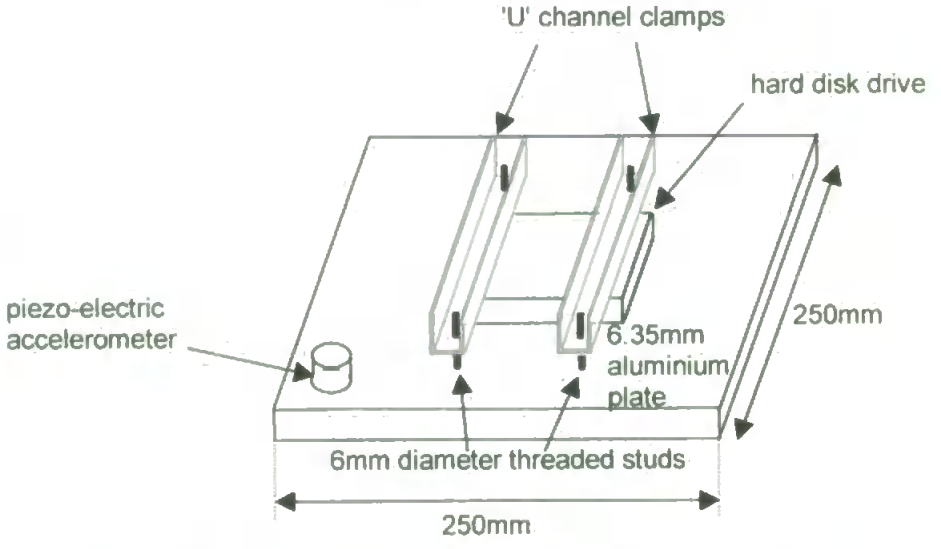

Fig. 25. Diagram detailing the original test system hard disk drive mounting.

To counteract this a number of modifications were made to the plate, as detailed in Figure 26. Firstly, the plate was made a lot smaller, only slightly bigger than the drive. This also has the benefit of reducing the load on the shaker. The accelerometer was then mounted as close to the drive as possible. Finally, a new mounting system was devised that held the drive more rigidly. The drive was mounted in such a way that its body is used to reinforce the plate rather than being 'sandwiched' in a vice like clamp. Finally, the data bus and power leads were re-routed to avoid them making contact with the plate, reducing any external interference to the plate.

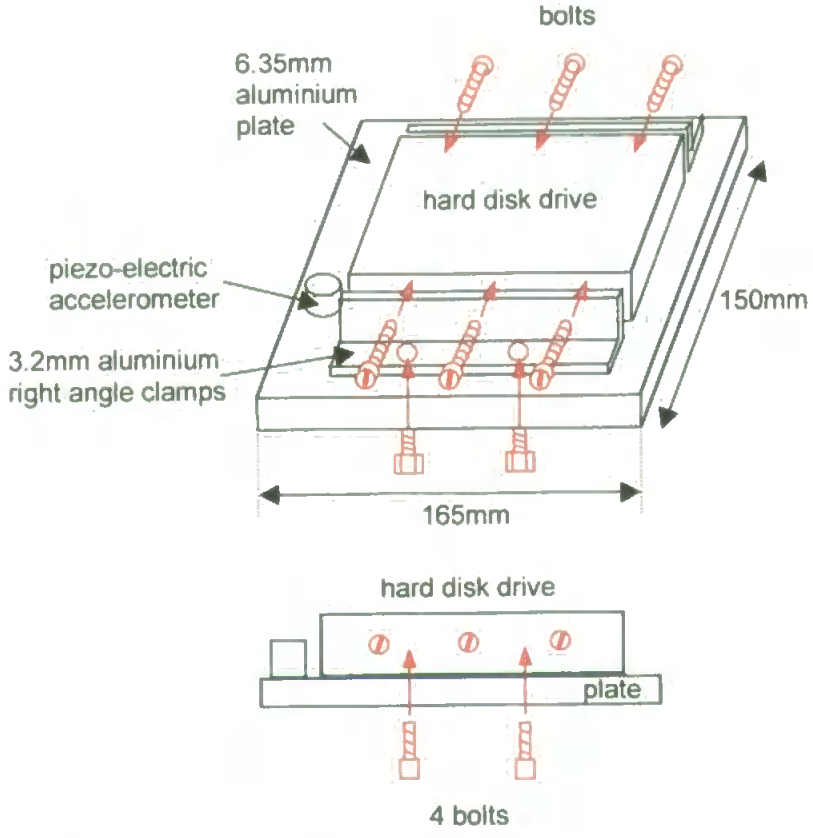

Fig. 26. Diagram showing the revised hard disk drive mounting plate for the vibration test rig.

5.2 Shaker Control System

A block diagram of the system used to test hard disk drives under vibration is shown in Figure 24. The whole apparatus is located in a laminar air flow bench, a Laminar flow systems Ltd Lamarflo, that provides a positive pressure, filtered air source. This ensures that the local environment is free of contaminates that could potentially damage any drive operating without its lid. A personal computer (PC) is used to control the sweeps of vibration and acceleration that the drive receives.

Whilst the drive is vibrated, the control PC is able to transfer data with it, whilst simultaneously monitoring the time taken for the data to be correctly transferred. Software, developed by Jepson [67], enables the control PC to transfer a file comprising solely of '1's, '0's or a pseudo random file to the drive under test. Another facet of the software is its ability to allow selection of the data transfer direction. The performance of the drive can be accessed whilst data is either read directly from the drive, or written to the drive. In the case of the latter, the data must then read back to confirm that the data was correctly written. As will be detailed later, the transfer rate of a drive is found to be dependent on the frequency and acceleration at which it is being vibrated. As the magnitude of vibration increases the drive's transfer rate slows down, eventually leading to total data transfer failure. This is the result of the error-correction system being progressively defeated, and calling for increasingly more track re-reads.

The Environmental Equipments Ltd 1531 power oscillator is used as a final stage amplifier that is capable of providing a driving source for the shaker of frequencies of up to 10kHz and sinusoidal accelerations of up to 50g. The power

amplifier can accept an external input or provide sinusoidal waveforms. It has been discovered, [68], that sinusoidal waveform sweeps for testing are:

- Time consuming
- Prone to over-stress mechanical components due to resonance
- Not an accurate reproduction of vibration conditions

A white noise generator, Marconi Instruments LTD TF2091B, with a bandwidth far in excess of that of the shaker, was used as an external input for the power amplifier that drove the shaker. This allowed for quick testing of the hard disk drive, and reproduced the more random nature of vibration that the drive would experience in its normal operating environment.

Software, written using the basic input/output system (BIOS) commands, controls which sector, track and head is used to read or write data. The software was written using C and created a powerful analysis tool. It enabled the drive to be tested with the head positioned at different circumferential points on the disk. Without the ability to do this, data would be simply transferred to the disk at indeterminate places, reducing the validity of any results.

The software makes use of the PC's interrupt routines, in this case the 13H disk commands, see Table 2. These commands allow direct control of the drive such as reading or writing to a given sector and track on the disk. This method of drive control is known as cylinder-head-sector, CHS, newer systems use the logical block address, LBA, system. A cylinder is a given track on each side of the disk, and for every disk in the drive. Once the head has been chosen, a given, individual, track on the drive can be observed.

To test the drive's operation under vibration, a chosen track and sector was written to with a known pattern of data. That track and sector was read back

repeatedly, whilst the drive endured vibration sweeps, with the read back data buffered in RAM and displayed on the monitor. The chosen read/write commands performed were devoid of error correction routines, other than that of the drive's on-board hardware, and returned a generated error correction code (ECC). This code is used by the PC's drive controller for error correction, but was used in these tests to observe the performance of the system. Any change in this code would indicate a data transfer error. The read back data pattern, generated error correction code and the returned drive status flag were observed throughout the vibration sweeps. When the drive failed to transfer correctly data, indicated by specific error correction codes, the drive status flag returns a code number identifying the reason for failure, as shown in Table 3.

00H	Reset Disk System	0CH	Seek
01H	Get Disk System Status	0DH	Reset Fixed Disk System
02H	Read Sector	0EH	Read Sector Buffer
03H	Write Sector	0FH	Write Sector Buffer
04H	Verify Sector	10H	Get Drive Status
05H	Format Track	11H	Recalibrate Drive
06H	Format Bad Track	12H	Controller RAM Diagnostic
07H	Format Drive	13H	Controller Drive Diagnostic
08H	Get Drive Parameters	14H	Controller Int. Diagnostic
09H	Initialise Fixed Disk Characteristics	15H	Get Disk Type
0AH	Read Sector Long	16H	Get Disk Change Status
0BH	Write Sector Long	17H	Set Disk Type

Table 2. Table of PC BIOS commands for the disk control interrupt routines.

00H	No error	0DH	Invalid no. of sectors on format (H)
01H	Invalid command	0EH	Cont. data address mark detected (H)
02H	Address mark not found	0FH	DMA arbitration level out of range
03H	Disk write-protected (F)	10H	Uncorrectable CRC[1] or ECC[2] error
04H	Sector not found	11H	ECC corrected data error (H)
05H	Reset failed (H)	20H	Controller failure
06H	Floppy drive removed	40H	Seek failed
07H	Bad parameter table (H)	80H	Disk timedout (failed to respond)
08H	DMA overrun (F)	AAH	Drive not ready (H)
09H	DMA exceeded 64KB	BBH	Undefined error (H)
0AH	Bad sector flag (H)	CCH	Write fault (H)
0BH	Bad track flag (H)	E0H	Status register error (H)
0CH	Media type not found (F)	FFH	Sense operation failed (H)

Table 3. Drive status return codes from disk control interrupt routine commands. (H) Hard disk drive, (F) Floppy disk drive.

[1] Cyclic Redundancy Check code

[2] Error Checking and Correcting code

5.3.1 Measuring Suspension Arm Movement using a PVDF Strain Gauge

All systems, when subjected to vibration, can go into resonance and hard disk drives are no exception. Therefore it is necessary to characterise fully data-transfer failure mechanisms. In order to do this, sensors have been incorporated within the hard drive housing to try to gain a more complete understanding of mechanical movements. However, it is important that the sensor system utilised is

unobtrusive. Hard disk drives are hermetically sealed to prevent dust contamination damage and this dictates that the *working* environment must be retained when applying sensors. Measuring the drive's internal components with the cover removed effects the drive's performance, [69]. With the cover secured an air cushion is created changing the natural frequencies of the components being measured, through damping. With the cover removed this damping is lost.

To measure the bending of the suspension arm a thin (110 μm) sheet of Poly Vinylidene Fluoride, PVDF, piezo-electric polymer sensor was bonded to the suspension arm to measure the average induced strain. The PVDF polymer membrane used was supplied by Precision Acoustics Ltd* with gold electrodes deposited on both sides. The sensor was cut from the sheet in the required shape, Figure 27, using a sharp scalpel. To ensure that a sort circuit between the two gold electrodes was not produced from the incisions, the electrical resistance between the electrodes was measured using an ohmmeter, and checked to maintain a resistance in excess of 20MΩ. The sensor was bonded to the suspension arm using a layer of Electrolube's silver conductive paint type number SCP03B, with a surface resistivity of 0.03Ω/square. This electrically connected the negative electrode of the sensor to the suspension arm and provided a flexible, thin and strong bond. After bonding the electrical resistance was checked to ensure that a short circuit was not present. If the silver conductive paint was found to have bridged the sensor's two gold electrodes then the electrical bridge was removed using a sharp scalpel. Finally the positive electrode of the sensor was connected to a signal wire connected to the data acquisition card. Co-axial wire, RS single core screened wire (part number 367-202) was used throughout for the hard disk

* Precision Acoustics Ltd, Poundbury House, Dorchester, Dorset, England. DT1 2PG

drive's novel internal sensors to minimise induced noise transmitted from the drive's control electronics. The co-axial wire has a conductor comprising 7 strands of 0.1 mm plain copper, it is poly vinyl chloride (PVC) insulated, lap screened and sheathed overall with PVC. It has a core to screen capacitance of 80 pF/m and a core to core capacitance of 83 pF/m. Where the signal wire connects to the sensor the wire was stripped 10mm of its outer sheath. The co-axial wires were twisted and bonded to the relevant sensor or ground point. The inner sheath was stripped 6mm and the multi-strand signal wire was cut to leave just one strand of wire. This wire was then bonded to the sensor, again using silver conductive paint. Using just one copper wire, of 0.1mm diameter, incurred a minimum obtrusion to the sensor and sensed structure, due to its minimal rigidity. To aid noise cancellation, an extra signal wire was carefully routed into the drive to replicate the signal wires connected to the sensors. The extra wire is subjected to the same noise environment as the signal wires, allowing for noise reduction through differentially measuring this and the signal wire.

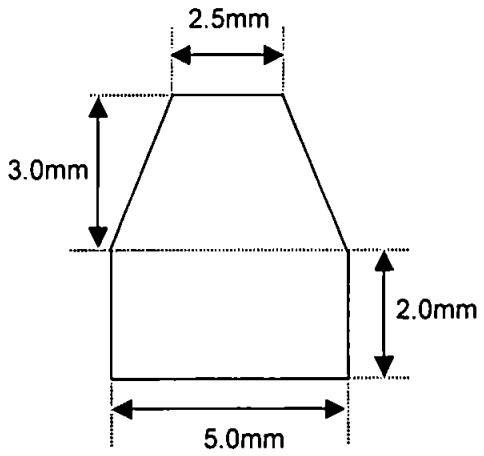

Fig. 27. Diagram showing the shape and dimensions of the PVDF suspension arm deformation sensor.

In order to mount both a sensor, and for future work an actuator, to the suspension it was necessary to bond the sensor and actuator to the bottom and top side respectively of the suspension arm. Bonding to the bottom side of the suspension arm proved to be impossible with the physical restrictions of the disk obscuring the underside. Therefore it was necessary to remove the suspension arm pack to allow unhindered access. When handling the suspension arm pack every care was taken to ensure that no contamination of the heads or arms is encountered through dust particles in the air. The laminar air flow bench was the source of contaminate-free air for working on the drive.

Another problem involved with removing the suspension arm assembly is created by the suspension arm's spring nature and the thickness of the disk. To remove the assembly it must be twisted to allow the heads to approach the edge of the disks. If the heads are pushed off the edge of the disk then the spring pressure from the suspension arm is great enough to force the heads together violently in a destructive manner. To prevent any damage a special tool was fabricated, see Figure 28. It was made from fibreglass, which is soft enough not to abrade the suspension arm and create micro-contamination. The tool is specially shaped such that it slots onto the disk and when the heads are pushed off the edge of the disk, uses the suspension arm to ramp the heads gently off the disk.

The coaxial wire, which was connected to the sensor, was bonded to the suspension arm allowing it to pivot at the same point as the arm pivots, as depicted in Figure 29. This prevents the problem of the voice coil motor not having enough torque to allow the suspension arm to track correctly across the disk.

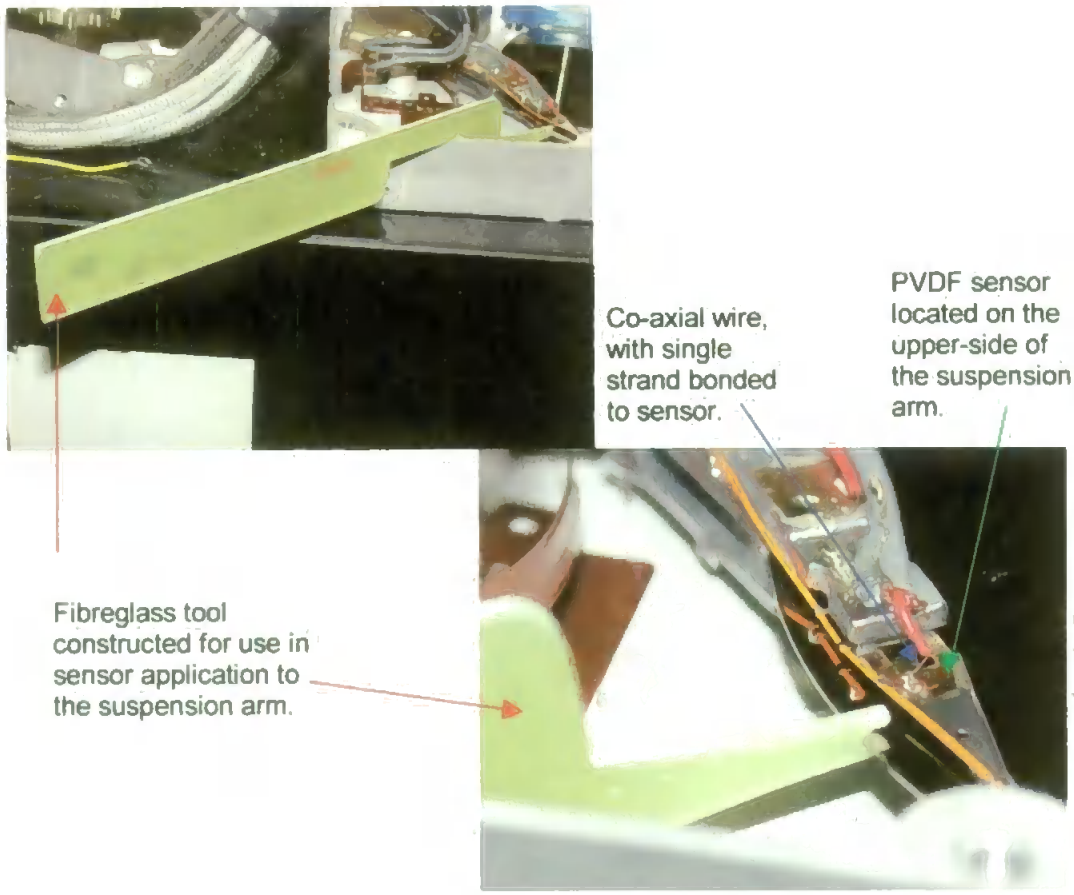

Fig. 28. Pictures of the fibreglass tool specially constructed to aid sensor application.

Since it is intended to extend this work to include active control of the head's flying height, see Chapter 11.3 Further Work, a further piezo-electric actuator was also mounted on the top of the suspension arm. Figure 30 shows the suspension arm with the actuator and sensor bonded to it. Tests show that the actuator has a minimal influence on the arm's mechanical characteristics.

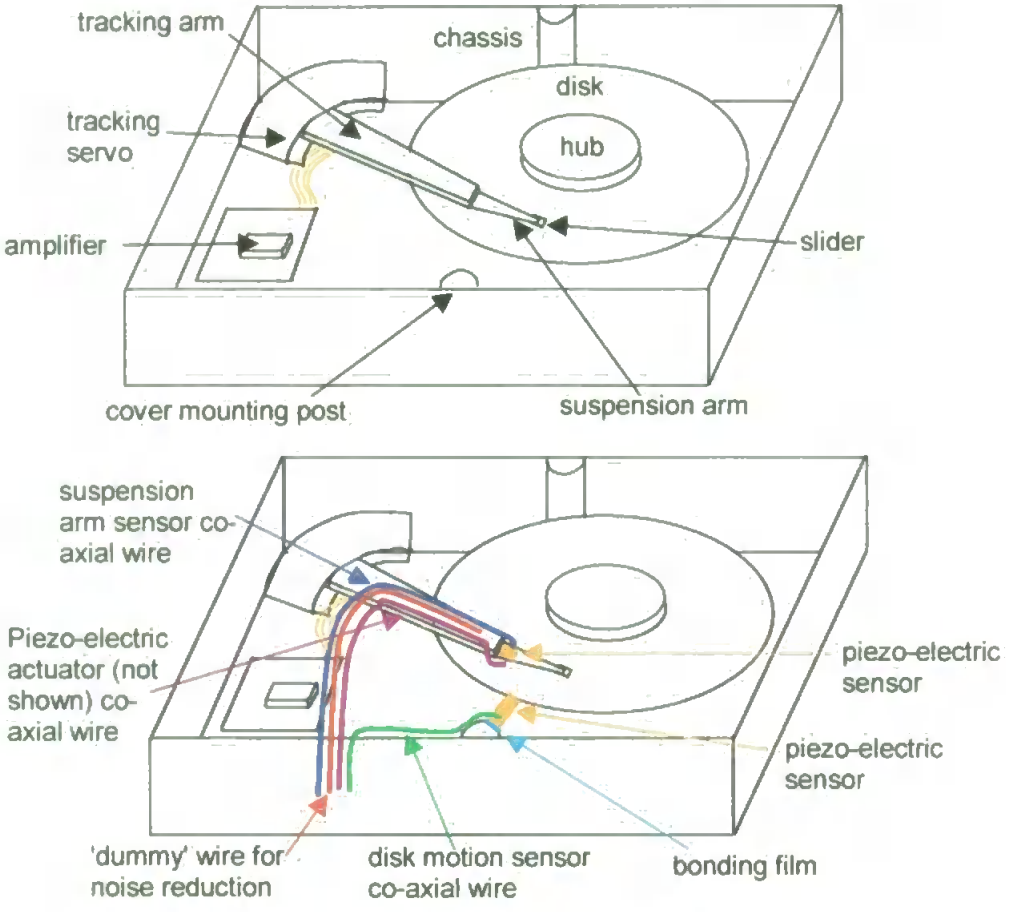

Fig. 29. Diagrams representing sensor positions in the hard disk drive.

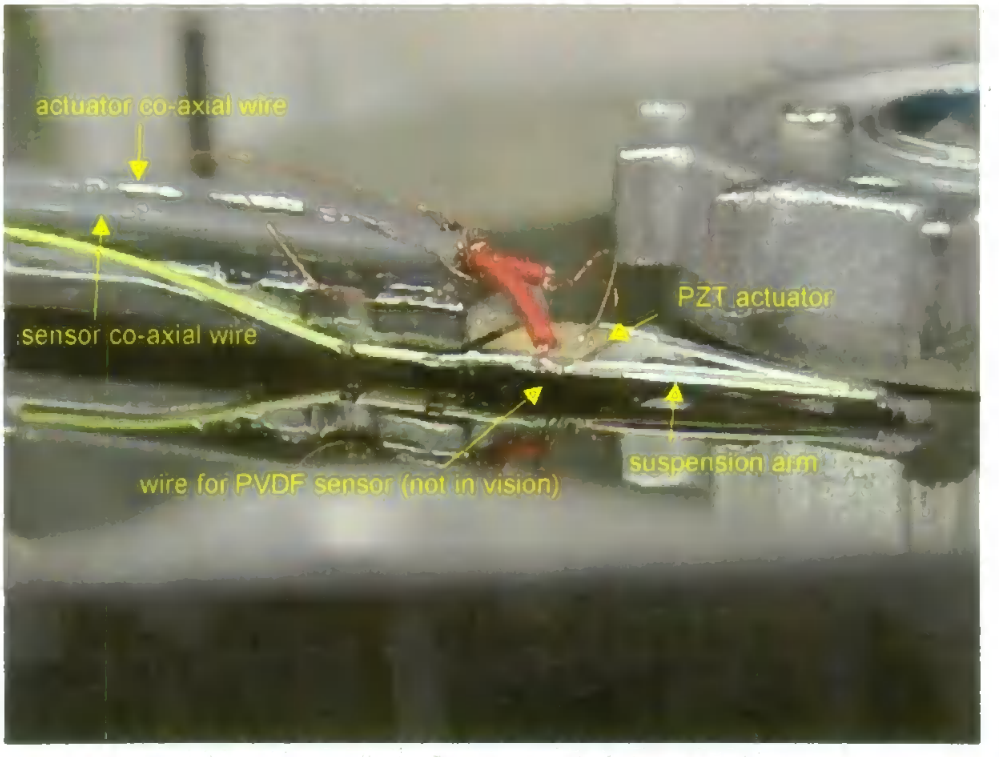

Fig. 30. Inside a modified hard disk drive. The piezo-electric element bonded to the top surface of the suspension arm is used for actuation (see text). On the lower side of the arm is the PVDF sensor.

5.3.2 Measuring Disk Movement Unobtrusively using PVDF Cantilevers

Measuring the disk movement is somewhat difficult as the rotating disk has many modes of resonance, both radial and circumferential.

It is necessary to measure the disk displacement and its spectral content to isolate disk and suspension arm movement. This will further the understanding of data-transfer failure mechanisms. The sensor located on the suspension arm will identify when it is moving, however movement due to tracking the disk resonance will need to be determined. Therefore a sensor need only measure the displacement of the disk in the region where the head is positioned above the disk. Using software that utilises BIOS commands it is possible for the head and suspension arm to read data from any chosen track on the disk. The BIOS commands enable the data to be transferred from the drive at a chosen cylinder, head and sector. Therefore, the head was placed at the outer edge of the disk to be positioned at the position most sensitive to disk fluctuations.

A further PVDF sensor was created, from the same material as the sensor discussed in 5.3.1, and used to measure the edge displacement of the disk due to flutter. This time the sensor used was in a cantilever configuration, with one end rigidly bonded to the drive chassis in a manner that pre-tensioned the cantilever against the disk, as shown in Figure 31. Any movement of the disk would change the strain induced in the cantilever. By pre-tensioning the cantilever a constant strain is induced, yielding a static dc offset. As the disk moves up or down then this voltage changes synchronously, enabling direction and displacement to be determined.

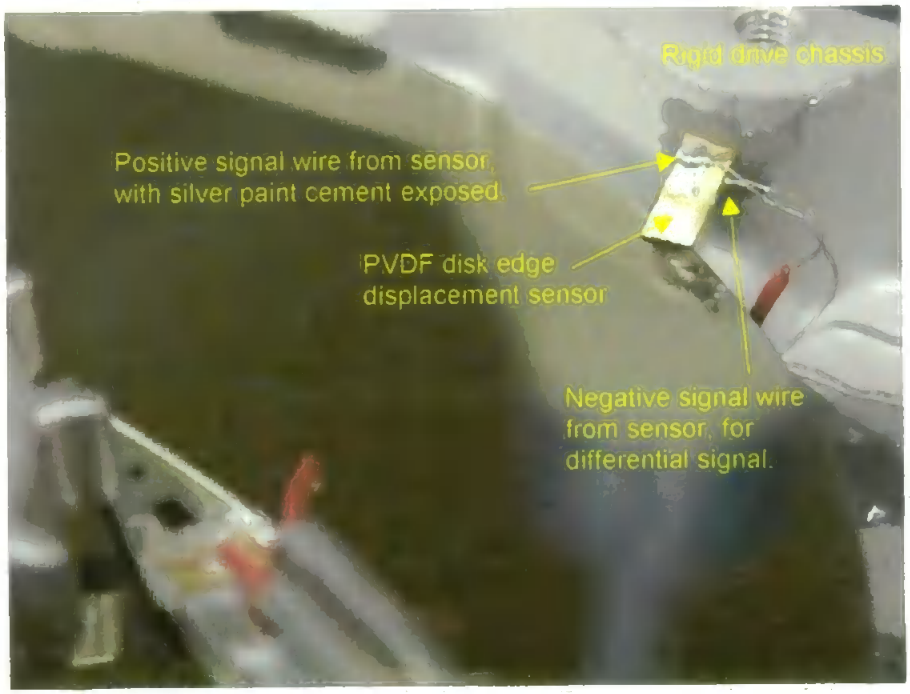

Fig. 31. A PVDF thin film 110μm polymer sheet has been bonded to the drive in a manner such that it is pretensioned. Note that it is positioned at the outer edge of the disk.

The bonding of the sensor to the drive's chassis needed to provide a rigid base for the sensor and locate the sensor near the head for meaningful results. Failure to position the disk sensor near the head would result in out-of-phase measurement of the head-disk variations. Failure to provide a rigid base for the cantilever would reduce signal strength and add noise due to its base resonating. One of the mounting posts for the lid is located close (4.0mm) to the slider and represents the greatest cross-sectional area of the chassis. The cantilever therefore required a minimum of 4.0mm span. However, due to the requirement of pre-tensioning the sensor the overall length is greater, 7.0mm, and is 4.0mm wide and rectangular in section.

The bonding medium used is Araldite Professional epoxy resin. This adhesive has resistance greater than 20MΩ and therefore does not electrically

connect, significantly, the sensor to the drive and hence does not earth the negative electrode of the sensor. This demands two wires to be connected to the sensor, one to the negative electrode and one to the positive electrode, in the same way as for the suspension arm sensor. The other end of the cantilever is in constant contact with the disk, but is not bonded in any way. The disk's surface is lubricated and finely finished to allow rotational freedom for the disk motor to spin the disks. The wear on the sensor proved insignificant throughout the tests undertaken. The negative electrode is therefore left in contact, both physically and electrically, with the disk. The resistance between the disk and earth was found to be approximately 3kΩ, due to the disk coatings and electrical resistance through the disk pack motor and spindle. Therefore the gold thin film negative electrode of the sensor was removed in the region of contact with the disk, and checked to give a total resistance in excess of 20MΩ.

5.4 Small Signal Measurement

A virtual instrument has been designed and implemented using National Instruments LabView for Windows software [70]. LabView for Windows is an industry standard software environment designed to allow virtual instrument to be graphically built using its G language [71]. The software has been designed to monitor one channel, using a differential input to reduce noise, and display it in the time domain. The software also enables a simultaneous real-time Fast Fourier Transform (FFT) sweep to display the spectral response in the frequency domain. Figures 32 and 33 shows the front-end virtual instrument created and the software behind it, a full size diagram of the front-end and code are included in the

Appendices. To reduce noise and build up a complete understanding of the frequency response of the component being measured, several FFT sweeps are undertaken to produce an average. Upon completion of using the software a snapshot of the last displayed FFT frame is saved so that the results can be recorded. The data is streamed off in a suitable form to allow Microsoft's Excel to reproduce the results easily in a manageable graphical form.

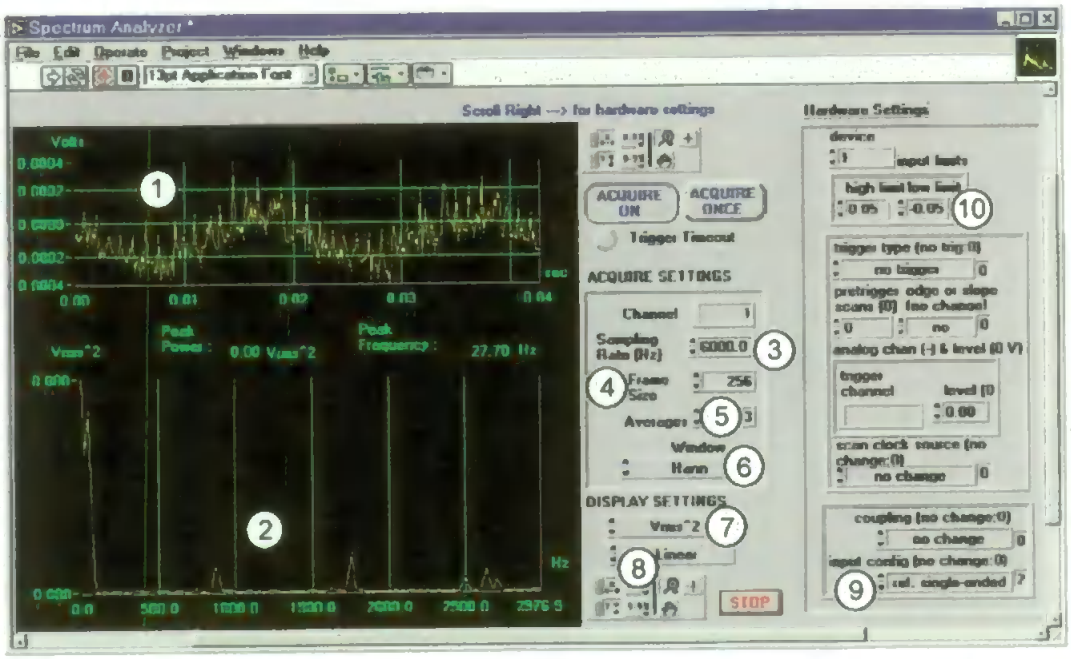

Fig. 32. Screenshots of the virtual instrument created from LabView for Windows. The text refers to the numbered regions.

The time domain trace, obtained in real-time, is displayed (1) on the screen and can be quickly scaled to allow for greater detailing of signal for accurate measurement or to give more insight to any dc offsets. The time domain signal is transformed and displayed as a frequency sweep (2). This graph is capable of scale adjustment enabling areas of interest to be 'zoomed' in, revealing greater frequency detail of the signal.

The sampling rate of the signal can be chosen (3). This dictates the maximum frequency of observed FFT signal, Nyquist theory stating that the required sampling frequency must be at least twice that of the highest frequency of interest. Shown in this example, Figure 32, the sampling rate is 6000Hz and the highest displayed FFT frequency is 2976.9Hz. The greater the frequency the less the accuracy for a given number of samples. The number of samples taken (4) can be adjusted to gain accuracy, at the expense of computational time. A number of FFT sweeps can be averaged for a more accurate review of the system's frequency sweep (5). The negative aspect of this is increased computational time and reduced refresh. This detracts from the system's real-time capabilities.

The FFT sweep graph can be filtered in a number of ways (6), including Hamming and Hann windows [42]. The *y* axis of the FFT graph (7) can also be scaled accordingly, such options are: Vrms, Vmean, $Vrms^2$, $Vmean^2$. $Vrms^2$ was used extensively as it exaggerated any resonant peaks allowing easier determination from the noise floor. The *y* axis of the graph can also be scaled (8) either linear, dB or dBm. Linear was used in general, as this further enhanced the resonant peaks.

The input can be configured to accept either single signal output sensors, differential output sensors and earthed connectors. The correct input configuration (9) was chosen depending on the sensor used. The signal level can be defined (10). The DAQ has an internal signal amplifier, the level of amplification depends on the signal range entered, +/-10V, +/-5V, +/-500mV and +/-50mV. The signals detected were in the 50mV range and limited the system to a resolution of 24.41μV.

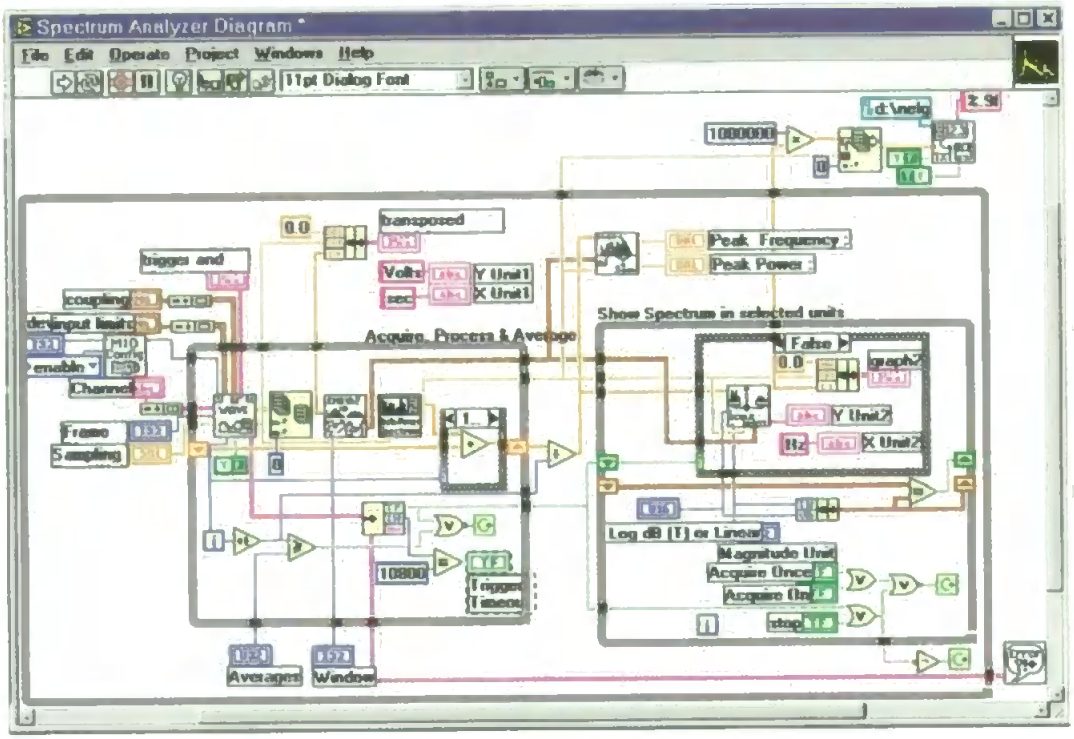

Fig. 33. Diagram used to generate the LabView instrument front end panel.

One disadvantage of this form of analysis is that the values recorded cannot be easily related to physical displacement. This means that any peaks in activity are relative to each other but their displacement is unknown.

A 12-bit data acquisition board (National Instruments PCI 6024E), capable of sampling the signal at up to 200 kHz, with a resolution of 24.41 μV, was used in conjunction with the LabView software to enable up to 8 differential analogue inputs to be monitored. The board also incorporates digital inputs and outputs as well as analogue outputs.

In order to optimise the system the signal-to-noise ratio must be maximised through the reduction of noise in the system. The data acquisition (DAQ) card is designed to work with the peripheral component interconnect (PCI) bus commonly used in PCs. The DAQ card is subjected to noise from its internal location within the PC, the card's noise level is known to be sensitive to its

position, [72]. In order to help minimise the noise the data acquisition card was mounted in the PC in a slot at least one slot away from any adjacent boards. As a matter of course the card was mounted in all the motherboard slots to confirm that the chosen one minimised measured noise. The change in noise level associated in motherboard slot position was not found to be greatly significant. The lead trailing from the back of the data acquisition card to the connector board was also shielded. A fine mesh shield was used to wrap the lead along its entire length from the back of the PC to the break out board. The mesh used was Warth International Ltd's Zemrex shielding strip*. The earth point on the break out board was then used as the central earth location and all earth connections were routed in a star configuration from this point. Hence, the shield along the lead was connected to earth at the break out board's earth point. This was found to minimise noise.

There are two PCs in this system, one controlling the hard disk drive under test, the other used to monitor the drive, as shown in Figure 34. Both of these contribute to noise generation. The PC controlling the drive powers the drive via +12V, +5V and earth. Therefore, the drive under test is connected to the electrical earth via a different source than from the monitoring PC. The drive chassis is directly connected to the electrical earth of the control PC, as are the embedded sensors. The DAQ card is electrically connected to earth via the monitoring PC. It was empirically found that the variation in voltage between the sensors' and DAQ card contributed to noise and was minimised through connecting the drive and shaker plate to the electrical earth point on the break-out board, adding to the star network at the break-out board. Care was taken to minimise the earth loop, with

* Warth International Ltd, Birches Industrial Estate, East Grinstead, West Sussex. RH19 1XH

all hardware connected to one electrical supply point via a multiple terminal adapter.

One serious problem with the apparatus was its susceptibility to external noise. The greatest source was in fact from the PCs themselves. To minimise the noise induced into the system it was found that re-positioning and turning off the visual display units (monitors) suppressed noise to a reasonable degree. Even the lead from the monitor to the PC was found to be critical.

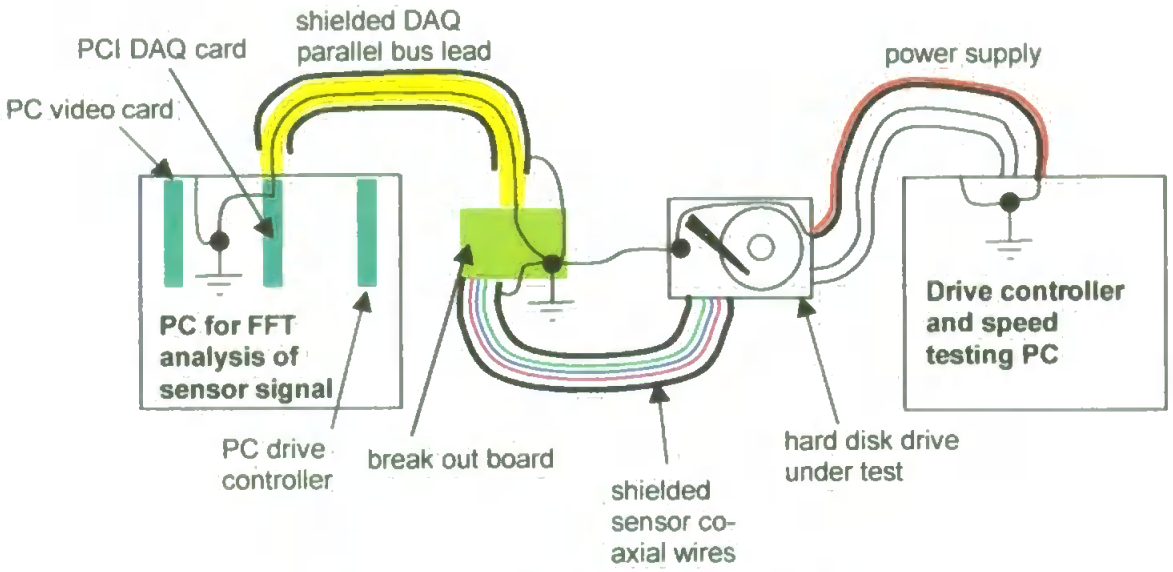

Fig. 34. Block diagram of the test and data acquisition

5.5 Measurement Methodology

To discover the frequency response of the disk, several tests were conducted. Initially, to determine the disk's natural frequencies, a typical 1.25mm thick disk was tested using a manually-controlled impact hammer with a small piezo-electric accelerometer mounted to the disk. Brüel & Kjær vibration analysis equipment was used for determining the frequency response of the disks

throughout these tests. For the next test, the disk was mounted to the shaker, with a clamp of similar dimensions to that used in a real hard disk drive, and driven with a white noise signal to obtain the disk's frequency response. The tests were carried out with two disks of identical manufacture to discover if manufacturing tolerances are significant. The disks were mounted as they would be in a real hard disk drive. A clamp was constructed with identical dimensions to the one used inside the drive.

To check the validity of the results obtained from using the accelerometer, an optical system developed by Katsikis, [73], was adopted to measure the disk's natural frequencies, see Figure 35. An optical sensor as previously used for a microphone was adapted for the task. The optical microphone comprises two optical fibres mounted at a critical angle and separation. A laser diode generates a beam that is transmitted through one of the fibres. This beam reflects off the surface of the microphone membrane, in this case the disk surface, back into the other optical fibre, which is monitored by a photo diode. If the disk's surface is placed at the optimum separation from the sensor nearly all of the optical power is coupled into the receiving fibre; however, if the separation changes the coupled optical power reduces. The static displacement between the disk under observation and the optical sensor was set to be exactly half way between maximum and minimum coupling. This allowed direction of displacement to be observed, and operation in the most 'linear' region. When the sensor was positioned at its optimum coupling position, the dynamic range of measurement is doubled because the coupled signal is reduced when the disk is brought both closer or further away. However, this provided no easy means of identifying direction, as the disk moved away from the maximum the signal reduced.

Furthermore, around the maximum coupling position, the measured response was found to be extremely non-linear. This was found to be the system's principal limitation.

The system's response was found to be 1.56mV/μm. The optical microphone's limiting resolution was found to be 2μm. Proving the system to be very sensitive to small displacements, confirming its high suitability for its designed task, but due to its non-linearity was not chosen for further hard disk drive sensing.

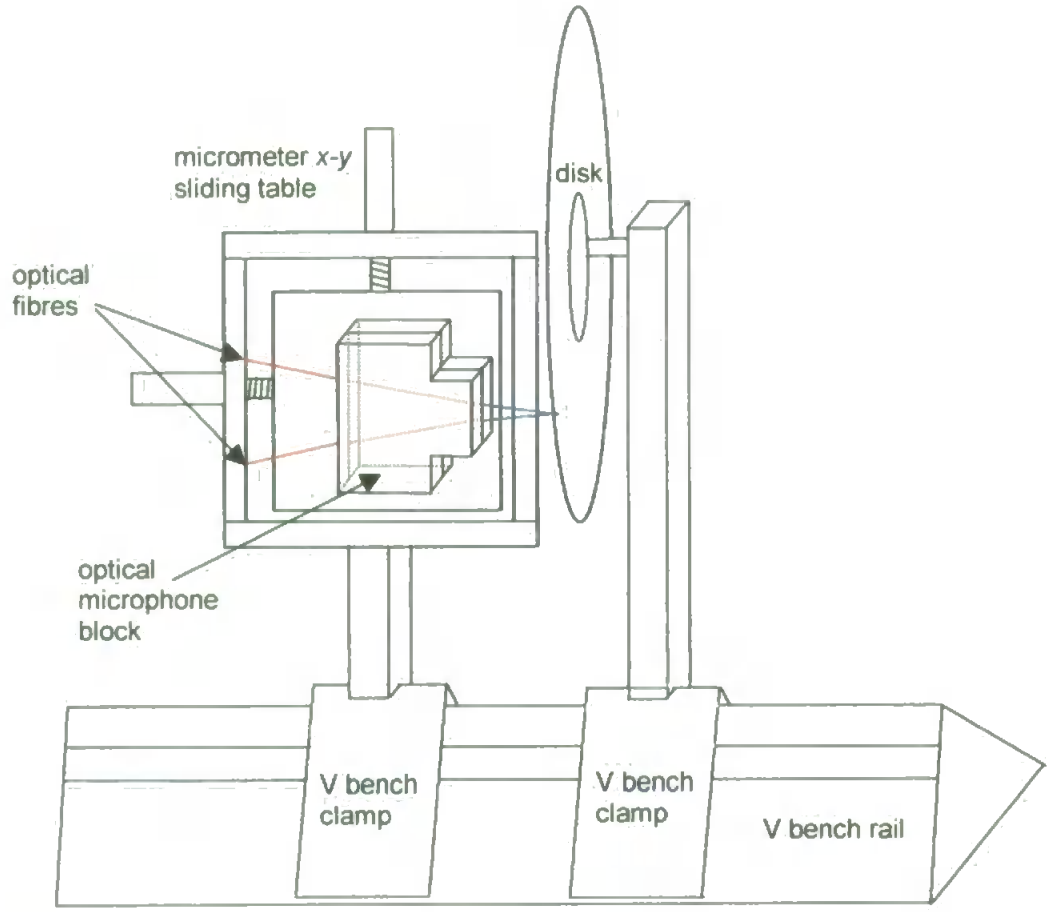

Fig. 35. Diagram showing the optical microphone test apparatus constructed from V bench equipment.

5.6 Piezo-Electric Actuation of Suspension Arm

In order to control the flying height the suspension arm must be actively moved by an additional actuator, other than the air coupling between the disk and slider. To do this a piezo-electric actuator, a 0.2mm thick, 4mm square ACL 4045 PZT plate, is bonded with Electrolube's silver conductive paint at the root of the arm in such that any movement created by the actuator is mechanically amplified through the arm's cantilever length. In order for the actuator to drive the suspension arm it must be efficiently coupled. As the actuator extends / contracts in its x axis, along the suspension arm which is comparatively unable to stretch in length, the arm tends to bend. This is analogous to the principle of operation of a bi-metallic strip. If the actuator increases in length then the suspension bends downwards, as it becomes the inner radius of the structure. If the actuator contracts then the head is lifted up, away from the disk as the suspension arm becomes the outer radius. Figure 36 shows this in more detail.

The suspension arm is attached at one end to a comparatively rigid duralumin structure, which can be considered to be both rigid and fixed. The other end has the aerodynamic slider attached to it. There is a boundary layer of air in contact with the disk, and as the disk spins round this layer of air spins with the disk, which creates a flow of air spinning under the slider. The slider is designed to use this airflow as a means of generating lift and the suspension arm pre-tension counteracts this. The air cushion therefore is in effect a pseudo-rigid second point for the suspension arm. In order for the piezo-electric actuator to effect the flying height of the head it must overcome the aerodynamic force exerted on the slider. See Figure 37 for a simple system force diagram.

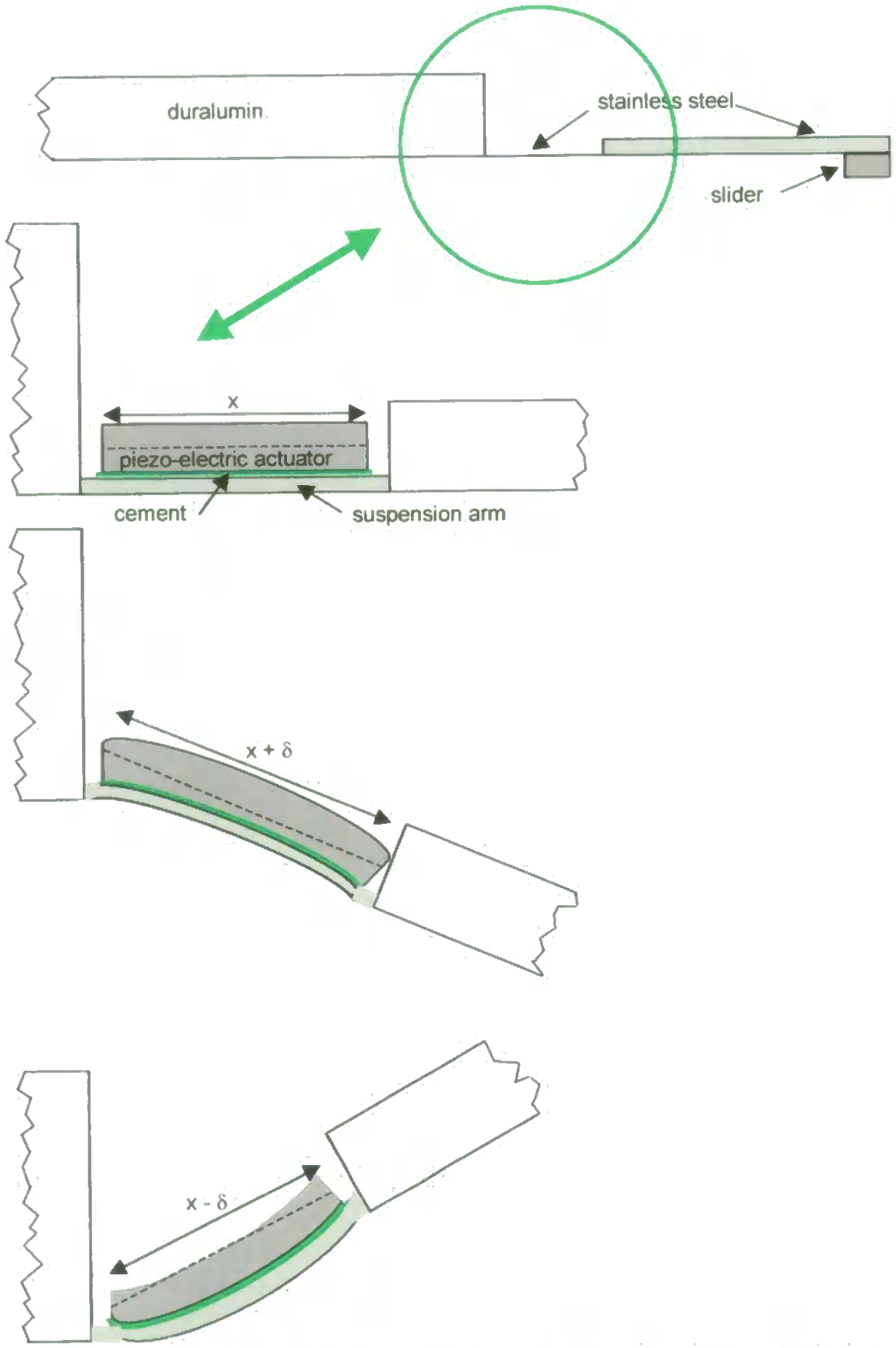

Fig. 36. Piezo-electric actuation of arm. The piezo-electric actuator is bonded to the top surface of the suspension arm/cantilever. The suspension arm is fixed in length and therefore if the actuator increases in length the suspension arm bends in a way that makes it the inner radius and if the actuator contracts the arm becomes the outer radius.

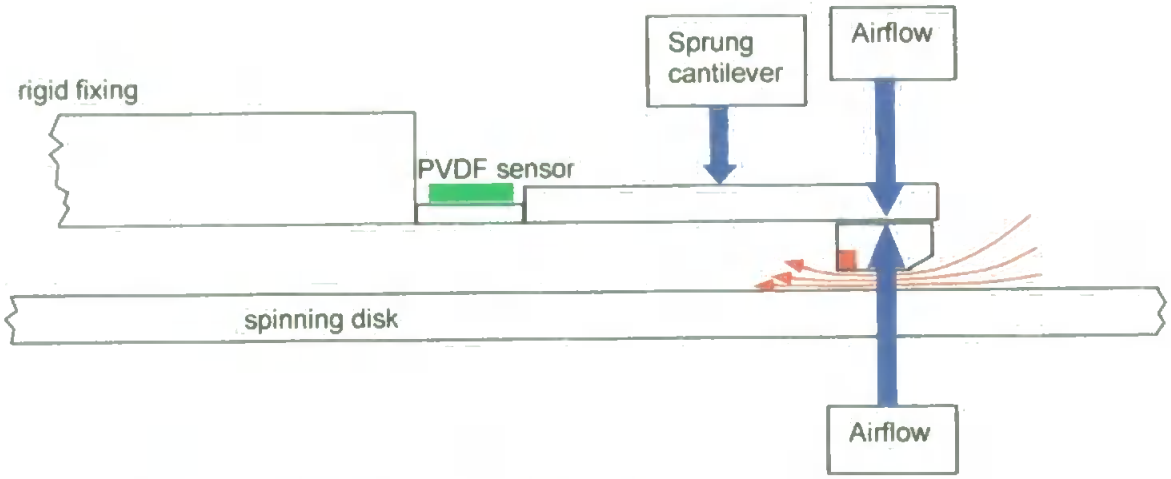

Fig. 37. Figure showing the forces involved when the disk is spinning, transforming the cantilever's characteristics.

To test the system initially, a signal generator was connected to the actuator. Sine waves of up to 20V peak-to-peak were used to drive the actuator, whilst the PVDF sensor output was monitored using a storage oscilloscope, comparing the input and output signals. Signal transference from actuator to sensor was minimal. This is attributed to the cantilever being effectively fixed at both ends, one at the tracking arm, the other at the air bearing.

Chapter 6. Vibration Testing Results

6.1 Vibration Testing of Hard Disk Drives

As the drive is vibrated its transfer rate slows down. The greater the acceleration with which it is shaken the greater the drive is affected and, in general, slower the drive transfers data, Figure 38. This is because the head fails to transfer data correctly in one, or even multiple, sectors. This forces the drive to wait for one full rotation of the disk to gain access to the sectors of data that were corrupted to re-attempt to transfer data. Ultimately, if the acceleration is great enough, data transfer fails on every re-attempt and the drive is forced to halt further operation after a pre-set time, set by the manufacturer of the hard disk drive.

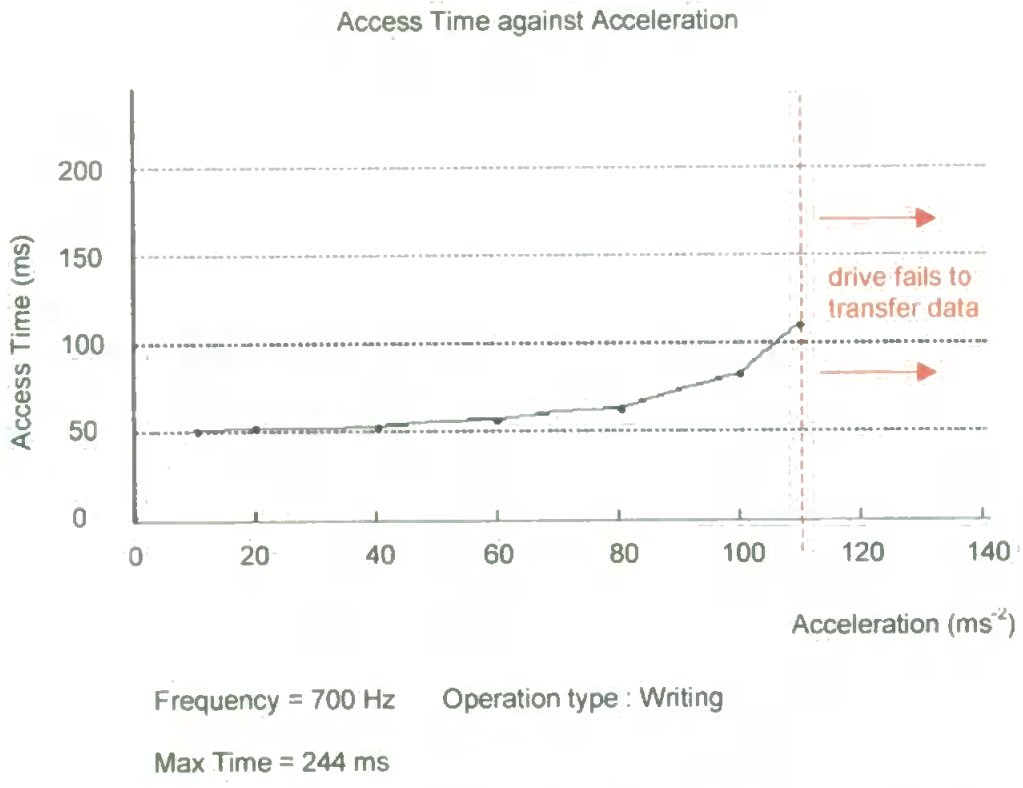

Fig. 38. Graph showing the decrease in data transfer rate speeds when the degree of vibration increases.

A number of tests were made to determine if drive failure was sensitive to the data pattern being written and read. The drive was vibrated sinusoidally at a given frequency, for each of three data patterns (all '1's, all '0's, and a random mixture), and the severity of vibration was increased until the drive completely failed to transfer data. The level of vibration was recorded and the test was conducted at the next chosen frequency. The test was conducted in a frequency band at which it was known from previous tests that the drive would experience difficulties. The results from these experiments, shown in Figure 39, show that any differences are small, +/- 0.5g, and are largely attributed to experimental tolerances.

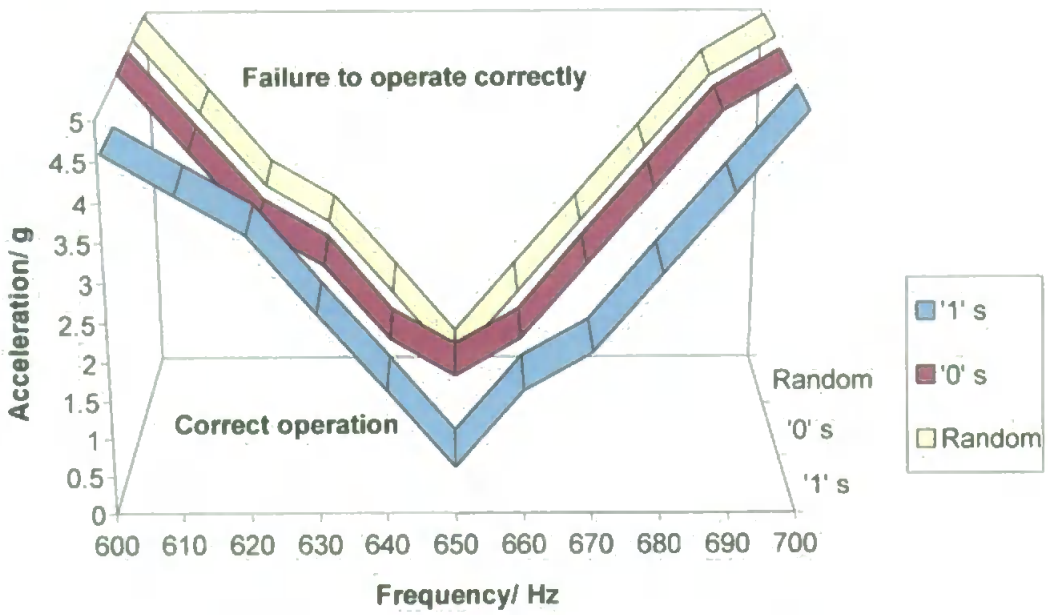

Fig. 39. 3D chart showing the performance of a 3.5" Quantum 230MB hard disk drive whilst transferring data files solely consisting of '1's, '0's or random in content.

Hard disk drives from different manufacturers were vibrated, whilst transferring data, at frequencies of up to 1kHz. The drive is capable of transferring data, albeit after many re-tries, successfully until the amplitude of vibration is so great that the drive is rendered incapable of transferring data. It is this amplitude

of vibration that is recorded. When the drive fails it invariably returns an error flag to the PC's drive controller, outlined in Section 5.2. The value of this flag has predominantly been 04H, indicating sector not found.

Some interesting characteristics of the typical 3.5" drive's performance is its inability to transfer data at acceleration levels greater than 1g in a 400 Hz – 600 Hz bandwidth, and yet the drive is resilient to about 45g of vibration at lower frequencies. These characteristics can be clearly seen in Figures 40 and 41.

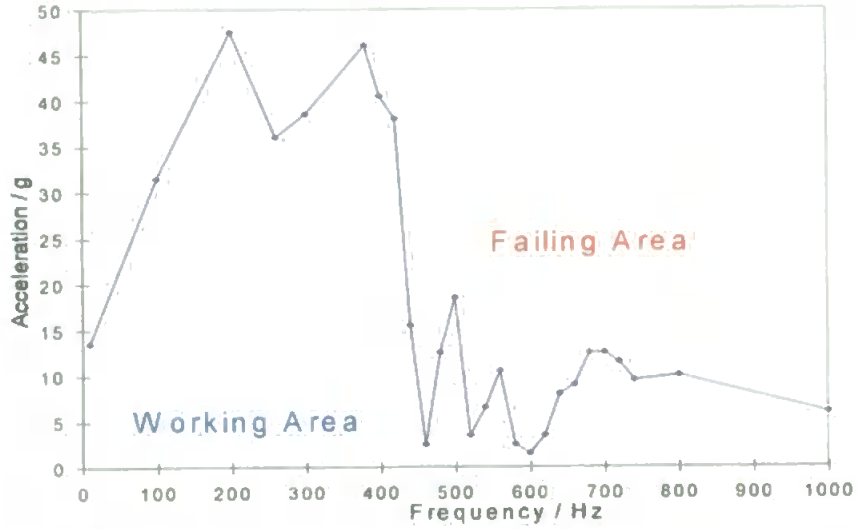

Fig. 40. Effect of vibration on a 3.5", 1GB, Seagate hard disk drive's operations, showing particularly poor data transfer in the 450-600 Hz region.

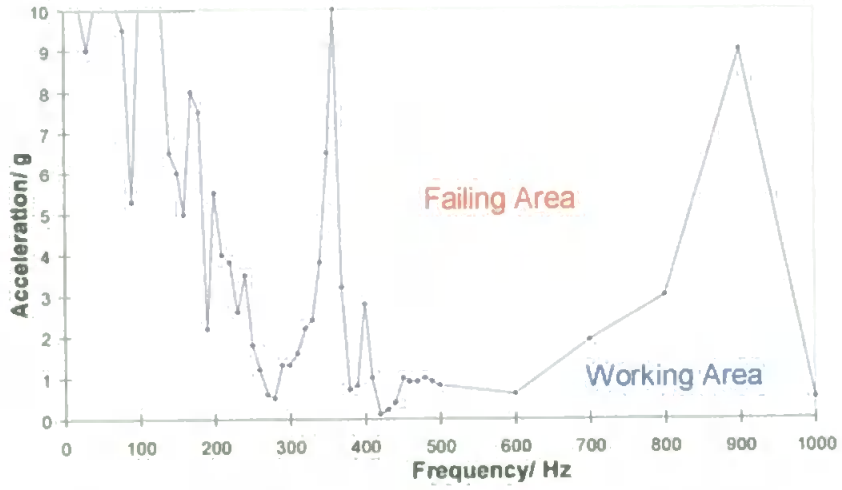

Fig. 41. Effect of vibration on a 3.5", 270MB, Quantum 270S hard disk drive's operations. This older drive exhibits inferior vibration performance than newer drives.

In these tests the drives were tested in their writing mode as this is a more arduous test, having data written to the drive and then read back to confirm correct writing. Reading from the drive involves having a file pre-written to the drive, and the drive read from whilst under test conditions.

It was found that all 3.5" hard disk drives tested, from a variety of manufacturers, showed poor performance under conditions of vibration at frequencies between 450 Hz and 700 Hz. These included: Quantum Seafury 230MB (x2), Quantum Lightning 350MB (x2), Seagate ST352A 1GB and the Quantum 270S Maverick 270MB.

The 1GB Seagate hard disk drive was driven at three, fixed frequencies 500Hz, 550Hz and 600Hz, where the drive is particularly susceptible to errors. The track from which the head was reading data was varied, using software described in Section 5.2, across the disk to see if the drive's performance varied. The results from these tests, in Figure 42, show that generally the drive performed much better with the head located near the inner diameter (ID) of the disk, where the disk displacement is at a minimum due to the clamp securing the disk.

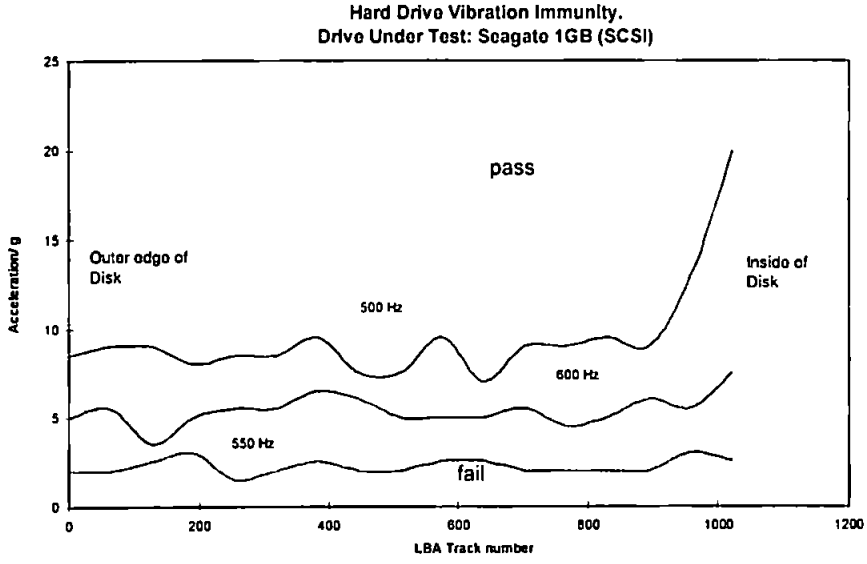

Fig. 42. Graph showing the drive's performance whilst being vibrated at three different, susceptible, frequencies with the head positioned at various points across the disk.

6.2 Frequency Response Testing of the Hard Disk

The results from impacting the disk, described in Chapter 5.5, with a piezo-electric accelerometer mounted to it, show that the 1.25mm thick disk's major natural frequency was at 564Hz. The disk also has another, lesser, mode at 660Hz. The tests were carried out with two disks of identical manufacture, as shown in Figure 43, and are in good agreement.

To confirm the major natural frequency of the disk, the disk was monitored optically with Katsikis' [73] 'optical microphone' and excited with an impulse shock. The natural frequency was measured on a digital oscilloscope to be at 570Hz, giving good agreement. The small difference can be attributed to the mounting of the piezo-electric accelerometer to the disk. Mounting the accelerometer to the disk will change its characteristics; also the mounting itself will not be perfect so the response of the accelerometer will be slightly different to that of the disk. Likewise, the means of mounting the disk to a sliding table micrometer is also likely to affect its frequency response, ie. it is an obtrusive technique, albeit minimal.

Results from white noise vibration testing the disk requires further analysis to extrapolate meaningful data. The principle modes are at 488Hz, 810Hz and 922Hz are shown in more detail in Figure 44. The 'signal' below 400Hz is predominantly attributed to DC noise and can be ignored.

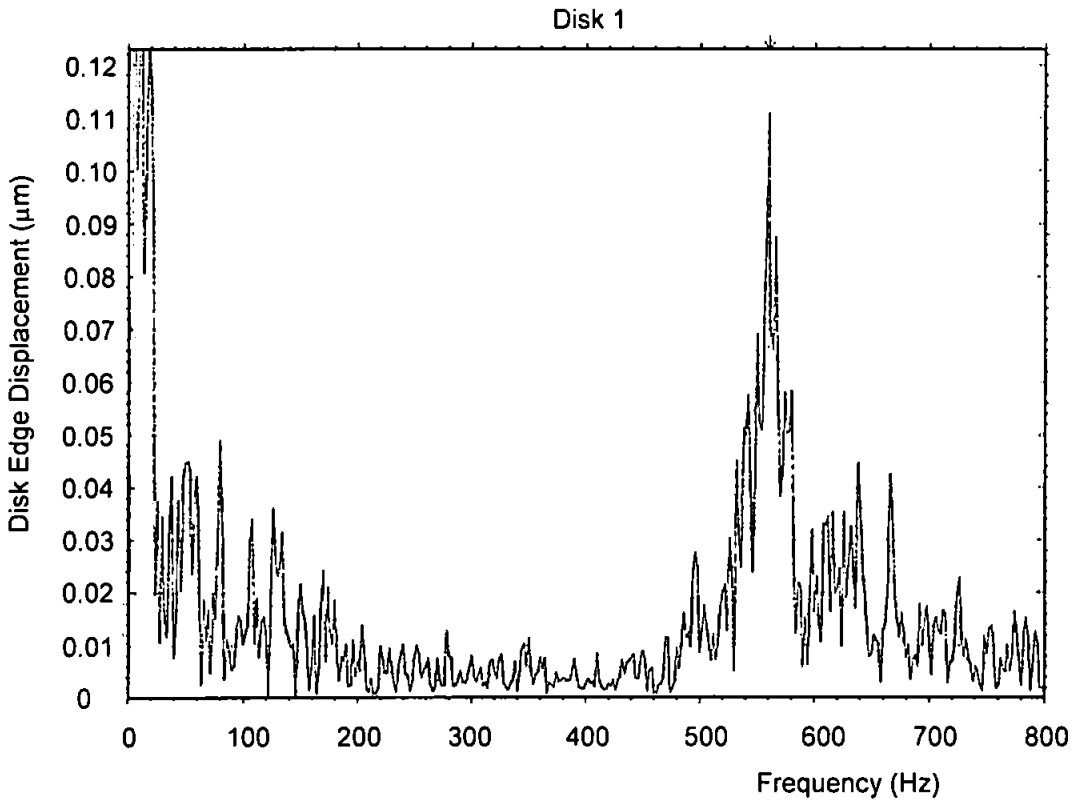

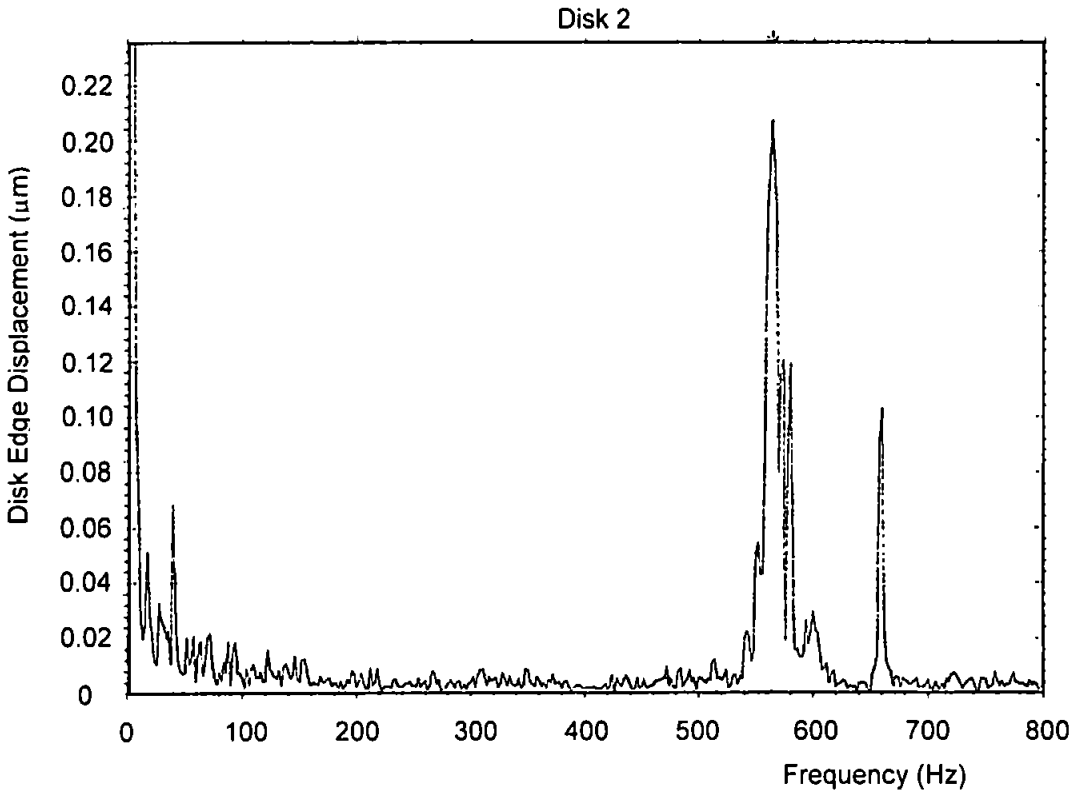

Fig. 43. Graphs showing the frequency FFT response from the disk mounted piezo-electric accelerometer, of two impulse excited 1.25mm thick, 3.5" diameter hard disks.

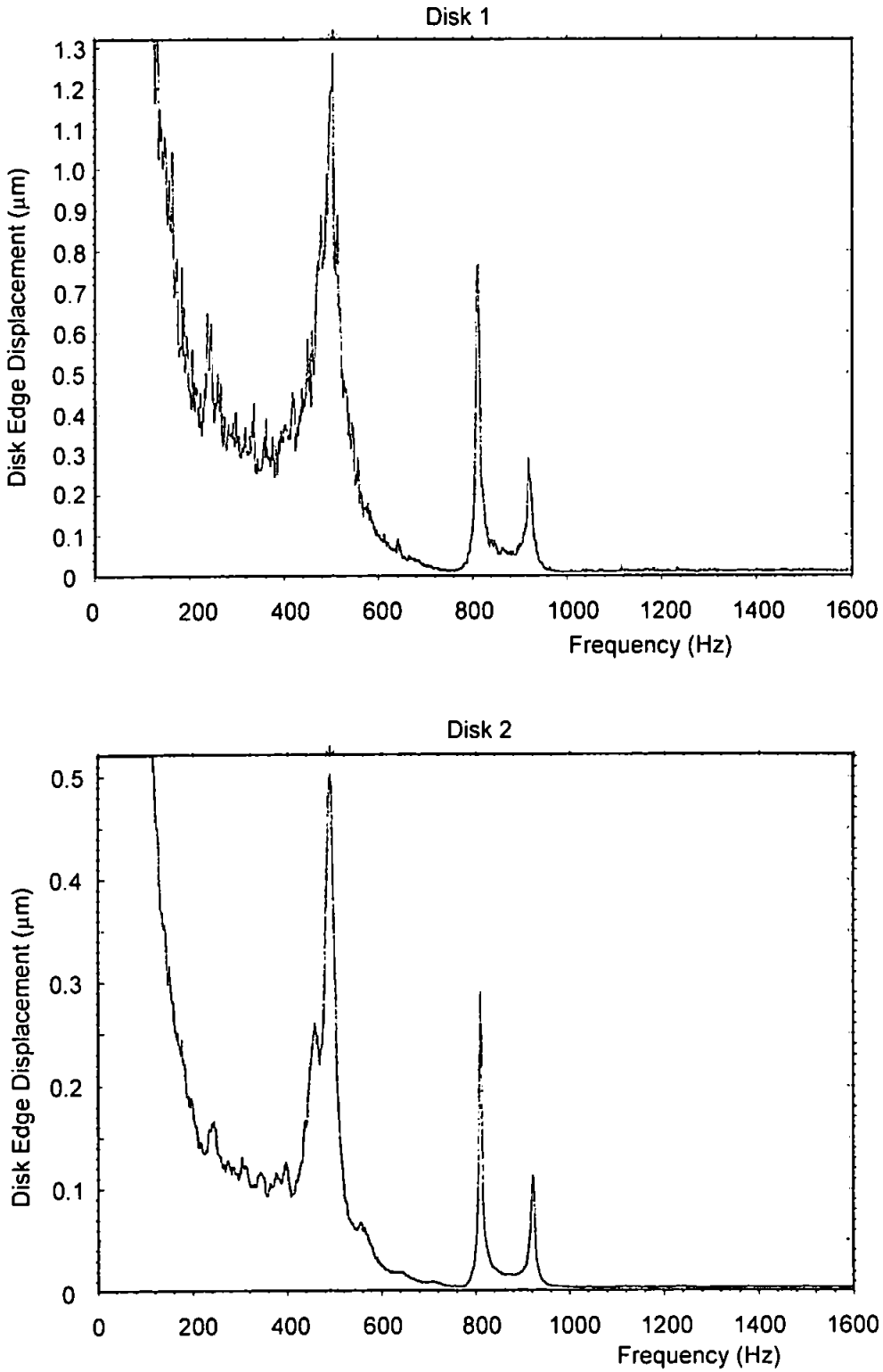

Fig. 44. Resonant frequency response of the same pair of 3.5" diameter, 1.25mm thick disks. This time clamped as in a real hard disk drive.

6.3 Piezo-electric Strain Gauge Measurement of the Suspension Arm and Disk Flutter

In order to validate the system, and enhance the understanding of the components being measured, some tests were undertaken to replicate other work [34,69,74]. These tests were designed to interpret the resonance frequencies of the disk. The drive was run with its lid on so as to conform to its normal working condition. The disk was then excited through shocks transmitted to it from impacting. The shocks were delivered in such a way as to excite all of its prominent modes of resonance and the frequency response calculated by FFT. Many identical tests were repeated to build up the picture of all the modes experienced and to average out noise in the system.

The first tests were performed to discover the resonant modes of the components whilst the drive was inoperative, as shown in Figures 45 & 47. This has the effect of testing the system without the air bearing. Then the same tests were repeated but with the drive running, Figures 46 & 48. In both cases the measured displacement of the arm will be combined to some degree with disk flexure. Many of the peaks on Figure 46 can be attributed to noise created from the electronics within the drive. However, new peaks were observed, as well as peaks frequency shifted due to the rotation of the disk.

In Figures 47 & 48 the frequency responses of the disk itself, as measured by the PVDF sensor described in Section 5.3.2, whilst it is static and whilst spinning can be seen. The responses show many characteristic changes. For example, the peaks detected during rotation are far sharper, showing a system with less damping.

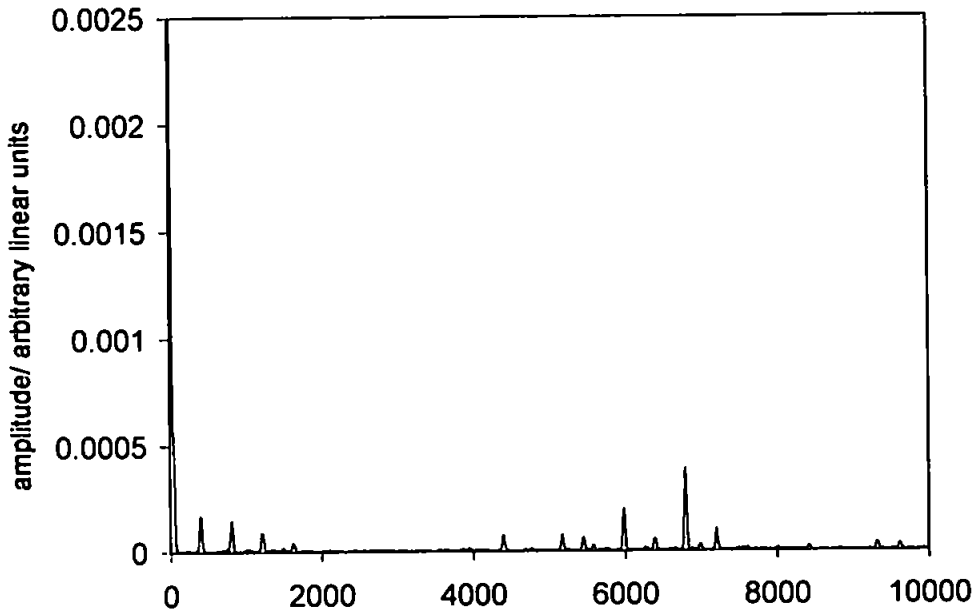

Fig. 45. Graph showing the frequency response of the suspension arm over a 10kHz range, as detected by the PVDF sensor, whilst the drive is in a state of non-operation with the disk pack not spinning.

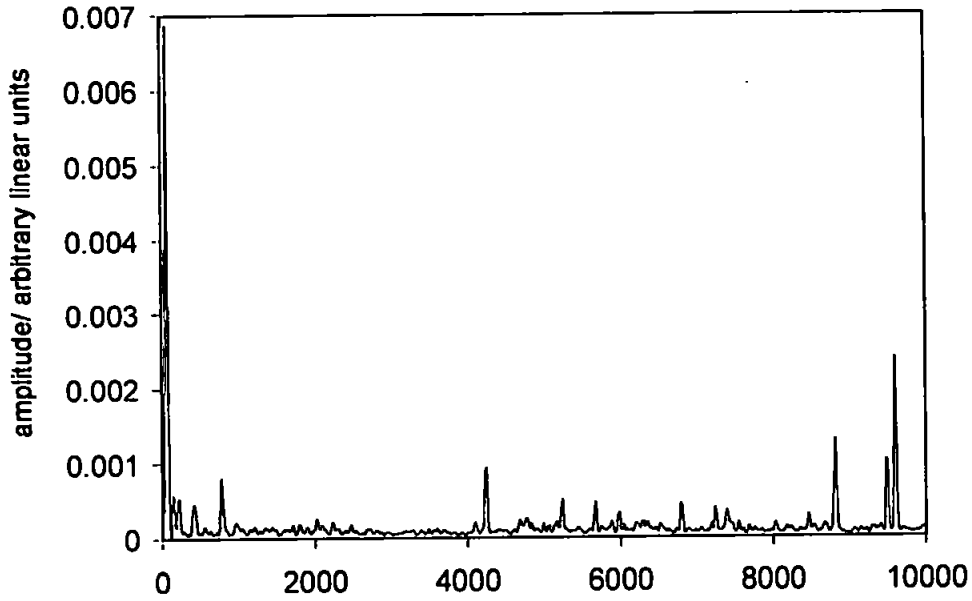

Fig. 46. Graph showing the frequency response of the suspension arm over a 10kHz range, as detected by the PVDF sensor, whilst the drive operational, with a rotating disk pack.

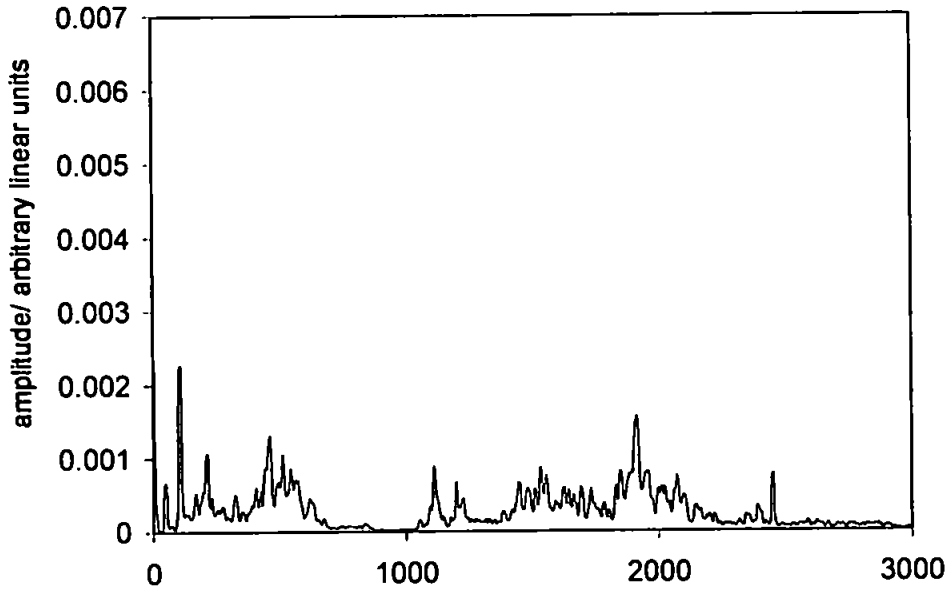

Fig. 47. Frequency plot of the PVDF sensor monitoring the disk, spanning over 3kHz. The drive was in a non-operational state, with a static disk pack.

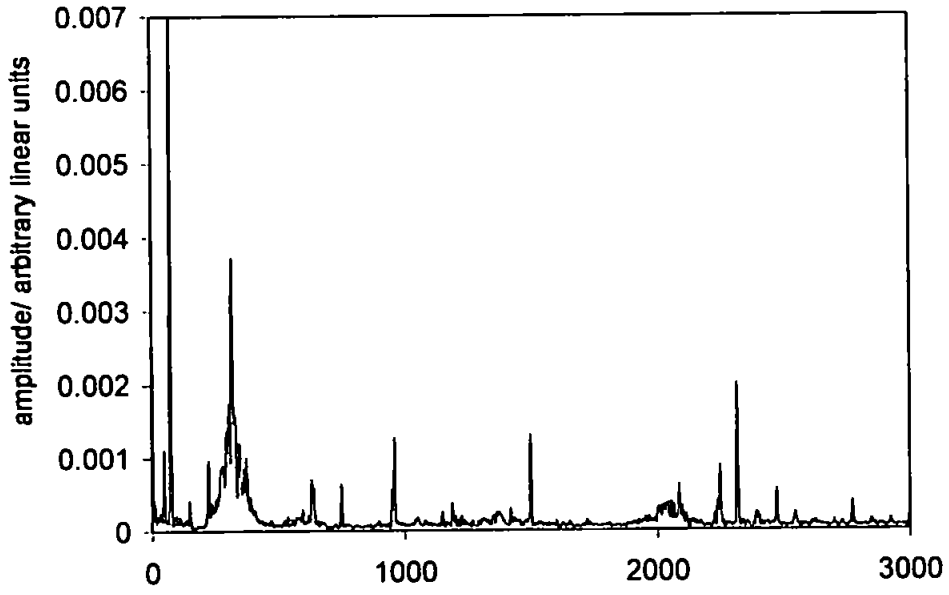

Fig. 48. Frequency plot of the PVDF sensor monitoring the disk, spanning over 3kHz. The drive was in a normal operating condition and the disk pack was rotating.

In the experiments undertaken, the main area of concentration has been in the lower frequency range, sub 3kHz, as these are the frequencies that drives are mostly subjected to in their normal operating environment and prevalently fail at.

The results shown in Figure 49 highlight the higher frequency activity of the suspension arm. At the lower frequency end, sub 3kHz, normal activity was detected. There is a dead-band between 3kHz and around 5kHz and then at approximately 6.5kHz, 8.25kHz, 10.5kHz, 11.75kHz and 14.25kHz large peaks were observed.

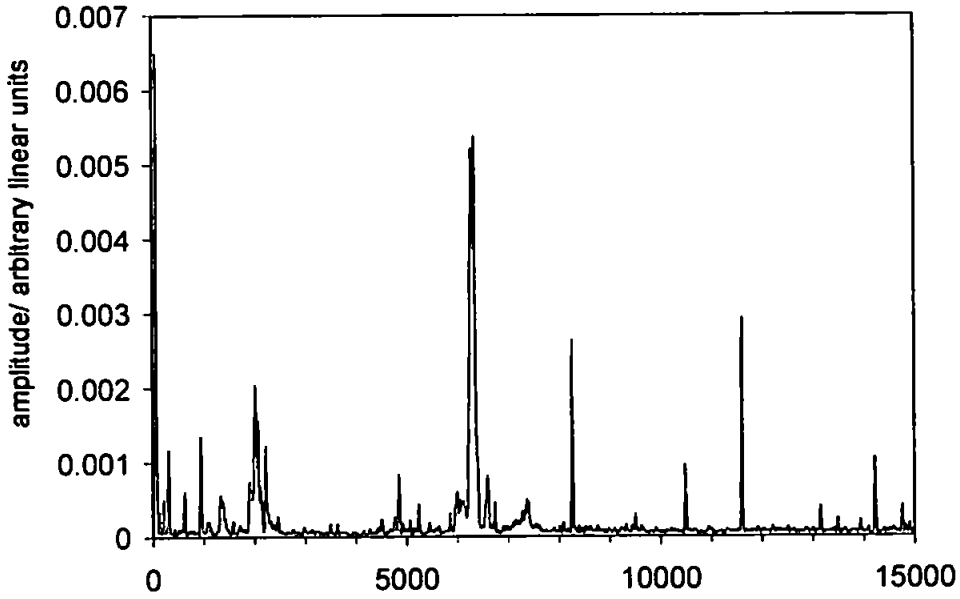

Fig. 49 A graph showing the frequency response of the suspension arm, as measured by the PVDF sensor, over a 15kHz range.

To discover which systems are resonating a direct comparison of the disk and suspension arm over the same frequency range is required. The test results shown in Figures 50 and 51 are restricted to evaluating drive performance at less than 3kHz. Above 3kHz very little activity occurs, and the drive is typically comparably vibration resilient at these higher frequencies. Therefore by sampling at 6kHz, giving a 3kHz frequency response from the Nyquist theorem, more processing power can be devoted to improving resolution, through increasing the number of samples taken.

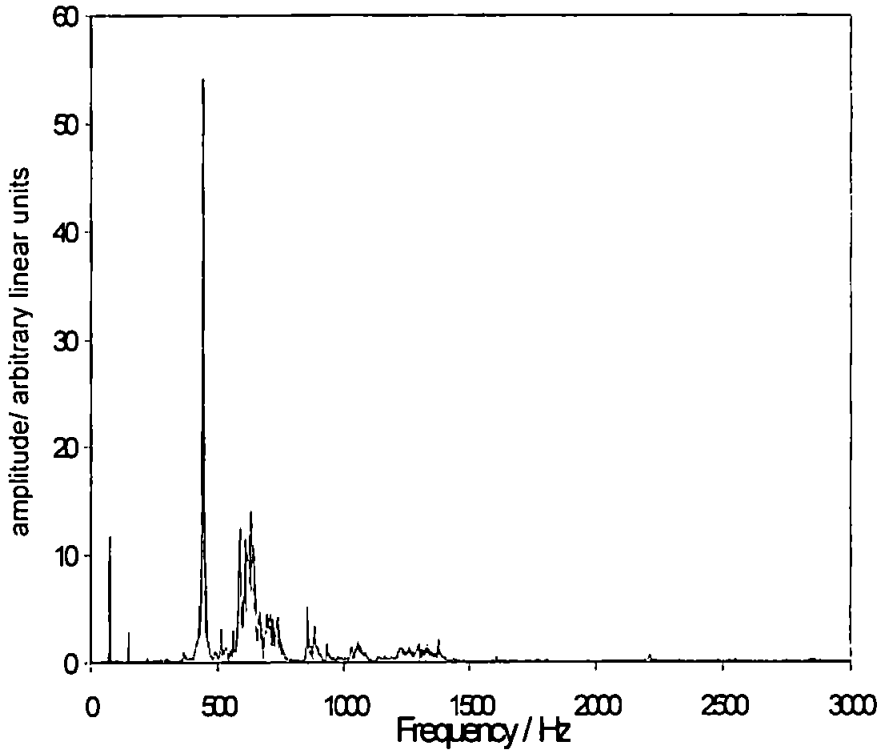

Fig. 50. Graph showing the frequency response of the disk, as measured by the PVDF sensor, alone when subjected to white noise excitation.

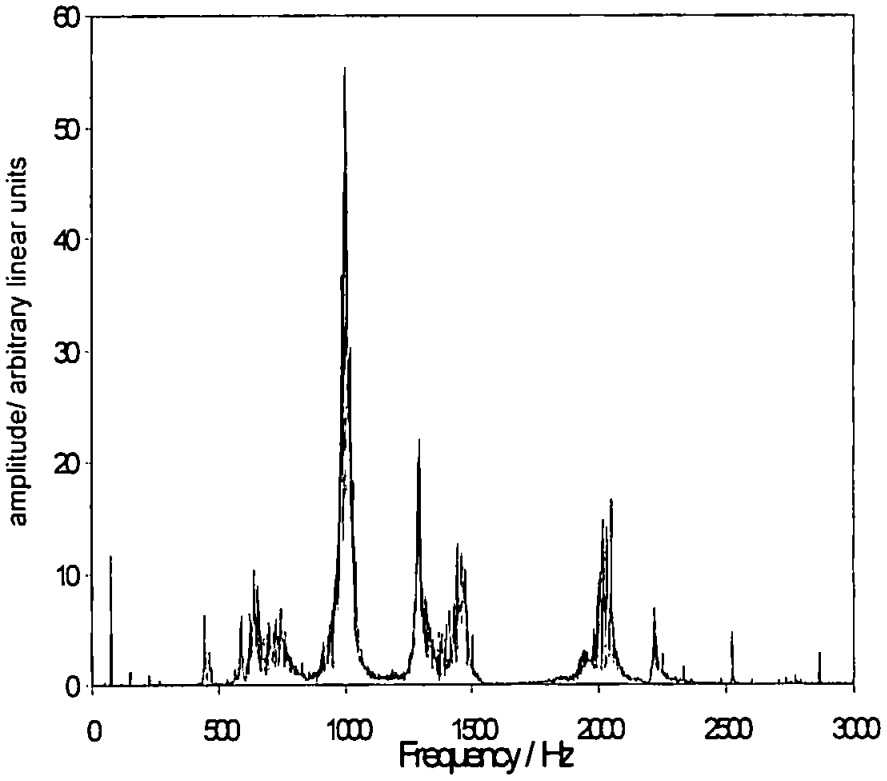

Fig. 51. Graph representing the frequency response of the suspension arm, obtained from the PVDF sensor, from the same drive in operation when subjected to white noise excitation.

6.4 Tracking Error Monitoring

A further means of identifying the components going into resonance is to monitor the off track movement of the head.

In order to reinforce the understanding of existing results a measure of tracking servo error was obtained. The drive was vibrated, from 50Hz to 3kHz, whilst the tracking servo signal was observed. The magnitude of this signal corresponds to the degree of track mis-registration. From Figure 52 it can be seen that large radial displacements were observed around 1775Hz and 1875Hz. This is probably attributed to the suspension arm going into resonance and causing the tracking servo to compensate for this 'apparent' misalignment. The peak observed at 575Hz is attributed to disk resonance. Displacements, although comparatively small, were repeatedly observed around 2225Hz.

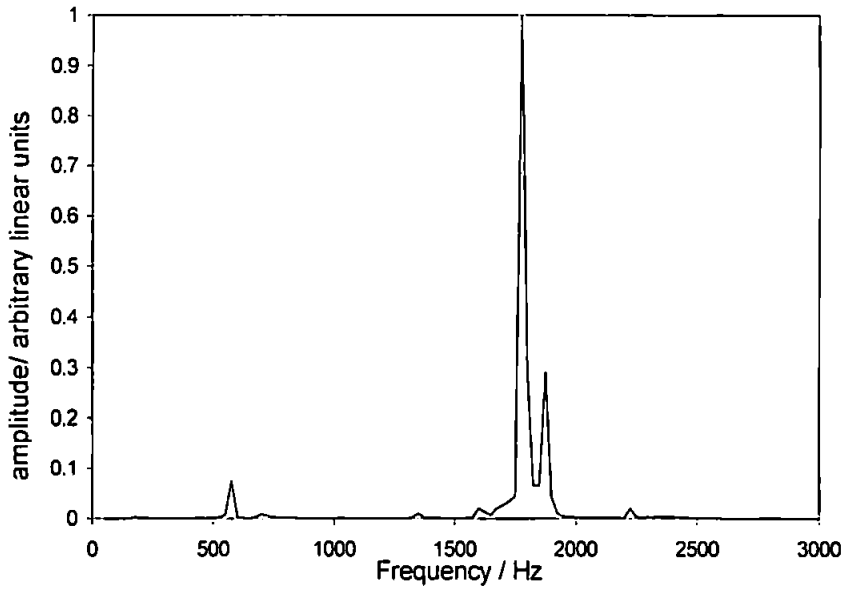

Fig. 52. Tracking servo error synchronous with applied drive vibration whilst the head followed the outside track.

Chapter 7. Compact Disk Optical System for Disk Vibration Response Characterisation

7.1 Compact Disc Player Optical System Overview

An alternative optical system was sought for measurement of the hard disk drive's internal components that provided ideally a linear response, was inexpensive, and could unobtrusively observe the head-disk interface and operate in the hostile vibration testing environment.

Compact disc (CD) players utilise a laser and photodiodes to read data from the disc. When the disc spins in a CD player it often has runout due to the disc not being absolutely flat. Therefore the laser has to move in two planes, horizontal and vertical, to maintain focus and tracking and hence correct data retrieval. The ability to move up and down, maintaining its focal distance from the disc, is of interest to this research. If reverse engineered, rather than applying a voltage to the voice coil to lift the focusing lens, the signal that would be going to the voice coil could be monitored to allow the distance from the disc to be found.

The photo detector comprises four sensors. When the laser is focused on the disc surface the reflected beam off the disc will be centrally located on the four sensors. The spot will then move either left or right to cover one pair of spots depending on the lens-disk distance, [75].

Figure 53 shows a diagram of one version of a CD head design of the type used in this research. The laser diode light passes through the prism and through the objective lens, focusing the beam onto the disc. The objective lens can be brought closer to or further from the disc to focus the light on the disc's surface.

The focused beam width is slightly larger than the data bits embedded on the compact disc, which are 0.5μm in width. From this it can be deduced that the spot size when focused is between 0.5μm and 1.0μm in diameter, Calimetrics CD ROM spot beam size being 0.87μm [76].

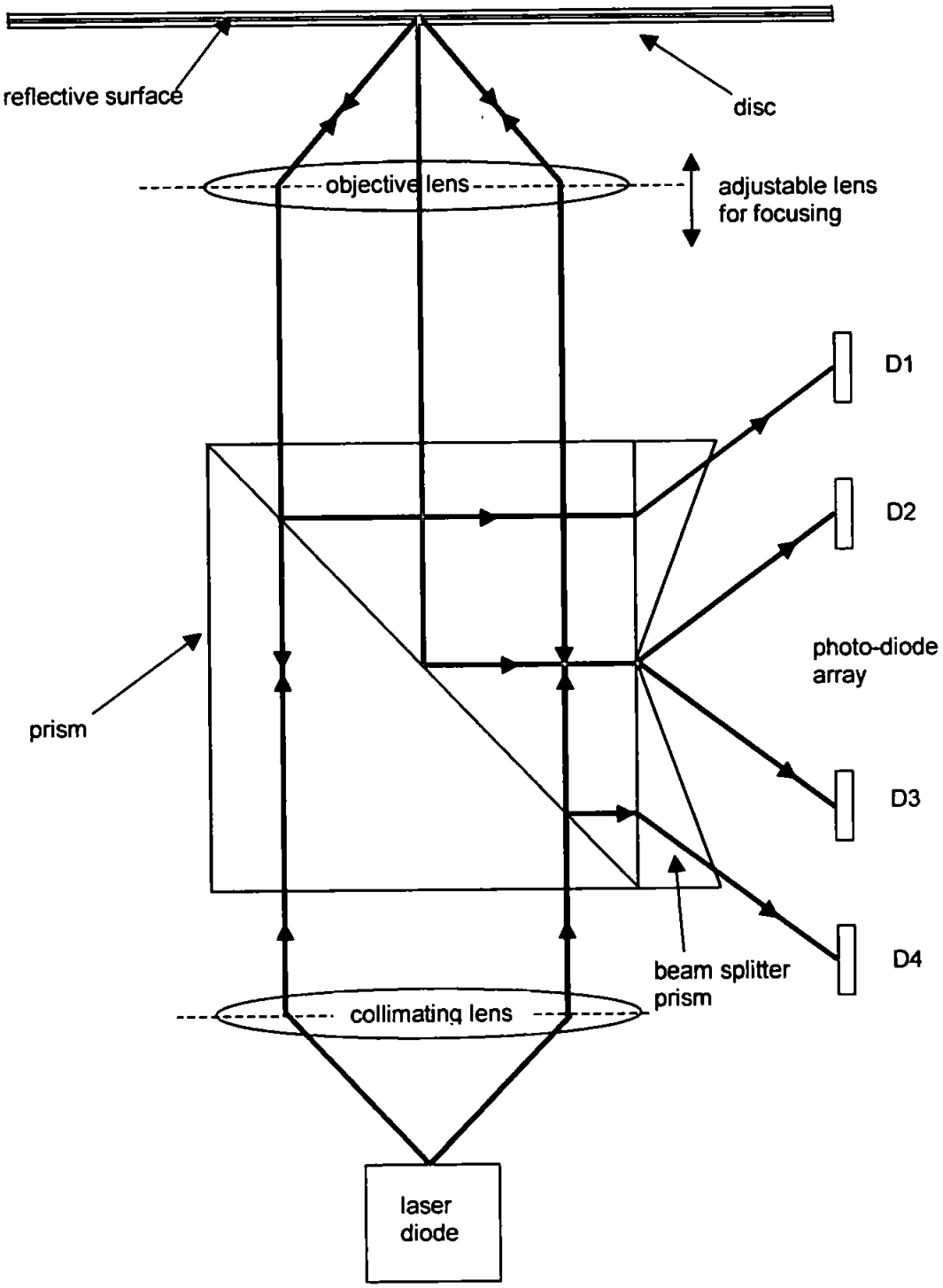

Fig. 53. Diagram of one type of CD optical head system. This is a quad-detector beam-splitting system.

When the disc-lens separation is such that the beam is perfectly focused, the light intensity from the beam splitter equally covers all the detectors, as shown in the centre example of Figure 54 (b.).

If the disc is too close to the objective lens then the beam will be reflected before its optimal focal distance. This means the reflected beam, when it passes through the beam splitter will focus the light intensity on the 'inner' pair of photodiodes. This is shown in the left-hand example of Figure 54 (a.).

When the disc is too far from the objective lens for perfect focusing the emerging beams from the beam splitter prism direct the majority of light intensity on the outer pair of photo-detectors, as shown in the right hand example of Figure 54 (c.).

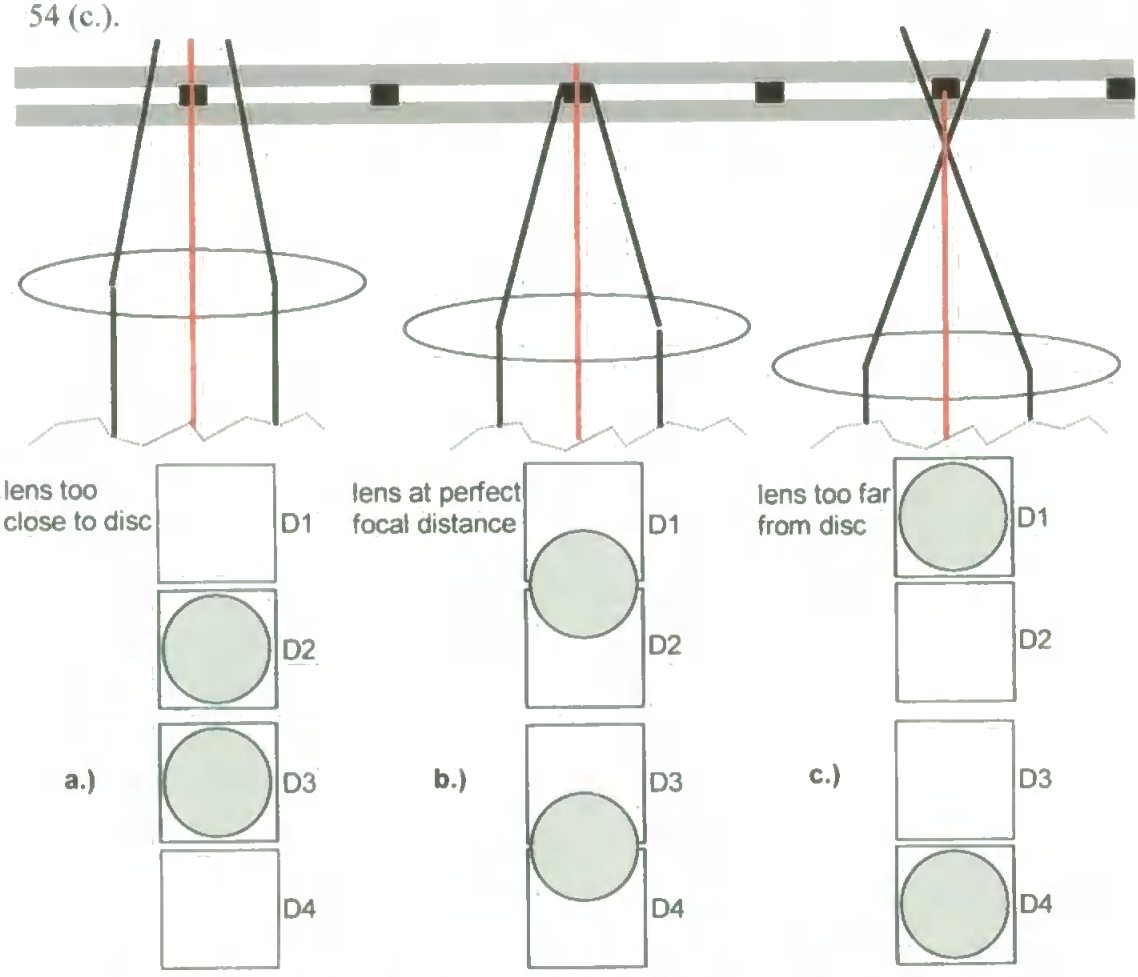

Fig. 54. Diagram highlighting the optical path's deformation due to focal distance changes and how the sensors observe these focal distance variations.

The second sensor of the pair of sensors used to measure differentially the flying height changes was of a later design. This design is called the critical angle prism, as shown in Figure 55. The prism is set at angle of around 42 degrees and any mis-focusing will have the effect of centralising the beam over one pair of the detectors.

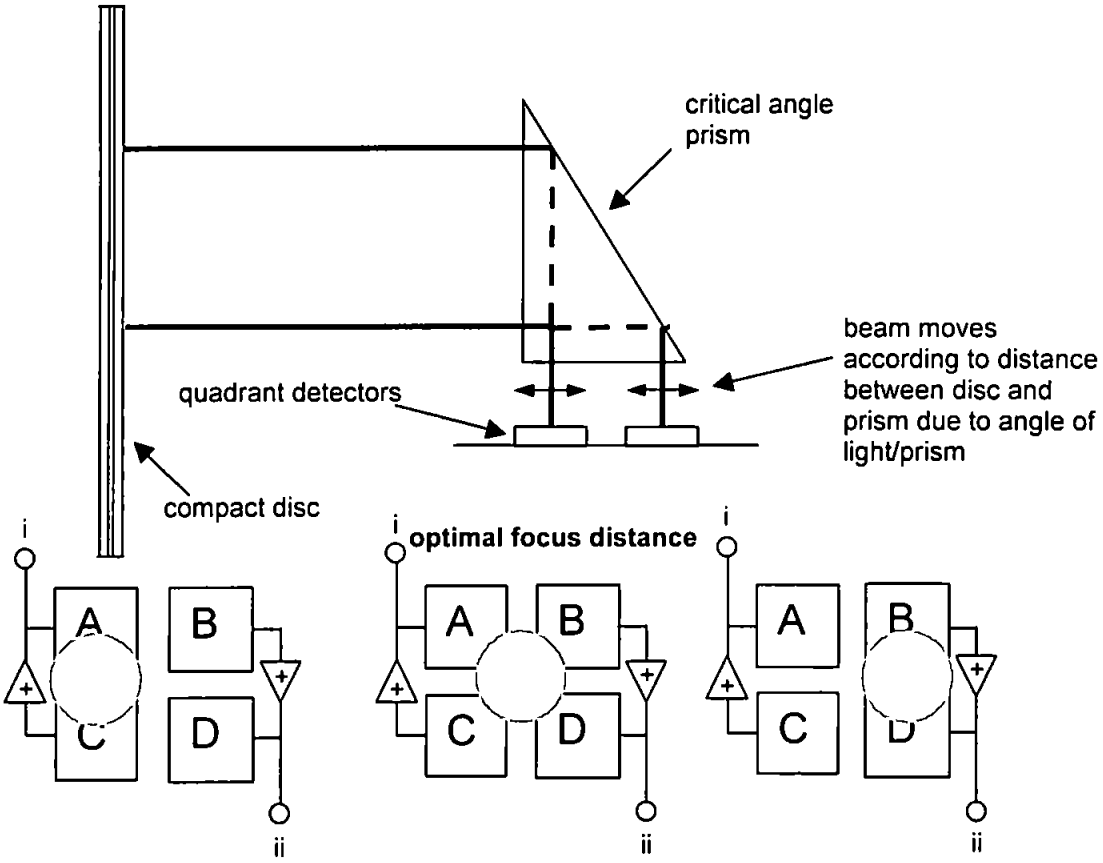

Fig. 55. Critical angle prism optical method of measuring focus distance. This diagram also shows the typical summing methods used to maximise signal detection. i and ii would typically connect as two inputs to a differential amplifier, however for the optical system developed here, they would connect to the differential inputs on the DAQ card.

7.2 System Appraisal

The CD heads were individually mounted to a micrometer-controlled sliding table and aligned so as to reflect off the disk from a hard disk drive. The reflected beam was monitored with an oscilloscope from one of the photo diode segments. By electrically adding together the outputs from the relevant pairs of the quadrant photodetector and observing the difference from the two pairs the system response is optimal, giving a signal four times greater then that observed from just the one segment.

When the 20mW laser diode driven four element photo diode array optical system was tested, it was observed that the peak voltage was achieved when the lens was 2.80mm away from the disk's surface, with an output from one detector segment of 30mV. The signal from the detector is the raw signal and is not amplified in any way. Linear response was observed when the disk was moved both closer to the lens and further away from it. There were 20mV swings observed when the lens was moved 200μm both closer to and away from the disk, giving a total linear region of 400μm. In order to ascertain direction the lens was mounted exactly halfway between the maximum and minimum points in the linear region, as shown in Figure 56, this means that a displacement of 200μm brought about a change of 20mV, giving a response of 0.1mV/μm. The single element sensor has a noise floor of 8mV, giving the response of 0.1mV/μm means the sensor has a limiting resolution of 80μm.

Similar results were obtained from the critical angle prism optical sensor with a 30mW laser diode. The peak distance was found to be 2.91mm, with a sensed voltage on one of the photo detectors of 100mV. The relationship between

distance and voltage was found to be 40μm to 80mV, hence giving a response of 2mV/μm for a single detector and 8mV/μm once the four elements have been appropriately manipulated. This sensor has a noise floor of 20mV, with a response of 2mV/μm, the single element sensor therefore has a resolution of 10μm. The sensors were observed to show no significant signal degradation over the maximum sweep range of the vibration equipment, 1Hz to 10kHz.

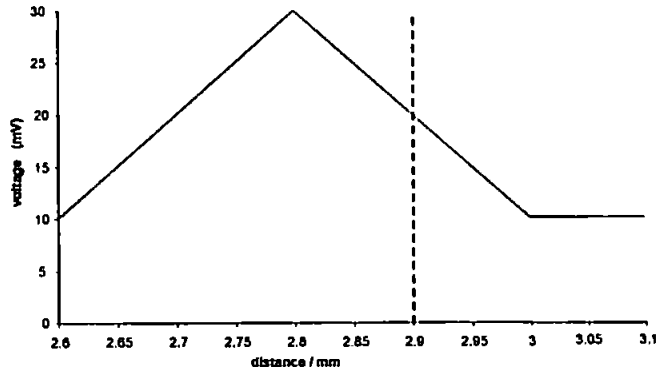

Fig. 56. Graph showing the voltage response from the quad-detector beam-splitting optical sensor as a function of distance from disk surface. Region of operation is

7.3 Test Apparatus Design

An optical system comprising two sensors has been used for monitoring both disk and flying height variation. The task of monitoring the hard disk drive whilst it is vibrating in the vertical plane is complex. The mounting of the optical system to the vibrating plate is precluded because the mass of any optical system would prove to be beyond the shaker's design parameters. Also structural rigidity would be compromised, creating spurious vibrations, and it would be impossible to know whether measured results were due to disk vibrating or the movement of

the optical system itself. For these reasons any optical system must be mounted externally to the vibrating hard disk drive.

Two optical sensors are required: one to measure the disk drive (i.e. chassis) movement as a reference, and one to measure the movement of the disk or the suspension arm. The difference between these measured signals gives the relative movement of the arm or the disk. Using two sensors enables the displacement of the disk and arm to be monitored synchronously with respect to each other. This enables an understanding of interactions between the two when one goes into resonance, and insight into the phase relationship between head and disk response. Since the sensors have to be mounted externally to the hard disk drive whilst the drive is moving and being vertically vibrated, they must be able to monitor small displacements from a relatively large distance or offset. The CD optical system is well suited to this application.

To produce the most meaningful results the sensors ideally need to be located to observe slider motion and disk motion directly beneath the slider. Since it is virtually impossible with this method of measurement to observe directly beneath the slider, every effort must be made to ensure that the sensors is observing the disk directly in front of and as close to the slider as is physically possible.

Other optical equipment used in this research laboratory [48,77] has been constructed using Spindler and Hoyer* Microbench components. These systems supported on from cradles forming a structure from four 6mm silver steel rods. This arrangement creates a very solid structure. However, it is very intensive on

* Spindler & Hoyer UK Ltd., 2 Drakes Mews, Crownhill, Milton Keynes, Buckinghamshire. http://www.spindelrhoyer.co.uk

materials, labour intensive for component positioning and comparatively large in physical size for use in these experiments.

A similar system to the Spindler and Hoyer Microbench was developed. However, only two rods were used instead of the four. With careful alignment of the rods it was possible to maintain strength and rigidity in the plane of vibration, yet minimise physical space taken by the equipment, as depicted in Figure 57.

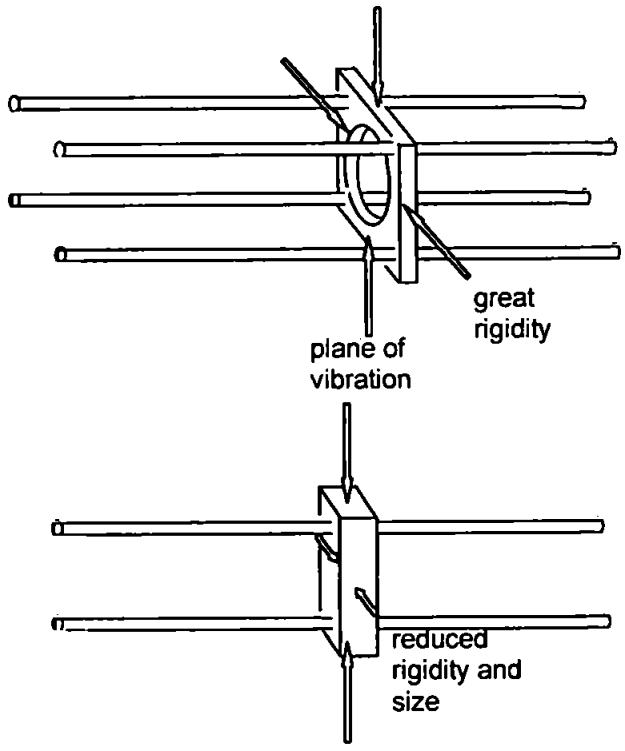

Fig. 57. Diagram representing the structural overview of the optical frame design.

The frame must allow the sensors to be moved independently across the drive to enable them to be correctly positioned above their respective components that are being observed. To achieve this separate sliding blocks have been created that allow for both movement in height, see Figure 58 and the other two planes across the drive, see Figure 59.

The rods and their separation are arranged with a hierarchy such that the blocks closest to the mounting bases house the rods furthest apart, offering maximum stiffness. 3mm grub screws have been used throughout in a way that when slack the sliding blocks move freely to allow repositioning, but when tightened they serve to clamp the blocks rigidly to their 6mm rods. This allows for an easily adjustable platform as well as a very rigid one.

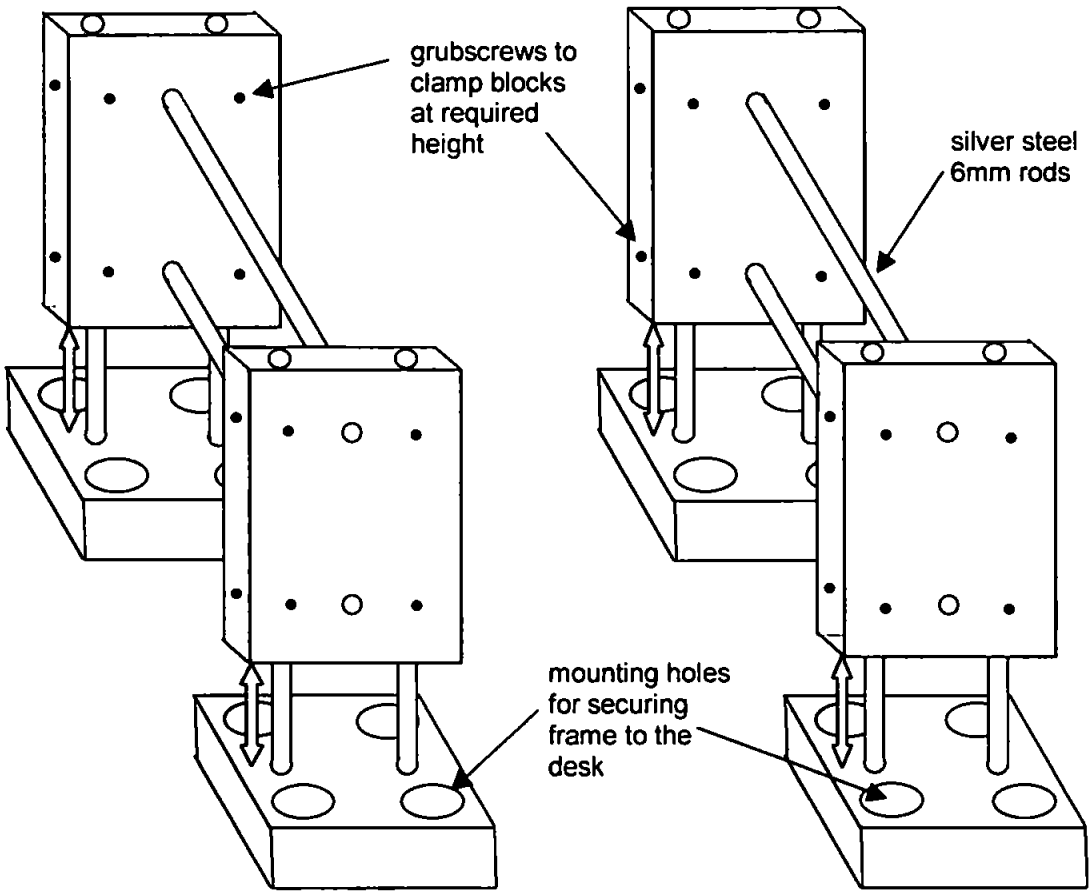

Fig. 58. Diagram showing how the vertical positioning of the dual optical sensor system can be adjusted.

The finalised frame for housing the two optical sensors is shown in Figure 60, and the quad-detector beam-splitting sensor, which is mounted to the frame (sensor 1), is shown on its own in Figure 61. The frame is secured to the desktop surrounding the shaker and plate with the four bases bolted down.

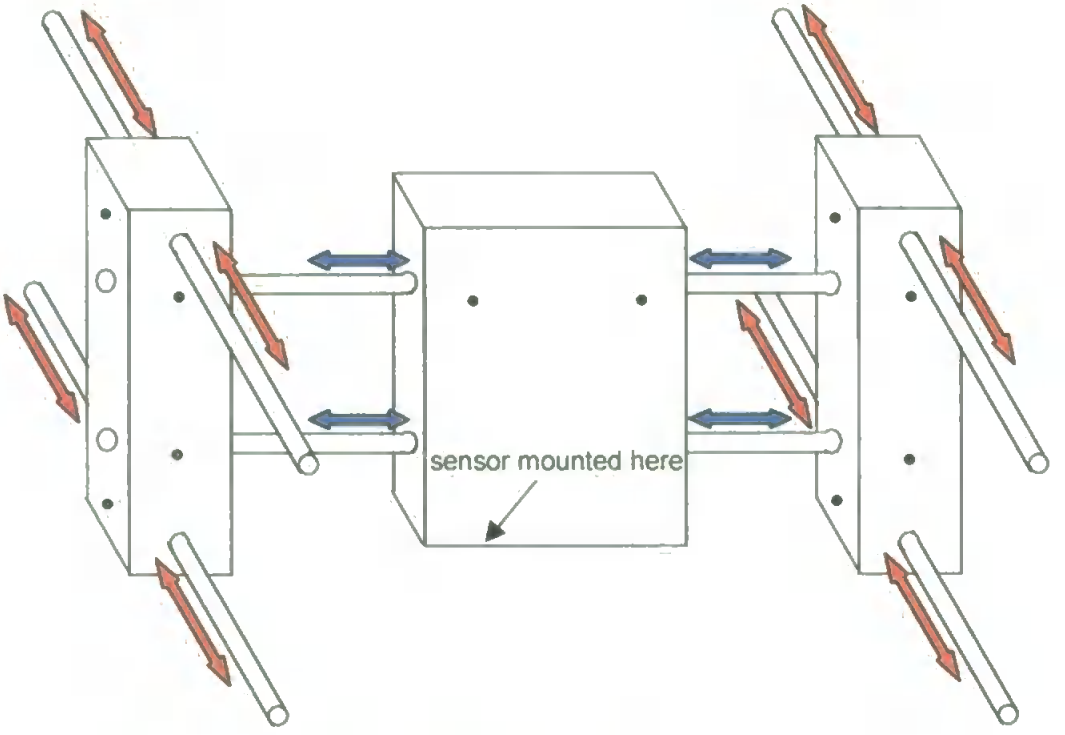

Fig. 59. Diagram showing the sensor's freedom in two planes.

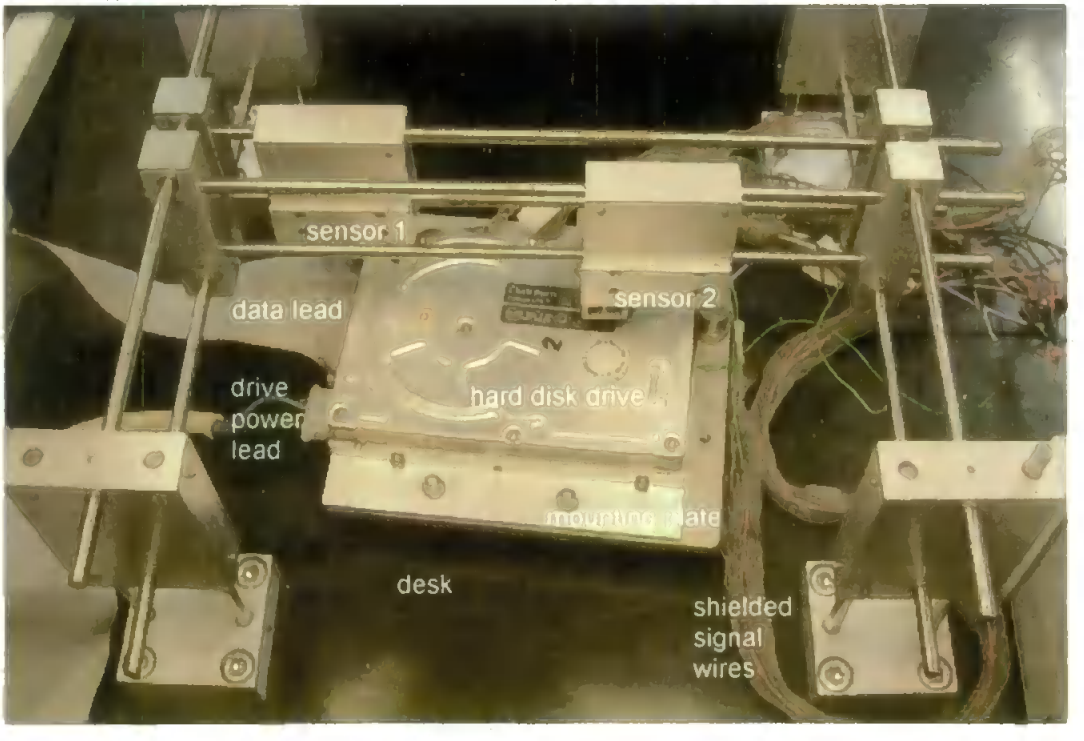

Fig. 60. Frame for housing the pair of optical heads for differential measurement of the head and disk within a hard disk drive. The optical heads are mounted to the two centre blocks allowing freedom of movement. The drive is mounted to the shaker plate beneath and is connected to a PC to control data transfer.

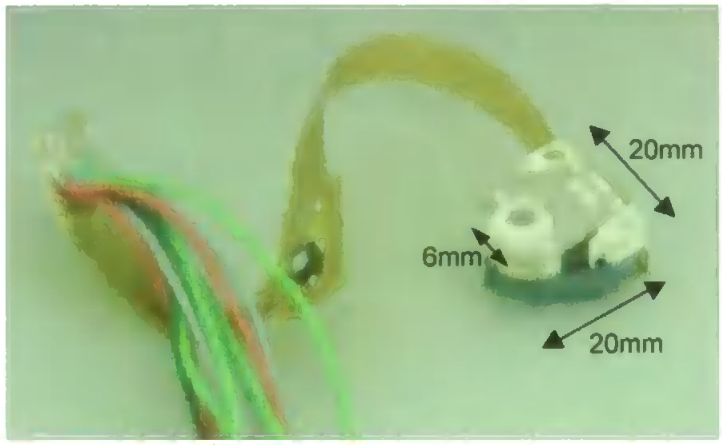

Fig. 61. Photograph of the smaller, quad-detector beam-splitting, sensor and its approximate dimensions.

7.4 Optical Measuring System Development

The system was built initially with a hard disk drive fitted without a lid, but protected from dust by the laminar flow clean-air bench surrounding the system. Although this affects the drive's performance it still enabled the optical system to be developed and evaluated. The fundamental mode of resonance was found to be at 540Hz, which is the disk's fundamental mode without the lid fitted, the slight change in frequency can be attributed to the lid's damping effect. The optical heads were positioned at the appropriate distance from the surface of the object that they were intended to measure. To aid positioning for reading data from a compact disc, the lens is mounted on a flexible mounting driven by solenoids to move the lens to and from the disc and left and right to keep on track. These solenoids were used to good effect to position the lenses where required. The drive was vibrated at 540Hz and the signals measured using a Tektronix TDS 3052, two channel digital phosphor oscilloscope with a bandwidth of 500MHz and capable of sampling 5,000,000 samples per second, are shown in Figure 62.

The drive was driven sinusoidally with a peak-to-peak amplitude within the sensors' range, ie 0.2mm. If driven too hard overflow errors occur.

The drive lid was then modified to include scope for optical measurement of the disk and suspension arm, Figures 63 and 64. The lid was carefully constructed to allow the CD lens to be positioned at its optimal distance from the object of concern, a distance of 2.9mm, this prohibited the use of an optically and physically thick 'window' material. The lid was modified by removing a section, of aluminium, and replacing it with 1.0mm thick Perspex. The Perspex screen was bonded to the lid, as a replacement of the aluminium section, using Araldite professional epoxy resin. Within the screen a recess, again made from 1.0mm Perspex, had to be created to allow the disk motion sensor to locate closer to the disk. As has been discovered, the lid acts as an air damper for any disk excitation and hence any change in the lid's material will change its characteristics. The inserts in the window also alter the aerodynamic conditions within the drive and possibly alter the slider's flying conditions.

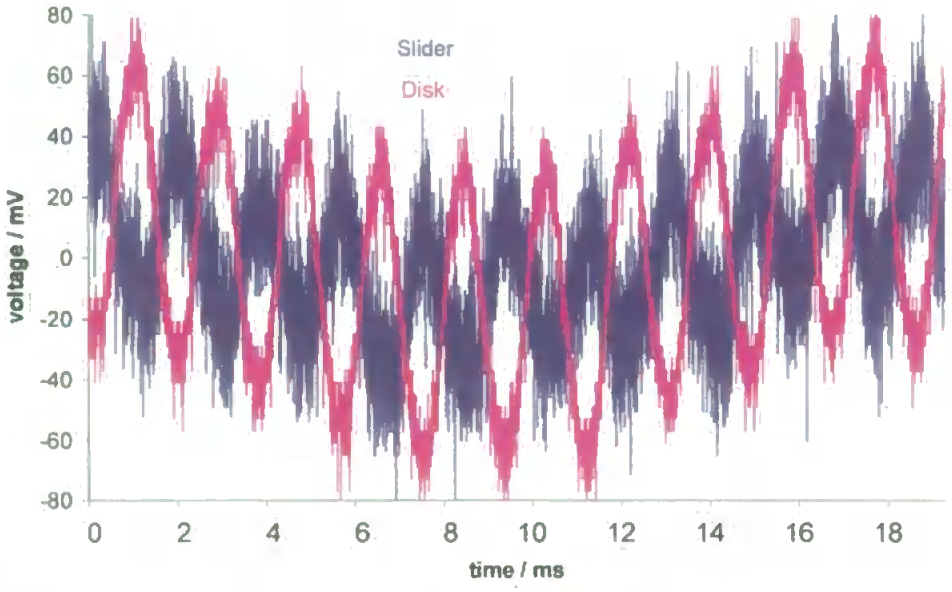

Fig. 62. Graph showing the measured response from the optical detectors. The sensors were measuring slider and disk motion whilst the drive was excited at 540Hz. This frequency represented the peak in resonant activity of the disk with the drive lid removed.

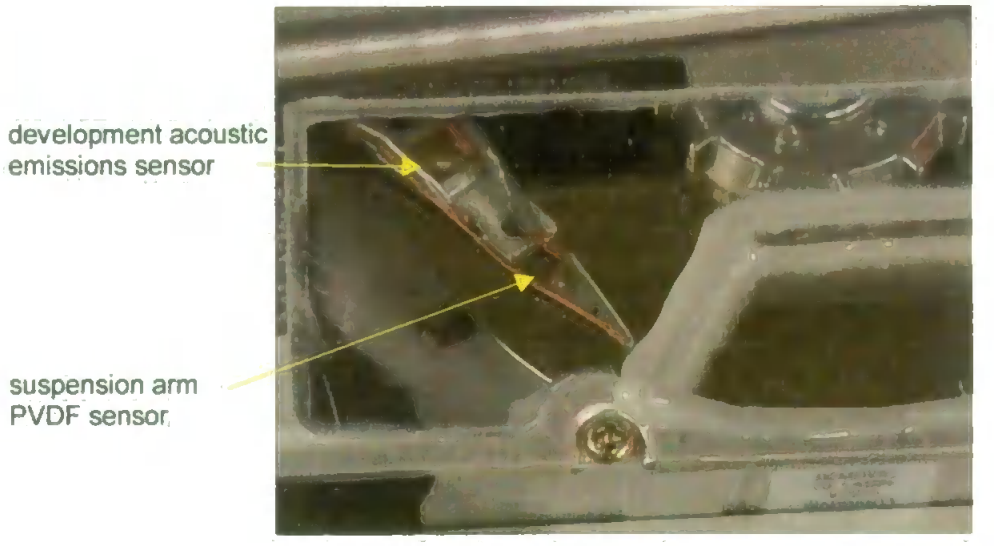

Fig. 63. Modified hard disk drive with clear Perspex screen to enable optical measurement of suspension arm and disk. Two PVDF sensors can be seen, the one on the suspension measures arm deformation and the other is a development version of an acoustic emissions sensor.

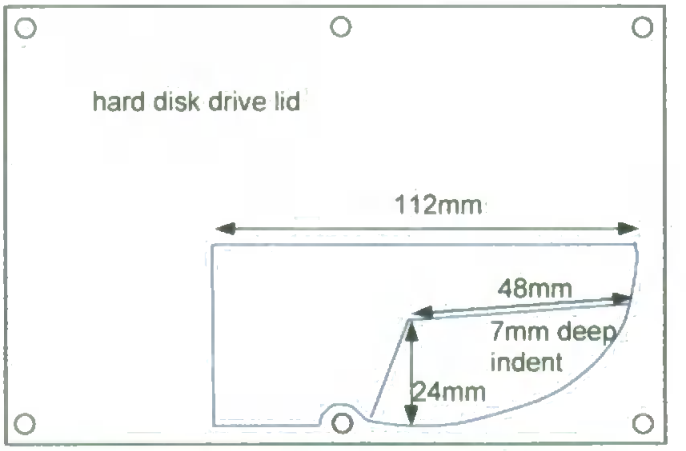

Fig. 64. Diagram showing the dimensions of the 1mm Perspex section of the modified lid and the indents allowing physical access for the optical sensors.

7.5 System Overview

In order to allow the optical system to measure and characterise head-disk interface performance whilst the drive is in operation the optical sensors were positioned to measure the motion of the slider and the disk directly in front of the slider.

The head units are relatively bulky, limiting how close to each other they can be located. The part of the disk observed is not directly underneath the head and therefore a phase delay, determined by disk speed and spacing, is induced into the system due to physical spacing. The beam separation, from slider to disk, is approximately 15mm. At a disk speed of 4500rpm, assuming a radial point, 45mm from the disk's centre, the disk beneath the sensor will be travelling at 21.2 ms^{-1}. Therefore the disk will take 0.71ms to travel from the disk sensor to the slider sensor.

The results, shown in Figure 62, have some 50Hz electrical mains pickup present. A future improvement would be to include a high pass filter in the system, suppressing this 50Hz signal. The period of the signals was 1.85ms, measured from the Tektronix oscilloscope. The disk on the drive under test spun anti-clockwise, looking from above, such that a fixed point on the disk would pass the slider sensor position before the disk sensor. The time delay between the measured peak displacements of the slider and disk was approximately 0.75ms. This figure is very close to the expected 0.71ms and indicates that little phase difference is present. However, the difference in phase is suspected to be very small due to the small head-disk separation. The signals' restricted resolution limit

the accuracy of phase measurement to currently prevent accurate head-disk phase behaviour measurements.

The lens of the head unit must be positioned 2.9mm away from the reflection surface. This imposes physical obtrusions on the system. To construct a transparent window to observe the operation requires a large indent to get the head units close enough. Also the window itself must not behave as a diaphragm when vibrated, as this will make the measurement system obtrusive. It is for this reason the profile of the window is restricted. The indent in the window has the effect of altering the aerodynamic influence of the slider. The fact that the lens must be very close to the surface being measured, and the unit is physically large compared to the slider, makes it very difficult to align the system.

The operating range of the standard compact disc read optical system is only 0.2mm. This limits the level of magnitude that the hard disk can be vibrated to just less than 0.2mm. This has been found to limit the severity of resonance peaks experienced.

However, despite the above drawbacks, the compact disc reader optical system represents a very economical means of measuring displacement with potentially great sensitivity.

Chapter 8. Finite Element Analysis

8.1 3D Modelling of the Disk Using Finite Element Analysis

Finite element analysis software from PTC, located in Needham, Massachusetts, USA, has been used to model the resonant characteristics of hard disks. Pro Engineer V20 was used to develop the physical structure of the models and Pro Mechanica motion was used to simulate the models' behaviour when vibrated. Models were created to determine the modal response for both free and clamped disks. In order to model the disk it is necessary to know both the material and geometric properties as parameters of the model.

When the disk resonates, the standing wave created differs in form depending on the mode of resonance at which it is excited. The waves either travel from the inner diameter of the disk to the outer diameter, radially around the disk or combinations of both. Common notation [34] has defined these modes as having m nodal circles and n nodal diameters, designated as (m,n), Figure 65 From McAllister shows modes (0,0) to (0,3).

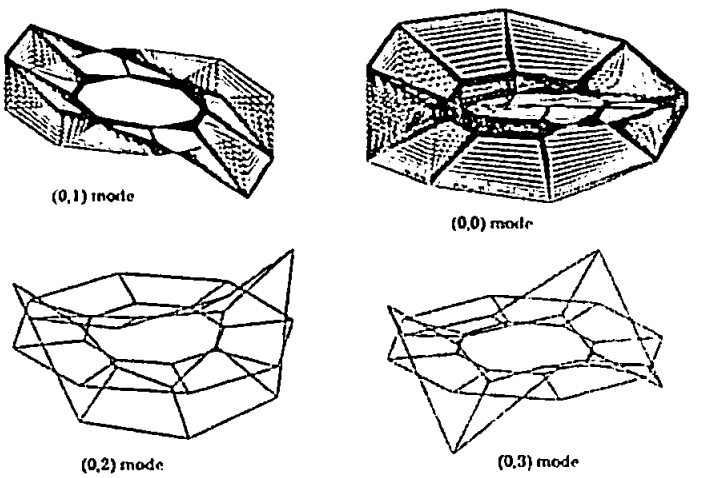

Fig. 65. Graphical representation of the modal designation of the hard disk, as presented by McAllister [34].

When modelling an object some thought must be given to the intricacy of the model. If the model is too complex it will take excessive time to simulate its behaviour. If the model is too simple the results will not be accurate enough to predict the measured results. Therefore a compromise must be made. It was found that the assumptions used here in the modelling had only a minimal effect on the outcome.

IDEMA* standards for hard disk drive substrates dictate that the disk edge should be chamfered for 0.178mm at an angle of 25 or 45 degrees [32,33]. However, to simplify the model the disk was assumed to be rectangular in cross section. Another limitation of finite element modelling, incurred by the finite element mesh size, prevents the disk from being a totally accurate circular model.

It is known that [34,78,79] the disk's resonant frequencies will be slightly altered due to the gyroscopic effect of the disk spinning. Further to this, it is also understood that due to the static position of the PVDF sensor and the nature of the disk's resonant undulations, a condition is created where the sensor detects two modes instead of the one static resonant frequency. These resonant peaks are detected at the static resonant frequency, modulated by the disks' rotational speed. The only mode that does not suffer from this effect is the 'umbrella' mode, where the entire outer circumference oscillates.

The first models were devised to discover whether different aluminium alloys significantly affected the disks' performance. Two disks of identical dimensions, 1.25mm thick with internal holes of 25mm diameter and total diameter of 95mm, one

*The International Disk Drive Equipment and Materials Association (IDEMA) is an international not-for-profit trade association that represents the HDD industry and its infrastructure. Founded in 1986, IDEMA provides more than 500 corporate and individual members worldwide with trade shows, technical conferences, symposia, education classes, networking events, and an active international standards program. It has an Executive Advisory Council (EAC) comprised of top industry executives: Bill Watkins (Seagate), Mike Cannon (Maxtor), Matt Massengill (Western Digital), Ichiro Komura (Fujitsu), Wayne Fortun (Hutchinson Technology), Ed Braun (Veeco Instruments) and John Dean (Salomon Smith Barney). www.idema.org

made of AlMg and the other pure aluminium were modelled. The results are shown in Table 5. The disks were meshed with 5 radial lines and 24 intersecting sections, shown in Figure 66.

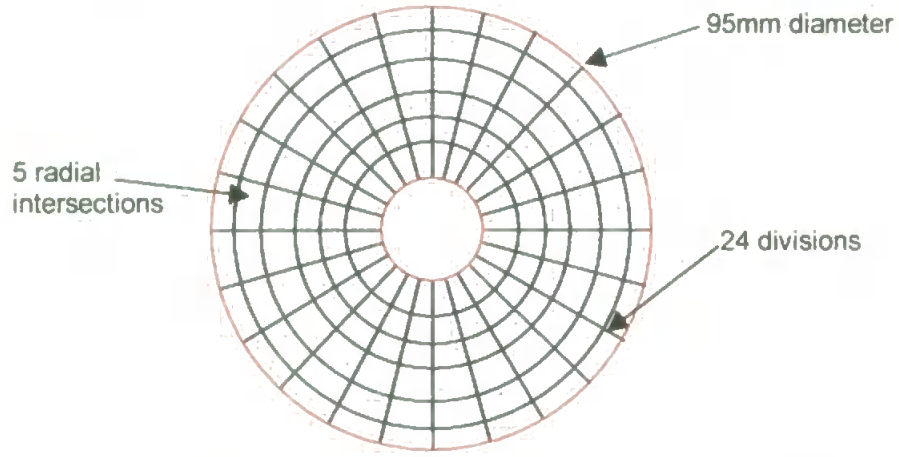

Fig. 66. Diagram showing meshing for the model of disk.

Model	Diameter	ID	Thickness	Density	Young's Modulus
a	95mm	25mm	1.25mm	2.66g/cm^3	71GPa
b	95mm	25mm	1.25mm	2.70g/cm^3	70GPa
c	95mm	25mm	1.25mm	2.66g/cm^3	71GPa
d	95mm	27mm	1.25mm	2.66g/cm^3	71GPa
e	95mm	33mm	1.25mm	2.66g/cm^3	71GPa
f	95mm	25mm	0.8mm	2.66g/cm^3	71GPa

Table 4. Definition of the physical properties of the disks modelled throughout this chapter.

	a.) AlMg	*b.)* Aluminium
Mode	Frequency/Hz	Frequency/Hz
1	427	423
2	427	423
3	465	461
4	792	784
5	792	784
6	1707	1690
7	1707	1690

Table 5. Table of results from finite element analysis of identical disks constructed from AlMg alloy and pure aluminium.

This test demonstrated that the mixture of aluminium alloy did not significantly effect the resonant modes of the disk. This is due to the Young's modulus properties of aluminium alloys not being greatly different, around 70Gpa [22,23].

The next test was undertaken to discover the effect of changing the diameter of the inner hole, the results are shown in Table 6. These models are a first step towards modelling the clamped disk on a real hub. The clamp used in a real hard disk drive has an outside diameter of 33mm, shown in Figure 68, and hence was one if the inner diameters for the disk chosen. An intermediate disk, with an inner diameter of 27mm was also modelled. The disk modelled was again a 1.25mm disk with an overall diameter of 95mm and made from AlMg.

	c.) 25mm ID	*d.)* 27mm ID	*e.)* 33mm ID
Mode	Frequency/Hz	Frequency/Hz	Frequency/Hz
1	427	442	485
2	427	442	490
3	465	469	490
4	792	805	853
5	792	805	853
6	1707	1711	1731
7	1707	1711	1731

Table 6. Results from Pro-Mechanica showing the resonant modes for disks with differing internal diameter holes.

The clamped disk has been modelled in three stages. Initially the disk alone is modelled. The second stage involved perfectly bonding the aluminium disk spacer to the under side of the disk. The spacer is used to separate the disks in the disk pack, creating physical spacing of the disks, and therefore is in contact with one surface of the disk. Finally the steel clamping plate was added to the model, as depicted in Figure 67 with dimensions shown in Figure 68. The results shown in Table 7 illustrate that the plate had little influence on the system once the spacer had been introduced, accounting for only minor changes in the disk's frequency response.

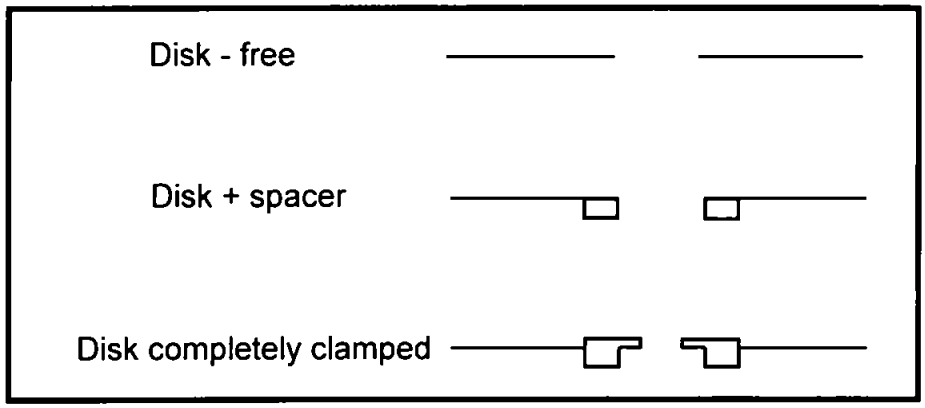

Fig. 67. Profiles of three disk and clamp variations used in the finite element analysis modelling.

Disk - Free /Hz	Disk + Spacer /Hz	Disk completely clamped /Hz
431	687	687
468	1165	1165
799	1694	1694
1719	2595	2595

Table 7. Results obtained from finite element analysis modelling of a 1.25mm thick disk, varying clamp configurations, showing the different modal frequencies.

The model was then applied to the 0.8mm disk. As expected the modal frequencies were lower for the more flexible 0.8mm disk, shown in Table 8.

f.) Disk /Hz	Disk completely clamped /Hz
277	440
298	742
512	1082
1097	1672

Table 8. Results obtained from modelling a 0.8mm thick disk, for both clamped and unclamped configurations, showing the different resonant frequencies.

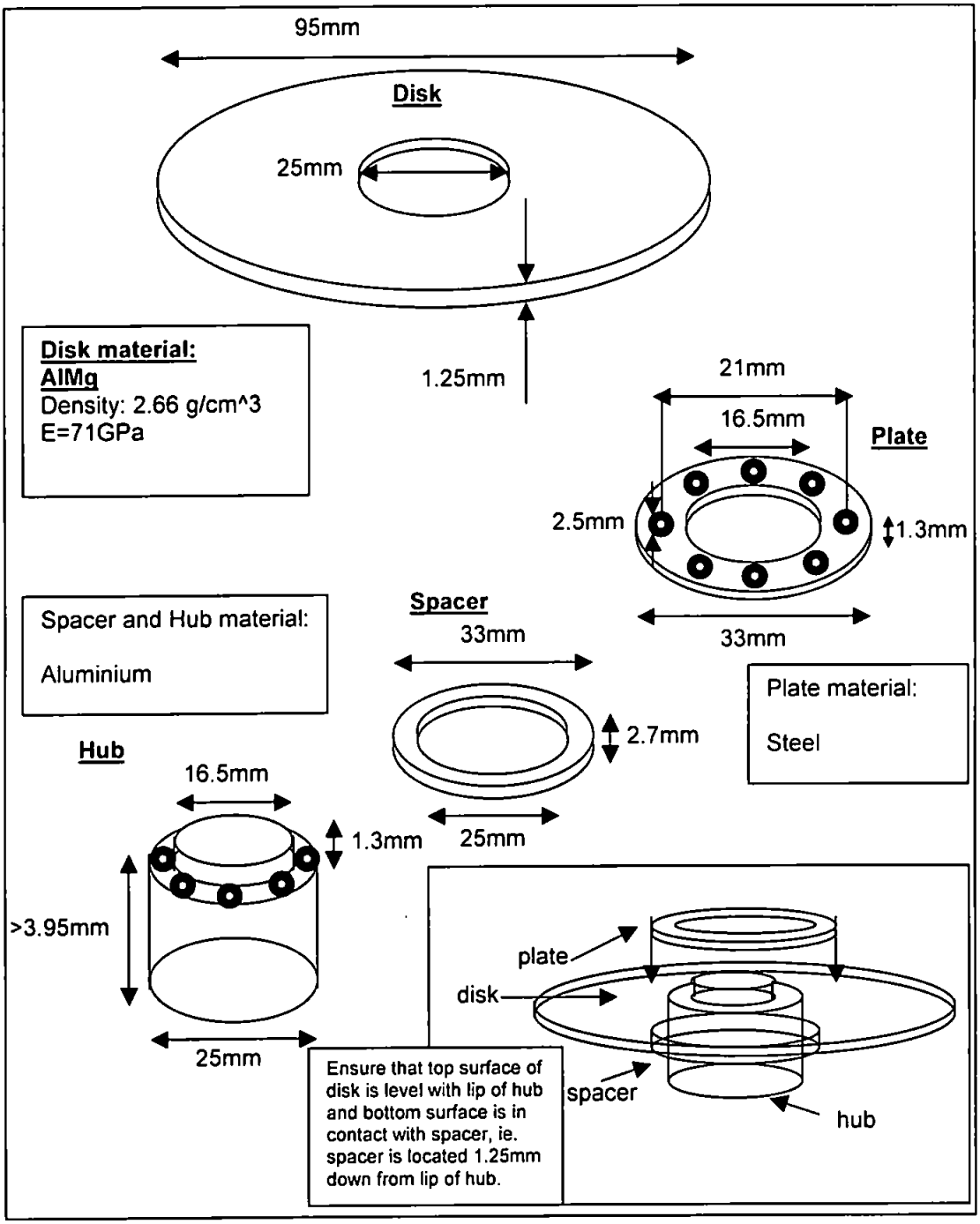

Fig. 68. Diagram outlining the key dimension and materials used for modelling the disk using ProMechanica Finite Element Analysis software.

8.2 Discussion of Finite Element Analysis Results

Several modes were observed in the frequency range of 10Hz to 10kHz, some maybe less significant than others. The lower order modes have been found to be those most destructive to data-transfer. A variety of different modes are shown in Figure 69, the potentially most troublesome 'umbrella' mode being shown in (a) and (b).

The modal frequencies of the free disk alone were slightly lower compared to the clamped disk. The clamp sandwiches the disk with a steel plate screwed into the aluminium hub, an aluminium spacer supports the disk from the other side. This has the effect of reducing the disk's span, stiffening it and raising the disk's resonant frequencies.

The thicker 1.25mm disk's resonant frequencies are higher than those of the thinner, 0.8mm disk. This has the effect of extending the drive's operational bandwidth under conditions of vibration from 440Hz to 690Hz.

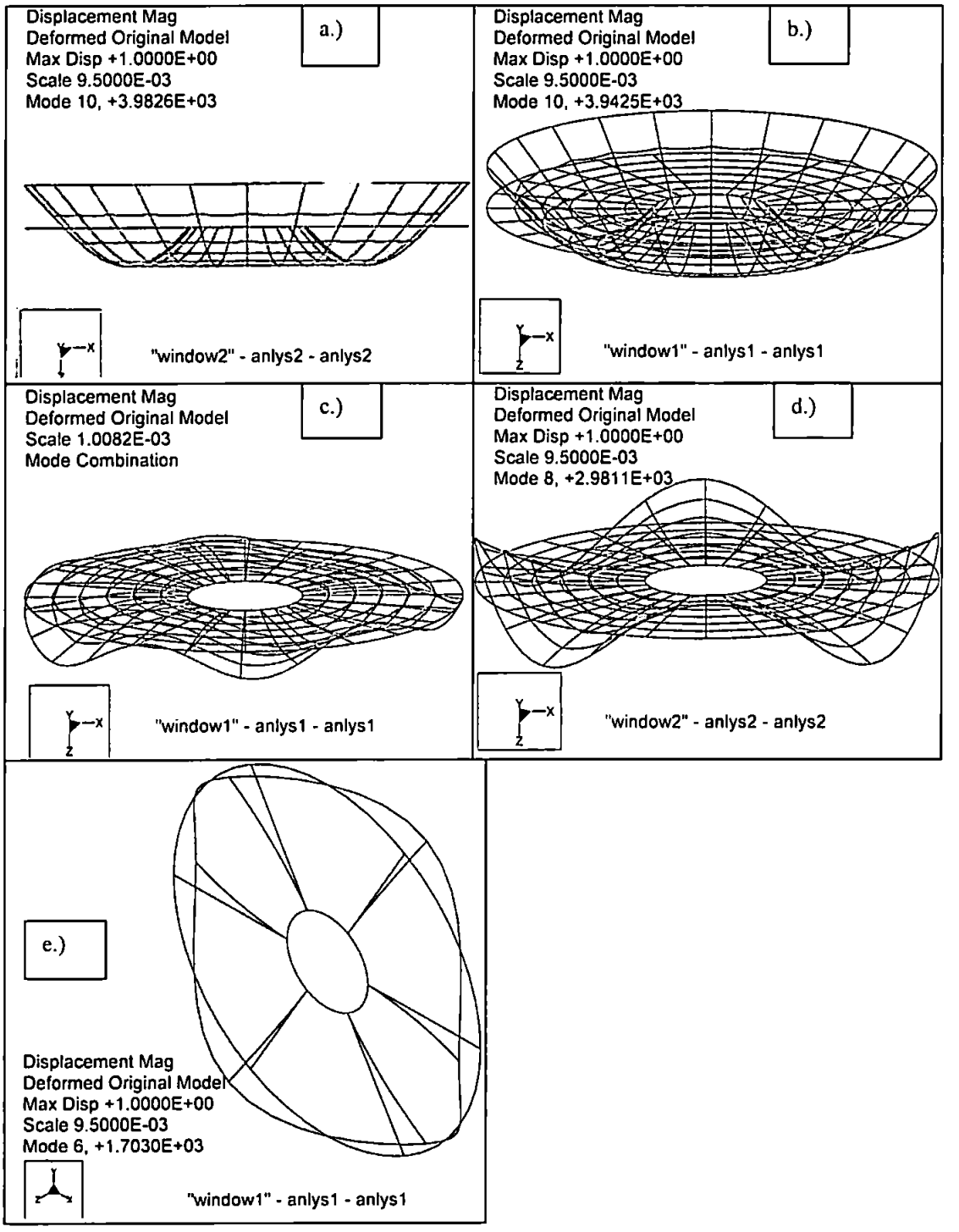

Fig. 69. Results from Pro-Mechanica showing the resonant modes: the upper two show the "Umbrella" mode.

9. Results and Discussion

It has been observed for all the hard disk drives tested that there are prevalent problems at frequencies around 450 Hz to 700 Hz. This is largely a feature of 0.8mm thick AlMg disks. It has been observed, shown in Figures 40 and 41 in Section 6.1, with most drives that a mere 0.5g of acceleration at key frequencies; 475, 525, 575 Hz, is enough to render the disk unable to transfer data.

The magnetic state of data has not been found to effect significantly the drive's performance. Figure 39, Section 6.1, shows only minor changes in data transfer performance of the drive whilst suffering induced vibration, which are attributed to limitations in accuracy from the piezo-electric accelerometer and the noise it experiences, explained in Section 5.1.

The drive, when tested at three individual frequencies; 500Hz, 550Hz and 600Hz, showed a tendency to be more immune to vibration when the head was positioned closest to the hub of the disk, shown in Figure 42, Section 6.1.

The tracking servo requires information to determine where to move the head to keep it on track. The servo information is stored on the disk at fixed points around the disk, between each sector. When the head is running at its outermost perimeter the physical distance between the servo data is greater. This means that the head has a greater distance to follow the track without servo information and hence has a greater chance of going off track, even though the time between servo data points is always equal, due to the rotational speed of the disk being constant. Therefore it is likely that the drive is more prone to transfer failures when the

head is reading the outer diameter of the disk, although this is not a factor greatly contributing to drive unreliability.

The greatest influence on drive performance operating under hostile conditions has been found to be disk flexing, both radial and circumferential, with disk displacement being greatest at its outer edge, shown in the results from finite element analysis modelling of the disk, clearly seen in Figure 69 a.) and b.), Section 8.2.

Figure 42 shows that the drive was not affected at 550Hz by the head's radial position. This is due to the disk not being the sole contributing factor, at this frequency, towards limiting drive performance under conditions of vibration. The drive's poor performance at this frequency is attributed to the suspension arm moving, observed in Figure 51, and the hub rocking through bearing tolerances [35,36].

The results from driving the disk with white noise with an accelerometer attached to the disk's edge, see Figure 36, showed an interesting fact. It can be seen that the disk, even though clamped, was still driven in its unclamped form to resonance due to an imperfect clamp. This was discovered from finite element analysis undertaken for the 1.25mm thick disk. The disk's (unclamped) resonant frequencies were found to be at 431Hz and 468Hz from the finite element analysis modelling, Section 8.1, Table 7, and are in good agreement with the experimental results, with the measured results being at 450Hz and 490Hz. It can be deduced from these facts that the disks within the hard disk drive are driven at their unclamped resonant frequencies as well as their clamped frequencies.

Considerable work has been undertaken by Bittner and Shen to produce waterfall plots of characteristic disk behaviour under vibration [69]. Table 9

shows their work with the measured harmonics of the disk when rotating at 4500rpm. Their results are compared with the results obtained from the piezo-electric strain gauge, Figures 50 and 51, Section 6.3.

It should be noted that the experiments performed by Bittner and Shen were carried out with the cover of the hard disk drive removed. This would effect the results slightly because the cover seals the drive with the air between the disk and the drive lid behaving as a damper.

Mode of Resonance	**Frequency / Hz** Measured by Bittner and Shen [69]	**Frequency / Hz** Results obtained in this work from the piezo-electric sensor
1st bending	550	515
2nd bending	585	590
Diaphragm (umbrella)	640	630
1st bending	680	660
2nd bending	850	855
3rd bending	920	940
3rd bending	1350	1375
4th bending	1600	1600

Table 9. List of results obtained empirically from other work compared to results obtained with novel piezo-electric strain gauge cantilever.

McAllister, [34], describes how when vibrations are "measured with a stationary probe, the observed amplitude will be modulated by the rotation frequency times the number of nodal diameters." This explains why there are two

distinct frequencies for each mode of resonance shown in Table 9, one with the rotational speed of the disk (75Hz) added to the resonant wave of the disk, the other subtracted.

The combination of the results obtained from measuring both the disk and suspension arm movement reveal some interesting facts, as shown in Figures 50 and 51, Section 6.3. The first observation was confirmation of the disk's rotation speed. From the spectral response of disk movement it can be seen that the disk's rotation speed is 4500rpm, found from the peak at 75Hz, Figure 50. The disk is slightly buckled when clamped onto the hub, and this causes vertical runout that the sensor is detecting. The subsequent peaks at 150Hz, 225Hz, 300Hz and 375Hz are harmonics of the 75Hz fundamental.

The results, from impacting the hard disk drive, show the disk to be driven into large excitation at 440 Hz. Disk movement at this frequency is so great that its displacement is coupled to the suspension arm. This is observed in the results for the suspension arm measurement, Figure 51, Section 6.3. The 440Hz resonance is the clamped disk's first mode of resonance, as confirmed through finite element analysis, Table 8, Section 8.2. It is at this frequency that the hard disk drive's data transfer performance, Figures 40 and 41, is most susceptible to vibration. In both cases 440Hz being the most sensitive frequency, proving that the disk's bending is the greatest contributing factor to drive data transfer performance under conditions of vibration. There is a lot of modal disk activity between 590Hz and 740Hz. This disk movement is mimicked by the suspension arm as the head and slider try to maintain a correct flying height.

At 1kHz the suspension arm clearly goes into resonance. However, there is very little movement in the disk at this frequency, which means the flying height

is fluctuating, ultimately leading to the head crashing into the disk. In fact the only time a hard disk drive being tested suffered from permanent damage was when it was vibrated at 1kHz. The suspension arm then goes into resonance once again at 1290Hz, 1450Hz, 2000Hz, 2250Hz, 2525Hz and 2870Hz. The suspension arm going into resonance was in fact large enough to cause the disk to bend at around 1kHz and 1290Hz. Not all of these modes are in the vertical, flying height, plane. Some will cause the tracking problems through arm twisting [79]. Others are from the suspension arm rocking, simply tilting the head. Figure 52, Section 6.4, identifies major tracking problems that occur between 1750Hz and 2000Hz. This reinforces the theory that the suspension arm activity at 2kHz is attributed to the tracking plane resonance of the suspension arm. Further evidence is the lack of disk flexing at these frequencies.

Figure 70 shows the results from the white noise vibration of the hard disk drive, observed by the PVDF sensors. The top graph shows the response of the disk, with all the significant peaks highlighted, and the bottom graph shows the frequency response of the suspension arm, again, with all the significant peaks highlighted. These peaks are cross-referenced with each other and the results gained from the finite element analysis modelling and shown in Table 10.

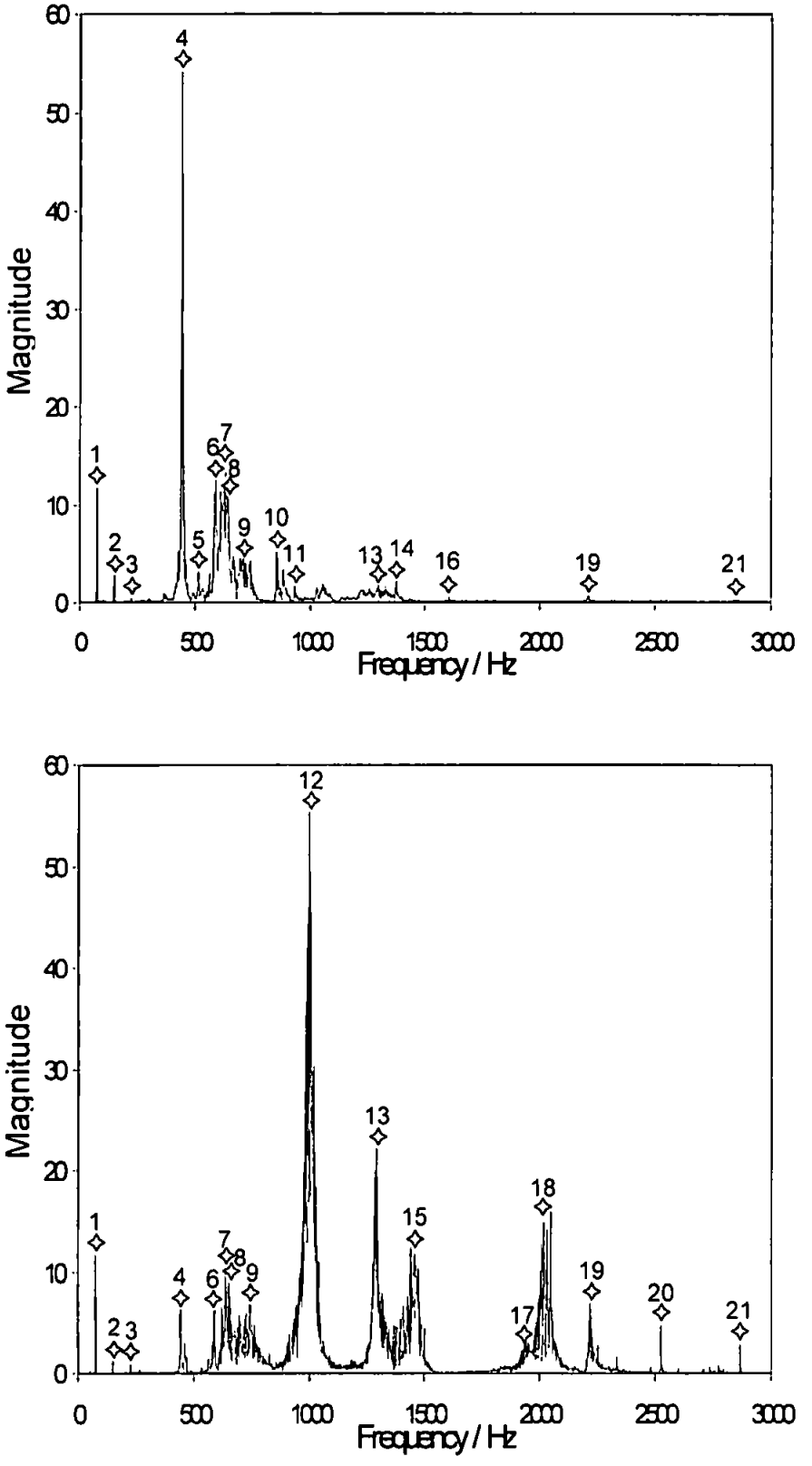

Fig. 70. Graphs showing the frequency response of the hard disk (above) and the suspension arm (below) with the resonant peaks highlighted.

High-lighted peak	Frequency of peak in Fig. 70	Resonant Component	Observed through
1	75	Buckled disk	
2	150	Uneven disk clamp	
3	225	Uneven disk clamp	
4	440	Clamped disk first mode	Finite element analysis
5	515	Unclamped disk first mode	Finite element analysis
6	590	Disk motion	Mimicked in suspension arm motion generating tracking error problems
7	630	Disk motion	Mimicked in suspension arm motion
8	660	Disk motion	Mimicked in suspension arm motion
9	740	Clamped resonant mode	FEA, generates minor tracking problems
10	855	Disk motion	
11	890	Disk motion	
12	1000	Suspension arm resonance	
13	1290	Suspension arm resonance	Coupled to disk motion, generates minor tracking problems
14	1375	Disk motion	
15	1450	Suspension arm motion	
16	1600	Disk motion	
17	1940	Suspension arm motion	Generates tracking problems
18	2000	Suspension arm motion	
19	2250	Suspension arm motion	Coupled to disk motion

20	2575	Suspension arm motion	
21	2870	Suspension arm motion	Coupled to disk motion

Table 10. Table of resonant peaks, shown in Figure 70, detected using PVDF sensors.

10. Conclusions

A test system has been developed which enables hard disk drives to be vibrated, at varying levels of amplitude, whilst the data transfer is timed and recorded. The data can be written to the disk, and then read back to confirm it has been correctly written, or just read from the disk. The data file can be comprised solely of '1's, '0's or of a pseudo random string. The magnetic state of the data, either '1's, '0's or a random string, has been found to be insignificant to the performance of the drive whilst being vibrated.

Data loss was found to be most significant at vibration frequencies between 440Hz and 700Hz. At other frequencies hard disk drives are able to transfer data reliably whilst subjected to as much as 45g of vibration. However, between 440Hz and 700Hz they may fail to transfer data at as little as 1g. These data failures can be attributed to two key components: the suspension arm and the hard disk.

The work performed is the first to measure disk and suspension arm motion in a hard disk drive that is both in operation and performing under its normal environment, with its lid on. This is an important contribution to knowledge, providing a clearer understanding of disk and suspension arm activity. The work performed is also solely providing excitation externally to the drive, as it would experience in normal operation. Previously published work has provided results from exciting the disk via impacting the disk itself by dropping either miniature hammers or ball bearings from a known height.

A CD ROM-based optical system has been successfully adapted to measure differentially suspension arm and disk movements. Two individual

sensors of different type have been used for this to test their suitability. One, the critical angle prism type, was found to have a response approximately eight times greater than that of the of the other, quad-detector beam-splitting type. This is more than can be accounted for by the fact that the former has a more powerful 30mW laser diode. Both have a peak operating distance of approximately 2.9mm, and are highly linear in operation.

PVDF sensors have been used to measure unobtrusively the suspension arm and the disk in a novel way. A virtual instrument created using LabView for Windows is capable of monitoring the signals in real-time and can perform FFT frequency sweeps. This rapidly provides the frequency response of the component under observation. The virtual instrument is capable of averaging multiple scans to reduce the noise level, varying the number of samples taken and the frequency of the FFT window to adjust the resolution of the FFT sweep.

Using BIOS commands, software, developed in C, has been developed which allows for the cylinder, head and sector of the disk to be individually selected when transferring data to and from the hard disk drive. This allows the position of the head to be controlled as well as observing any error flags returned by the drive should the drive's error correction be overcome by the vibrations. From this it was discovered that the drive predominantly failed for one reason. When the drive completely failed to transfer data due to vibration it was registering tracking errors. The drive was tested with the head positioned at radial locations across the disk from the inside of the disk to the outside, and this showed the drive's prevalent weakness to transfer data with the head located at the outer edge of the disk.

Finite element analysis software, Pro Mechanica Motion, has been used to model the disk and simulate its resonant activity. The models were created in Pro Engineer V20 and also included a clamp of identical materials and dimensions to that of the clamp used in real drives. The disk was modelled with and without the perfectly bonded clamp. The results show that the disk's first mode of resonance changed from 277Hz to 440Hz when clamped, proving that the clamp acts to stiffen the disk significantly.

The PVDF sensor detected the disk's vertical run-out, and through the FFT sweep performed by the LabView software the disk's rotational speed has been confirmed as 75Hz, 4500rpm. Harmonics of this have been detected at 150Hz and 225Hz, caused by buckling from the disk's clamp. Further resonant peaks have been detected at 440Hz and 515Hz. These modes have been confirmed from finite element analysis to be the disk's first mode of resonance when perfectly clamped and its third mode when unclamped. Therefore the disk is resonating at both its clamped and unclamped frequencies, indicating that the disk is not perfectly clamped.

It was found, experimentally, that when the disk goes into resonance the movement is such that the disk and suspension, coupled via the air bearing, move synchronously together. However, there is an initial lag between disk motion and arm motion. This creates a variation in the flying height, a major contributing factor to data transfer errors. The air bearing is acting as a damper for the coupled movement, which has a further effect on the head's flying height. Suspension arm displacement has been observed to peak at 1kHz. The disk, however, does not experience a similar movement. This indicates that there is a flying height variation at this frequency and hence a potential weakness in drive operation.

This information gained through this work will help enable future hard disk drives to operate under wider conditions of shock and vibration then at present. Critical frequencies have been discovered and, by using a combination of novel sensors, the failure mechanisms identified. Future drives will almost certainly at some stage include active control of the suspension arm through use, probably, of a piezo-electric actuator as described in this thesis. Knowing the frequencies, amplitudes and modes of resonance also aids the design of the control system, which will be used to regulate the flying height of such a head.

11. Further Work

11.1 Optical Measurement Techniques

An optical system that has a reasonably large dynamic range and great sensitivity is required for the type of measurements made during this work. A CD ROM-based optical system has been developed to achieve this and used as a first step towards differentially measuring flying height variations. This system has been found to be lacking in dynamic range and the limited focal distance forcing restrictions on the system. The two CD optical units used are of slightly different types, although they both use quadrant detectors for focusing; one uses the critical angle prism method and the other a beam splitting prism.

There are a few ways of altering the beam splitting prism focal distance, and hence range in this application. One would be to move the quadrant detector array closer to the beam splitting prism. This would have the effect of moving the laser spots, from their previously too great a focus distance position, towards the middle of the detectors, restoring their 'null' position, as shown in Figure 71.

Another method would to be to change the objective lens to another one of different focal length, thus focusing the beam to a point much further away. Alternatively a second lens could be fitted to achieve this. Changing the lens, or adding lenses is not a preferred method as it does add cost, complexity and potentially adds bulk to the system.

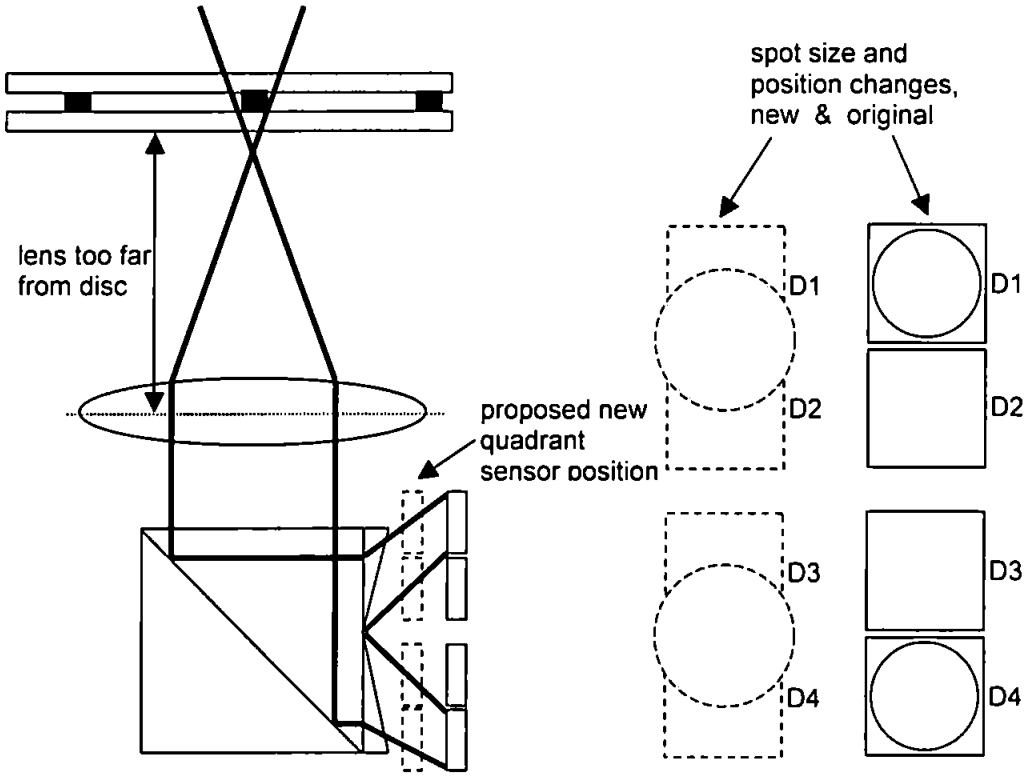

Fig. 71. Diagram showing proposed revision to quadrant sensor position to increase focal and working distance for the beam splitting prism type of CD optical unit.

To increase the operating distance the critical angle prism would need to have the prism twisted slightly to make the emitted beam closer to orthogonal with the surface being observed. This would allow a greater distance between the surface and the prism for a given optical path, refer to Figure 55 in Chapter 7 to see how this is illustrated.

11.2 Tracking Motion Disturbances

When the drive is in operation the data is stored on the magnetic disk in catalogued fragments throughout the disk. The location of data is not necessarily uniform and constant throughout. Naturally the obvious means of storing data is to stream one file or program after the other around the disk. However, when one file is deleted an 'empty' area is left on the disk. The next file that might be required to be stored on the disk may be too big to fit into the space left by the previous file. Hence this file will be either split up to fit into multiple 'gaps' or will be stored elsewhere where more file space is available, shown in Figure 72 for a simple representation.

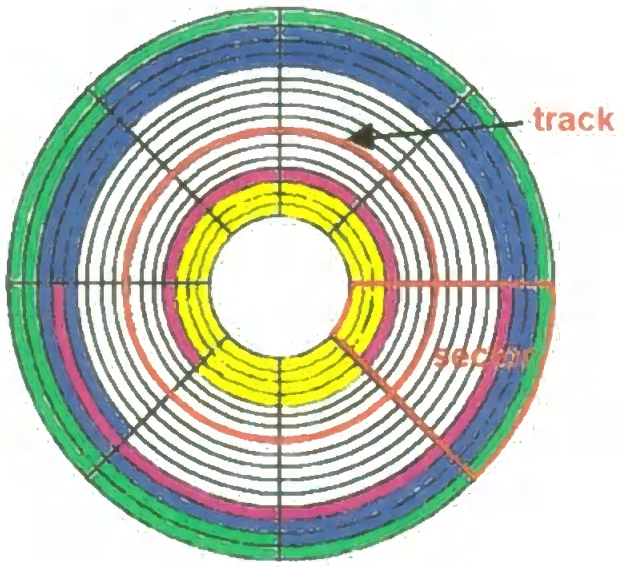

Fig. 72. Diagram showing a simple representation of data allocation on a disk. The magenta cells represent a file that has been split and placed in gaps in data created through file removal.

By virtue of having files fragmented throughout the disk, when reading just one file the head might be required to scan across the disks in many steps. To do this

the tracking arm traverses the head across the disk as quickly as it can. Due to the fact that the head, suspension arm and slider all have mass, they exhibit momentum and do not settle to their new position instantly. Even when the tracking servo stops, the head and suspension arm etc will try to continue beyond the predicted position. This system, largely made from spring steel, has little in the way of natural damping. The air bearing will act as the principle damper to this system, but acts predominantly in the vertical, flying height, plane. As a result, a lot of overshoot is present, as has been widely discovered [80]. The proposed passively damped drive mounts have been evaluated to counteract this phenomenon [81] but bulky mounting mechanisms are not the ideal solution. This overshoot in the tracking system causes poor data transfer through the system due to erroneous signal detection caused from off track cross-signals.

Therefore when the head arcs across the disk there is a finite period of tracking oscillation. This oscillation is largely due to the suspension arm bending in its lateral plane, or rocking, as shown in Figure 73.

Rocking of the slider, from suspension arm rocking, will have the affect of reducing the head and slider area directly above the data bit. As the head is twisted it rotates out of the plane that it is designed to operate in, potentially reducing the thickness and stability of the air bearing. Since the slider's design is optimised for flying with zero twist, rocking of the slider will impair its aerodynamic thrust (be it positive or negative thrust) and render the head more susceptible to flying height variations due to vibration. The slider will eventually stabilise this, since it is designed to self-stabilise aerodynamically. However, there will still be a finite time for complete stabilisation.

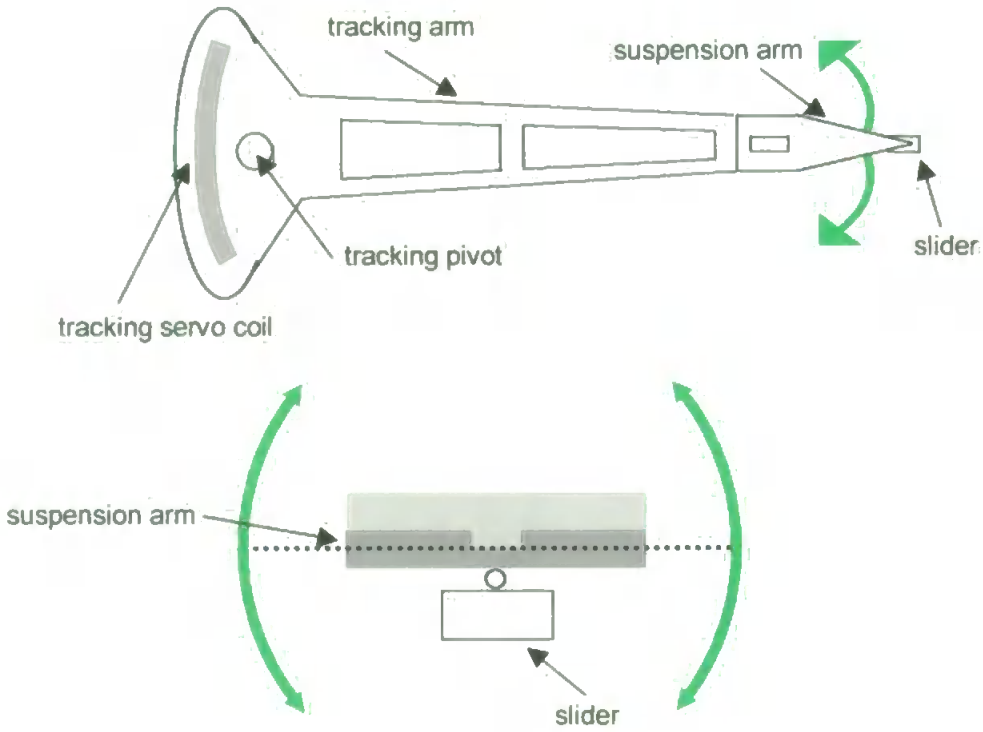

Fig. 73. Diagrams representing the main forms of suspension arm deformation during rapid tracking changes.

The piezo-electric sensor mounted on the root of the suspension arm can be used to detect the lateral modes of resonance. These lateral modes exist in the sensor's least efficient mode of operation, its g_{33} mode.

The rocking motion encountered by the sensor can be averaged out over the whole sensor area. This is due to piezo-electric sensors measuring the average induced strain. Over the entire area of the sensor in its g_{31} and g_{32} modes the net strain will be zero when the arm is purely rocking. To overcome this the sensor can be split down the centre, as shown in Figure 74. This creates two individual sensors, hence requiring two channels to monitor, but capable of measuring the motions of the arm from side to side. Polarity sensitivity would provide essential information. If both sensors were of the same polarity the arm would therefore have to be bending uniformly up or down. If, however, the two signals were not of the same magnitude or

taken to an extreme, different polarities, then the arm would therefore be rocking with or without a coupled bending deformation.

If the sensor were to be split it would be very important that both sections are of identical area. Failure to achieve this would result in unequal voltage measurements from side to side. This can be accounted for, if the differential response of the two sensors is known, however it would be impractical to account for any 'zigzagging' of the division caused by machining tolerances.

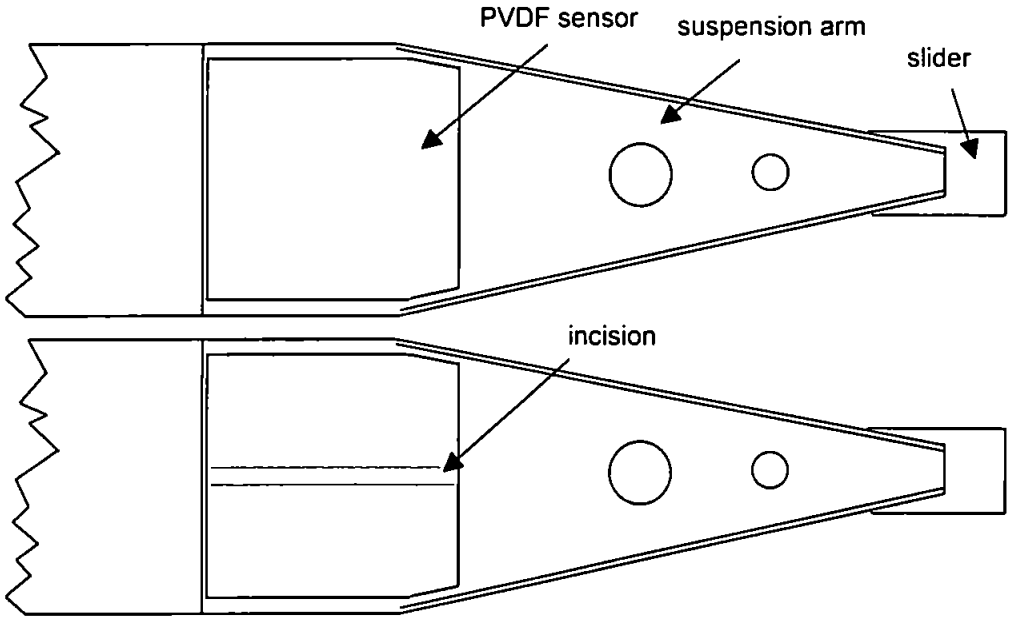

Fig. 74. Diagram representing the PVDF sensor and how it is positioned on the suspension arm, and how it could be modified by separating it into two equal sensors to observe rocking motions.

11.3 Piezo-Electric Control of Suspension Arm

One of the major obstacles to overcome when trying to control the head in this manner is the problem that the actuator is operating at the base of the cantilever. Therefore it is operating very close to the fulcrum and whilst any motion it provides is

magnified through the cantilever's length, any force present at the head, located at the end of the cantilever/suspension arm will also be magnified. This means that the actuator, although providing sufficient motion for the head is lacking the driving force to move the head should a significant load be present.

The force generated from the air bearing of a typical sub-ambient tri-pad slider has been found, experimentally by Khurshudov and Talke, to be between 1mN and 2.5mN [82]. The 1mN to 2.5mN force generated from the air bearing represents less than 10% of the typical suspension arm load. For example, a suspension arm could be pretensioned against the disk with a 3mg load suspension arm, see Figure 37, Chapter 5.

2.5mN / 9.81 = 0.255mg

Whilst this air bearing force is not large in comparison to that of the suspension arm it has been found to be significant towards defeating the actuator's control of the head.

It has already been discussed in Chapter 1 how the take-off procedure for the head is mechanical and very crude. The head literally scrapes across the disk whilst the disk increases its rotational speed until enough airflow is created to allow the slider to fly off the disk. To reduce the mechanical wear between the head and the disk, the piezo-electric actuator on the arm could be driven to lift the head physically off the disk just prior to the disk spinning up. This way any scraping between the head and the disk due to disk start-up can be eliminated. If the drive is of the ramp variety, such that it parks the heads up on a ramp in non-operation, there is still friction and scraping between the suspension arm and the ramp. Whilst this scraping does not

wear the head or disk it still creates micro-contamination [12,13,14] contributing to long term drive failures. In the same way that the piezo-electric actuator can be used to lift the head off the disk it is possible to lift the suspension arm off the ramp, to an extent.

If the head system is to be optimised for use with a piezo-electric actuator to control lift-off and parking then the aerodynamics of the slider will need to be adjusted to match that of the new system. The slider will probably need to generate a slightly lower total operational force because the piezo-electric actuator will be contributing to add and to detract from this force to control flying height variations. The low disk speed aerodynamic characteristics will also need to be altered to account for the piezo-electric actuator lifting the head up off the disk on start-up and gently placing the head back down on power down.

11.4 Sensor-Actuator Integration

The piezo-electric elements work as both sensors and actuators, as described previously in Chapter 4. The extent of how well they work as either is predetermined through their structure and material. A piezo-electric actuator, through its very nature, will work as a sensor, albeit at a reduced performance to that of a dedicated sensor. It is therefore possible to multiplex the piezo-electric transducer's tasks to include both sensing and actuation.

Integrated sensor-actuators have been developed already in research. The main advantages of using an integrated sensor-actuator is that it reduces the cost, complexity, mass and total size of the system.

12. References

[1] The Era of Magnetoresistive heads, http://www.storage.ibm.com/hdd/ipl/oem/tech/eraheads.pdf , IBM.

[2] Coding for Digital Recording, John Watkinson, ISBN 0-240-51293-6

[3] Coding Techniques for Digital Recorders, Kees A. Schouhamer Immink, ISBN 0-13-140047-9

[4] APS News Online, www.aps.org/apsnews/0301/030111.html

[5] Rock-Solid Server Hard Drive puts IBM back on Top http://www.storage.ibm.com/hdd/press/20020709.htm, IBM.

[6] Naohiko Ishimaru. Experimental Studies of a Head / Disk Interface Subjected to Impluse Excitation During Nonoperation. *Journal of Tribology*, Vol. 118, October 1996, p807-812.

[7] E. Schrek, R. Kimball and R. Sonnenfeld. Magnetic Readback Microscopy Applied to Laser-Texture Characterization in Standard Desktop Disk Drives. *IEEE Transactions on Magnetics*, Vol. 34, No. 4, July 1998, p1777-1779.

[8] Jia Jay Liu and Wenjun Li. Tribology Optimization of Laser Zone Texture Using a Green CW Laser. *IEEE Transactions on Magnetics*, Vol. 35, No. 5, September 1999, p2373-2375.

[9] B. M. Barnes, J. J. Kelly, J. F. MacKay, W. L. O'Brien and M. G. Lagally. Correlations Among Sputter Pressure, Thickness, and Coercivity in Al/Co/Cu Magnetic Thin Films. *IEEE Transactions on Magnetics*, Vol. 36, No. 5, September 2000, p2948-2950.

[10] Y. Liou, ching-Ray Chang, C. K. Lo, C. P. Chang, Y. D. Yao. Influence of Chromium in Co/Cr(100) Multilayers. *IEEE Transactions on Magnetics*, Vol. 33, No. 5, September 1997, p3652-3654.

[11] Raymond-Noël Kono, Myung S. Jhon, Hyoung J. Choi and Chul A. Kim. Effect of Reactive End Groups on the Rheology of Disk Lubricant Systems. *IEEE Transactions on Magnetics*, Vol. 35, No. 5, September 1999, p2388-2390.

[12] Li Hong Zang and Ramesh Koka. Lost data: How a little dirt can do a lot of damage. *Data Storage*, March 1999, p15-20.

[13] Lihong Zhang, Ramesh Koka, Yewwah Yuen and Edwin Lam. Particle Induced Damage on Heads and Discs Due to Fine Particles of Different Materials. *IEEE Transactions on Magnetics*, Vol. 35, No. 2, March 1999, p927-932.

[14] Shuyu Zhang, Larry Wang, Paul Jones, Gerald Lopatin. Numerical and Experimental Study of the Particle Contamination in a Head/Media Interface. *IEEE Transactions on Magnetics*, Vol. 36, No. 5, September 1999, p2442-2444.

[15] Wei Yao, David Kuo and Ramesh Sundaram. Dynamics of Glide Head in the Proximity Contact Regime. *IEEE Transactions on Magnetics*, Vol. 35, No. 5, September 1999, p2469-2471.

[16] Joshua C. Harrison, Kenneth J. Altshuler, and Chris M. Huynh. An Explanation of the Observed Frequency Domain Behavior of Head-Disk Interface Resonances in the Proximity Recording Regime. *IEEE Transactions on Magnetics*, Vol. 35, No.2, March 1999, p933-938.

[17] M. Suk and D Gillis. Effect of Slider Burnish on Disk Damage During Dynamic Load/Unload. *Transactions of the ASME Journal of Tribology*, Vol.120, April 1998, p332-338.

[18] Shuyu Zhang and David B. Bogy. Variation of the Heat Flux Between a Slider and Air Bearing when the Slider Flies Over an Asperity. *IEEE Transactions on Magnetics*, Vol. 34, No. 4, July 1998, p1705-1707.

[19] Li Chen, David B. Bogy and Brian Strom. Thermal Dependence of MR Signal on Slider Flying State. *IEEE Transactions on Magnetics*, Vol. 36, No. 5, September 2000, p2486-2489.

[20] Nano magnetism, http://csns.snu.ac.uk.kr/content/magne/magne.htm

[21] Magnetic Recording Technology, Second Edition, C. Dennis MEE and Eric D. Daniel. ISBN 0-07-041276-6

[22] ASM Handbook. Volume 2. Properties and Selection: Nonferrous Alloys and Special-Purpose Materials. ASMInternational. The Material Information Society. 10th Edition, ISBN 0-87170-378-5.

[23] Smithells Metals Reference Book. Seventh Edition. Brandes Brook, ISBN 0-7506-1020-4.

[24] N Dennis. Wideband Passive Mechanical Mounting Systems for Disk Drives on Boats in Rough Seas. *IEEE Oceans* October 1997, p1488-1495.

[25] J. S. McAllister. Characterization of Disk Vibrations on Aluminium and Alternate Substrates. *IEEE Transactions on Magnetics*, Vol. 33, No.1, January 1997, p968-973.

[26] Baekho Heo and I. Y. Shen. Taming Disk and Spindle Rocking by Damped Laminated Disks - An Experimental Study. *IEEE Transactions on Magnetics*, Vol. 35, No. 5, September 1999, p2304-2306.

[27] David Kuo, Ramesh Sundaram, Nagappan Thangaraj, Jin Hui Ou-Yang and I-Yeu Shen. Mechanical Performance Of Laminated Discs, *IEEE Transactions on Magnetics*, January 2000, p166-170.

[28] Jaing Z. Head Disk Interface Subjected to Impulsive Excitation. *prepr of Jpn, soc Mech Eng.* No 920-67, 1992, p75-78.

[29] Suresh Kumar, Vijay D. Khanna, M. Sri-Jayantha. A Study of the Head Disk Interface Shock Failure Mechanism, *IEEE Transactions on Magnetics*, Vol. 30, No. 6, November 1994, p4155-4157.

[30] Schrek E. Magnetic-Readback-Mapping and its Application to Slider/Disk Interface Damage due to Shock Impact, 1994, STLE Special Publication, SP-16, p5-10.

[31] T. Kouhei, T. Yamada, Y. Kuroba and K. Aruga. A Study of Head-Disk Interface Shock Resistance. *IEEE Transactions on Magnetics*, Vol. 31, No. 6, November 1995, p3006-3008.

[32] IDEMA standards D15-98, http://www.idema.org/stand/stand_standards.html

[33] IDEMA standards D2-91, http://www.idema.org/stand/stand_standards.html

[34] Jeffery S. McAllister. The Effect of Disk Platter Resonances on Track Misregistration in 3.5 inch Disk Drives. *IEEE Transactions on Magnetics*, Vol. 32, No. 3, May 1996, p.1762-1766.

[35] Joseph Wang. On the Dynamics of Rocking Motion of the Hard-Disk Drive Spindle Motor System. *Advances in Information Storage Systems*, Vol. 7, 1996, p251-267.

[36] C.P. Roger Ku, I.Y Shen. Effect of Disk Flexibility on Rocking Mode Frequencies of a Disk Drive Spindle Motor System. *Tribology Transactions*, Vol. 39, 1996, 3, p579-586.

[37] A. Miller Allen and D B. Bogy. Effects of Shock on the Head-Disk Interface. *IEEE Transactions on Magnetics*, Vol. 32, No.5, September 1996, p3717-3719.

[38] J R. Edwards. Finite Element Analysis of the Shock Response and Head Slap Behaviour of a Hard Disk Drive. *IEEE Transactions on Magnetics*, Vol.35, No.2, March 1999, p-863-867.

[39] Thomas C. McMillan, Frank E. Talke, Joshua C. Harrison. Identification of Slider/Disk Contacts Using the Energy of the Acoustic Emission Signal. *IEEE Transactions on Magnetics*, Vol. 34, No. 4, July 1998, p-1819-1821.

[40] Q. H. Zeng, M. Chapin and D. B. Bogy. Two Calibration Methods of AE Measurement Channels for Slider-Disk Contact Detection. *IEEE Transactions on Magnetics*, September 1999, p-2367-2369.

[41] The Art of Electronics, Horowitz and Hill, second edition. ISBN 0-521-37095-7

[42] Digital Signal Processing, A Practical Approach. Emmanuel C. Ifeachor and Barrie W. Jervis. ISBN 0-201-54413-X

[43] Felix P. Lu and Deva Ramaswamy, Ph.D. Characterization of head and media interface of hard disk drives using acoustic emission and strain gauge measurements at the drive and component level. Micropolis USA September 19th, 1996, University of California San Diego

[44] Thomas Y. F. Liew, M. C. Chai, S. Weerasooriya and T. S. Low. Head-Disk Interaction of Proximity Sliders Studied by the Acoustic Emission Probe, the Dynamic Flying Height Tester, and the Laser Doppler Vibrometer. *IEEE Transactions on Magnetics*, Vol.33, No. 5, September 1997, p3175-3177.

[45] Amei Li, Xinqun Liu, David Jenkins, Warwick Clegg, and Paul Davey. Parameter estimation method for real time flying height detection of hard disk drives. Accepted for presentation at the 8th Joint MMM-Intermag Conference, San Antonio, Texas, January 7-11, 2001. Accepted for publication.

[46] Physics, Parts 1 and 2. Third Edition. David Halliday and Robert Resnick. ISBN 0-471-02456-2

[47] Head Media Dynamics Measurement in Glide and Ramploa, Thomas Truong, Thu-Thuy Truong, Nigel Funge, 2/26/99, http://www.tti-us.com/doc/papers.htm

[48] Xinqun Liu. Development of Improved Head-Disk Spacing Measurement Methods for Magnetic Disk Drives. PhD Thesis, December 2001.

[49] Xinqun Liu, Warwick Clegg, Bo Liu. Interferometry method for measuring head-disk spacing down to contact. Part of the *OSJ/SPIE Conference on Optical Engineering for Sensing and Nanotechnology* (ICOSN '99), Yokohama, Japan, SPIE Vol. 3740, June 1999, 0277-786X/99, p598-601.

[50] Xinqun Liu, Warwick Clegg, Bo Liu and Chongtow Chong. Improved Intensity Interferometry Method for Measuring Head-Disk Spacing Down to Contact. *IEEE Transaction on Magnetics*, Vol. 36, No. 5 September 2000, p2674-2676.

[51] Xinqun Liu, Warwick Clegg and Bo Liu. Normal Incidence Polarization Interferometer for Measuring Flying Height of Magnetic Heads. *IEEE Transactions on Magnetics*, Vol. 35, No. 5, September 1999, p2457-2459.

[52] Xinqun Liu, Warwick Clegg, Bo Liu. Ultra low head-disk spacing measurement using dual beam polarisation interferometry. *Optics and Laser Technology*, Vol. 32, 2000, p287-291.

[53] Warwick Clegg, Xinqun Li, Bo Liu, Amei Li and Chongtow Cong. Normal Incidence Polarization Interferometry Flying Height Testing. *IEEE Transactions on Magnetics*, Vol. 37, No. 41, July 2001, p1941-1943.

[54] Yufeng Li, Aric K. Menon and Peter R. Goglia. The Development and Implementation of a Flying Height Tester Calibration Standard. *IEEE Transactions on Magnetics*, Vol. 30, No. 6, p4131-4133.

[55] Kok Lue, Christopher Lacey and F. E. Talke. Measurement of Flying Height with Carbon Overcoated Sliders, *IEEE Transactions on Magnetics*, Vol. 30, No. 6, November 1994, p4167-4169.

[56] Li Yufeng. Flying Height Measurement on Al_2O_3 Film of a Magnetic Slider. *Journal of Tribology, Transactions of the ASME*, Vol. 119, p681-686, October 1997.

[57] Richard Sonnenfeld. Capacitance Methods in Head-Disk Interface Studies. *IEEE Transactions on Magnetics*, Vol. 29, No. 1, January 1993, p247-252.

[58] Piezoelectric Ceramics & Components - Data Sheet, 2002. Physik Instrumente Ceramic, Lindenstrasse, D-07589 Ledarhose, Germany.

[59] Jenkins, D.F.L., Chilumbu, C., Tunstall, G., Clegg, W.W., Robinson, P. Multi-layer bulk PZT actuators for flying height control in ruggedised hard disk drives. *Proceedings of the 12th IEEE International Symposium on Applications of Ferroelectrics*, (ISAF 2000), Vol. 1, 2001, p293 -296.

[60] D F L Jenkins, W W Clegg, C Chilumbu and G A Tunstall. Actuators for tomorrows ruggedised hard disk drives. *Datatech* Vol. 3, 1999, ICG Publishing.

[61] E. F. Crawley and J de Luis. Use of Piezoelectric Actuators as Elements of Intelligent Structures. *Am. Inst. Aeronaut. Aeronaut* Journal,, Vol. 25, No. 10, 1987, p1373-1384.

[62] S. J. Kim, and J. D. Jones. Optimal design of piezoactuators for active noise and vibration control. *Am. Inst. Aeronaut. Aeronaut* Journal, Vol 29, No. 12, 1991, p2047-2053.

[63] Moftah Mohamed Bakush. Actuators and Sensors for Active Vibration Control. PhD Thesis, Manchester University, 1996.

[64] G. Plantier, C. Guigou, J. Nicolas, J. B. Piaud and F. Charette. Variational analysis of a thin finite beam excitation with a single asymmetric piezoelectric actuator including bonding layer and dynamical effects. Acta Acustica 3, 1995, p135-151.

[65] John Bates. Computer Controlled Vibration Test Rig. M.Sc. Dissertation, University of Manchester, 1994.

[66] Colin D'Souza. Development of a Vibration Test Station. M.Sc. Dissertation, University of Manchester, 1995.

[67] Stephen D. Jepson. The Development of a Computer-Controlled Environmental Test Rig. M.Sc. Dissertation, University of Manchester, 1997.

[68] 1990 Proceedings Annual Reliability and Maintainability Symposium, p316.

[69] H Bittner and I Y Shen. Taming Disk / Spindle Vibrations through Aerodynamic Bearings and Acoustically Tuned-Mass Dampers. *IEEE Transactions on Magnetics*, Vol. 35, No. 2, March 1999, p827-832.

[70] www.ni.com

[71] G Programming Reference Manual, January 1998 Edition, Part Number 321296B-01

[72] National Instruments DAQ PCI-6023E/6024E/6025E User Manual Multifunction I/O Boards for PCI Bus Computers, October 1998 Edition, Part Number 322072A-01

[73] Ioannis Katsikis. Optical Microphone. M.Sc. Dissertation, University of Plymouth, 1998.

[74] I Y Shen and C P Roger Ku. On the Rocking Motion of a Rotating Flexible-Disk/Rigid-Shaft System. ISPS-Vol. 1, *Advances in Information Storage and Processing Systems* ASME 1995, p271-282.

[75] Understanding and Servicing CD Players. Ken Clements. Newnes. 1995.

[76] http://www.calimetrics.com/Products/CDSpecs/CD-ROM/cd-rom.html

[77] David Jenkins, Warwick Clegg and Xinqun Liu. A combined polarising interferometer and optical beam deflection system for MEMS characterisation Presented at SPIE 46th Annual Meeting, San Diego, USA, July 2001. *Published in Proceedings of SPIE*, Vol. 4442, 2001, p15-25.

[78] C. D'Angelo III, C. D. Mote, Jr.. Natural frequencies of a thin disk, clamped by thick collars with friction at the contacting surfaces, spinning at high rotation speed, Journal of Sound and Vibration, 1993, 168(1), p1-14.

[79] Dynamics of Structures. W C Hurty, Moshe F Rubinstein , Prentice Hall. ISBN, 0-132-22075-X

[80] Weilu Wang, Guoxiao Guo and T.-C. Chong. HDD Actuator Resonance Detection Through Acoustic Signal Analysis, *IEEE Transactions on Magnetics*, Vol. 36, No. 5, September 2000, p3585-3587.

[81] Masaya Suwa and Keiji Aruga. Evaluation System for Residual Vibration from HDD Mounting Mechanism. *IEEE Transactions on Magnetics*, Vol. 35, No. 2, March 1999, p868 - 873.

[82] A. G. Khurshuddov and F. E. Talke. A Study of Subambient Pressure Tri-Pad Sliders Using Acoustic Emission. *Transactions of the ASME, Journal of Tribology*, Vol. 120, January 1998, p54 - 59.

13. Appendices

13.1 Software Written in C for Reading Data from a Hard Disk Drive at a Chosen Cylinder Head Block

```
#include <conio.h>
#include <stdio.h>
#include <dos.h>        // for int86(), REGS
#define FUNCTION2 // service no
#define INTER 0x13  // Disk BIOS interrupt number

void main (int argc, char*argv[], long address)
        {
                union REGS regs;
                long start, end;
                if (argc !=3)
                        {
                        printf ("Example usage: C>READ 147 209");
                        exit ();
                        }
                _ES = 0;
                start=atoi(argv[1]);
                end=atoi(argv[2]);
                regs.h.ch=(long)start;
                regs.h.cl=(long)end;
```

```
                regs.h.dh=1;
                regs.h.dl=129;
                regs.h.bh=4;
                regs.h.bl=208;
                regs.h.al=1;
                regs.h.ah=FUNCTION;        //service number
                int86(INTER,&regs,&regs);  //call interrupt
                printf("Status (0=good, 4=sector not found) %d,",regs.h.al);
//-------------------------------------------------------------------------------------------
                for (address=0x4CF; address<0x6D7; address++)
                {
                        printf("%x",peek (0,address));
                }
                exit ();
        }
```

13.2 Results from Finite Element Analysis Modelling of a 0.8mm Thick Disk

Mode	Free	Clamped
1	277	440
2	277	440
3	298	742
4	512	1082
5	512	1082
6	1097	1672
7	1097	1682
8	1916	1913
9	1916	1913
10	2555	2938
11	2816	2939
12	2816	2984
13	2939	2987
14	2939	4037
15	3602	4157
16	3602	4157
17	4158	4598
18	4158	4601
19	4882	4759
20	4882	4922
21	5569	4990
22	5569	5327
23	6568	5327
24	6569	5568
25	7169	5568
26	7172	6464

27	8209	6468
28	8510	6959
29	8510	6995
30	8569	7168
31	8569	7168
32	8634	7593
33	8963	7593
34	8963	8536
35	9420	8539
36	9420	8546

13.3 Results from Finite Element Analysis Modelling of a 1.25mm Thick Disk

Mode	Free	Partially Clamped	Fully Clamped
1	431	677	690
2	431	677	692
3	468	1147	1166
4	799	1669	1751
5	800	1669	1751
6	1719	2561	2651
7	1719	2561	2651
8	3002	2952	3194
9	3003	2952	3802
10	4004	4533	4742
11	4405	4533	4890
12	4405	4585	4911
13	4605	4585	4911
14	4605	6364	6340
15	5624	6416	6340

16	5625	6432	6515
17	6518	7062	7918
18	6538	7062	7918
19	7622	7675	8086
20	7622	7675	8086
21	8681	8669	9615

13.4 Virtual Instrument Used for Analysing Signal from Embedded Piezo-electric Sensors

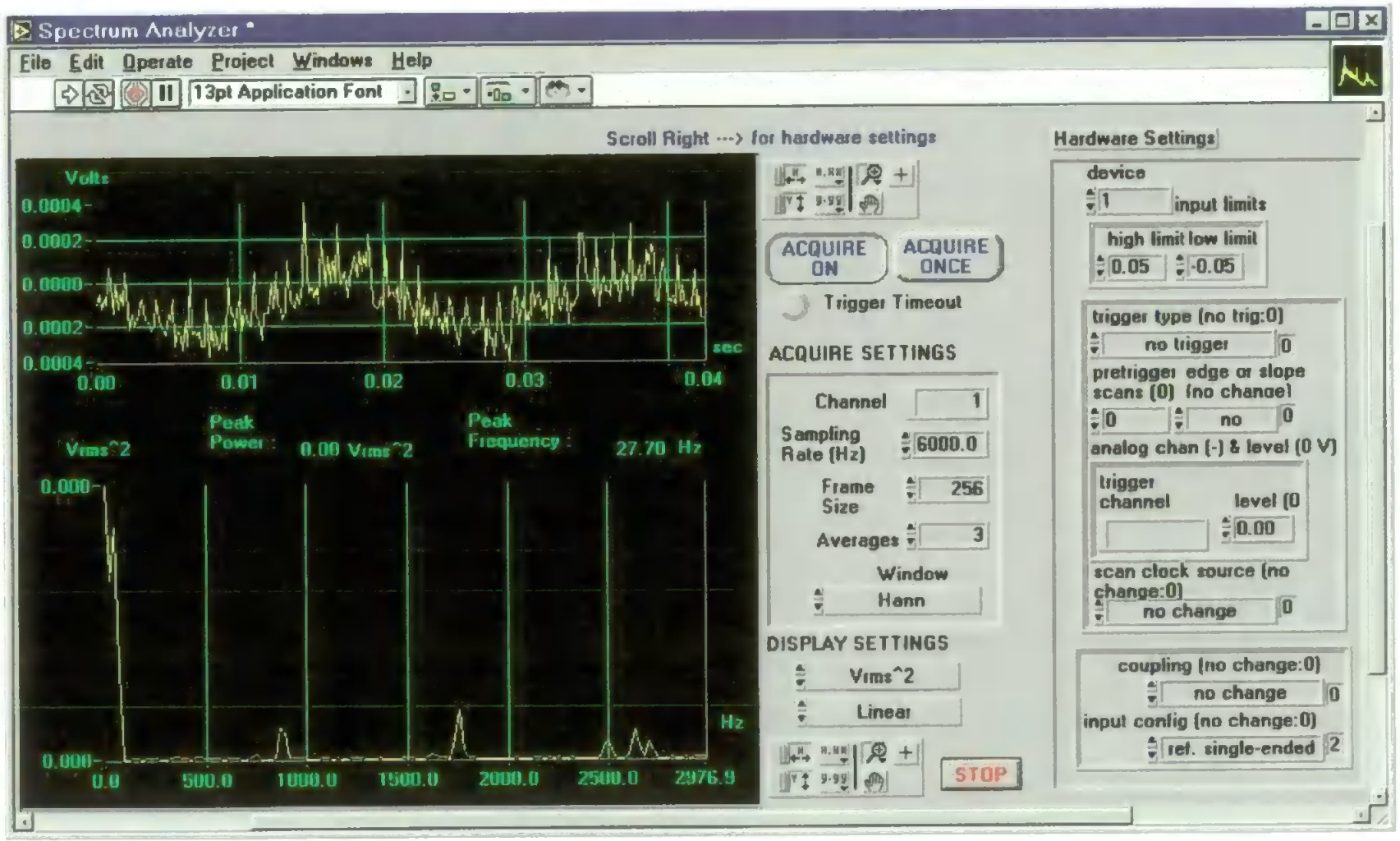

13.5 Screenshot of Virtual Instrument Diagram

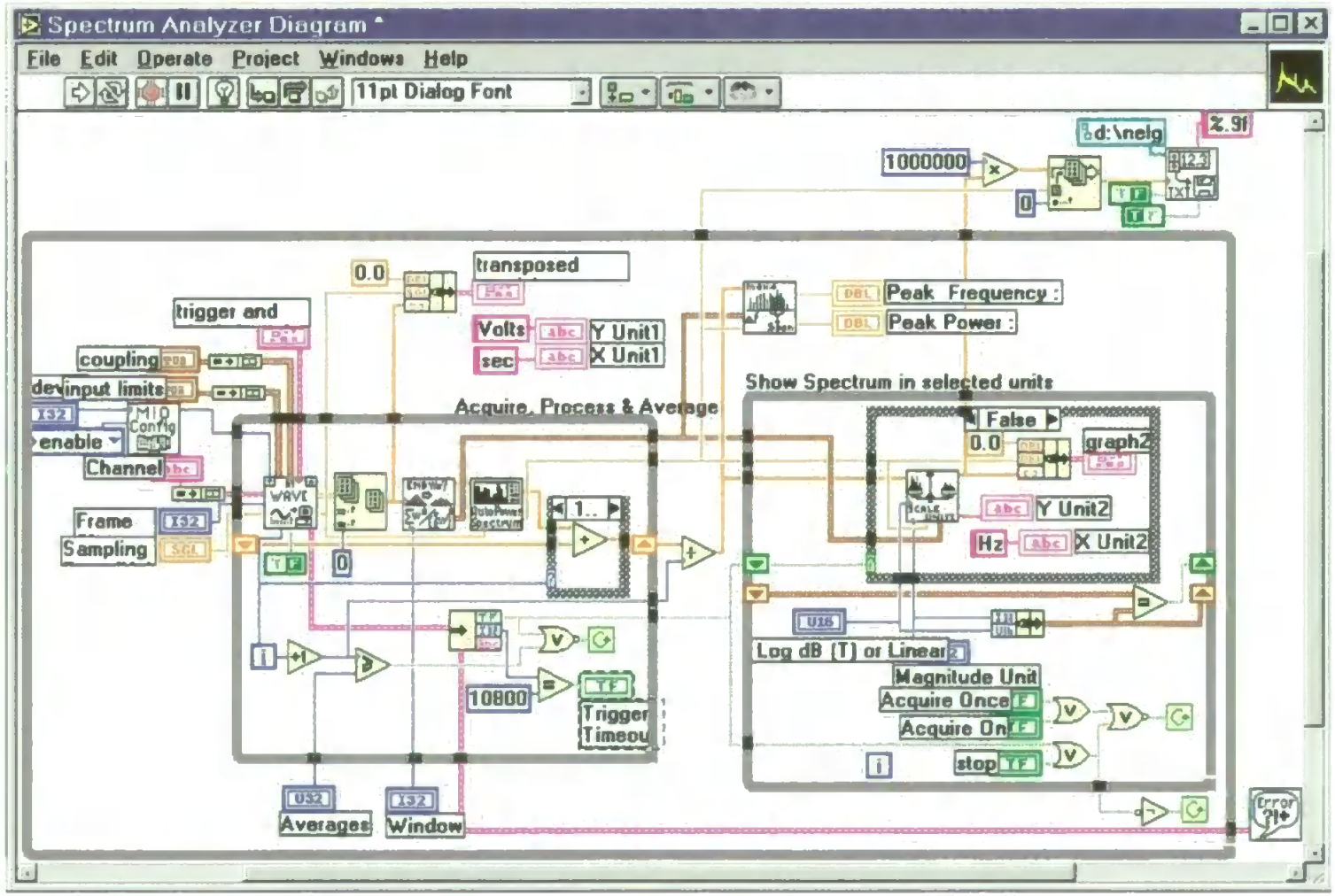

Published Papers

Sensors for Dynamic Characterisation of Magnetic Storage Systems, DFL Jenkins, WW Clegg, L He, J Windmill, G Tunstall, X Liu, C Chilumbu, A Li, Sensors Review, Vol. 20, No. 4, 2000, Page(s): 307-317, invited paper.

Head-media interface instability under hostile operating conditions, Tunstall, G.; Clegg, W.; Jenkins, D.F.L.; Chilumbu, C. , IEEE Transactions on Instrumentation and Measurement, Volume: 5, Issue: 2, Apr. 2002, Page(s): 293 -298

Actuators for tomorrows ruggedised hard disk drives, D F L Jenkins, W W Clegg, C Chilumbu and G A Tunstall, Datatech Vol. 3, 1999, ICG Publishing.

Multi-layer bulk PZT actuators for flying height control in ruggedised hard disk drives, Jenkins, D.F.L., Chilumbu, C., Tunstall, G., Clegg, W.W., Robinson, P.,
Proceedings of the 12th IEEE International Symposium on Applications of Ferroelectrics, (ISAF 2000), Vol. 1, 2001, Page(s): 293 -296.

Research articles

Sensors for dynamic characterisation of magnetic storage systems

D.F.L Jenkins
W.W. Clegg
L. He
J. Windmill
G. Tunstall
X. Liu
C. Chilumbu and
A. Li

The authors

D.F.L Jenkins, W.W. Clegg, L. He, J. Windmill, G. Tunstall, X. Liu, C. Chilumbu and A. Li are all at the Centre for Research in Information Storage Technology (CRIST), University of Plymouth, Plymouth, UK.

Keywords

Inspection, Magnetic, Distance measurement

Abstract

The areal (surface area density of bits) storage density of magnetic hard disks is continually increasing, with typical available commercial storage densities being around 10Gbits/in^2. It is predicted that densities in excess of 40Gbits/in^2 will be possible before the year 2003. A number of key issues arise from this development, such as the need to determine and control accurately the dynamic flying height (z-axis) of the read-write head, which is affected by the apparent distortion of the disk surface due to rotation-induced disk resonance. As a result of the increasing storage density the positional control of the head in the plane of the disk (x-y plane) also becomes more critical. This paper deals generally, but with a particular emphasis on optical and piezoelectric sensors used in our laboratory for characterisation of storage media and systems.

Electronic access

The research register for this journal is available at http://www.mcbup.com/research_registers/aa.asp

The current issue and full text archive of this journal is available at http://www.emerald-library.com

Sensor Review
Volume 20 · Number 4 · 2000 · pp. 307–315
© MCB University Press · ISSN 0260-2288

Introduction

There is a vast array of sensors available to us at present. Sensors are selected according to the particular measurand and in many cases, the particular application, e.g. interfacing to a control system. Sensors are generally required to work in parallel with signal conditioning electronics, and may then be either used as a stand-alone measurement system or incorporated into a control system for real-time sensory feedback.

Depending on the measurand there is a vast array of sensors that can be used for surface and textural characterisation. One of the standard methods for investigating the surface profile is to use a profilometer[1]. A profilometer utilises a stylus much in the same way as a record player follows the variations along the track of a record, the main difference being that the profilometer uses optical sensing to determine the attitude of the stylus. In a record player the stylus generates a signal by electromagnetic induction (moving coil or moving magnet). The potential disadvantage of the stylus-based systems is modification of the surface, due to contact being made by the stylus. However, the use of optical based profilometry is able to circumvent this, and a number of systems have been developed so far. Abou-Zeid and Wiese developed a compact interference profilometer that uses a wavelength-tunable diode laser as an optical stylus, with a measurement uncertainty of around 10nm[2]. A number of profilometry systems based on interferometry have also been reported[3,4]. Cuthbert and Huynh[5] have designed an optical system for fast non-contact measurement of surface texture, based on the optical Fourier transform pattern of the surface, which is correlated with the surface roughness obtained using a stylus based instrument.

Moving into the new millennium we are faced with the increasing demands of hard disk drive technology. Data storage density continues to increase, necessitating that the head flies even closer to the disk surface: state-of-the-art flying heights currently being around 15nm. This is coupled with the increasing demand for faster track access, which means that the disk drive is required to operate at increasingly higher speed. This represents a challenge for PCs operating in the office environment, but presents more

serious difficulties for computers working in conditions where they are subjected to shock and vibration. This is of particular interest to military and aerospace applications; and to a lesser extent will also affect users of laptop computers.

This paper looks at a variety of sensor systems used in the CRIST research laboratory for the characterisation of magnetic media and data storage systems, namely: scanning laser microscopy, magnetic force microscopy, dual beam polarisation interferometry, CD-ROM optics and thick film piezoelectric sensors. Finally, there is a brief look at a complete sensor-control-actuator system, which includes optical beam deflection for displacement (or topography) sensing, which is currently being investigated for the improved operation of hard disk drives.

A. Dynamic scanning laser microscopy

Scanning laser microscopes are extremely useful tools for high-resolution point-by-point imaging of sample surfaces. The most common configuration employs a stationary laser beam, which can have either continuous or modulated (intensity or polarisation) output. The laser is brought to a focus using a microscope objective to yield a diffraction-limited spot, which is typically around 1mm on the sample surface. The sample can then be micro-positioned, with a motorised *x-y* stage, with respect to the sample and the reflected light collected by one or more detectors. An alternative configuration employs a pair of scan mirrors to move the spot on the sample surface. This set-up is significantly more complex as it requires auto focusing to maintain the same size spot at all points of the scan, and there is a trade-off between scan area and resolution. For example a 5mm × 5mm area can be scanned with a resolution of around 30mm[6]. However, the two systems are often combined: scan mirrors (high speed scanning) and *x-y* stage (large area scan). The use of different detectors and polarisation sensitive/insensitive optics enables different information to be acquired.

In our laboratory a scanning laser microscope has been designed and built to observe the dynamic behaviour of domain switching during the thermo-magnetic write process and the subsequent magnetisation state (domain orientation) in thin-films and devices[7-9]. It can also be used to write to magneto-optic disk material thermo-magnetically prior to imaging. Images are derived from the longitudinal and polar magneto-optic Kerr effects, which are wavelength dependent.

The microscope system has been made modular, which enables the imaging system to be flexible and allows further functionality to be added as required. An overview of the system is shown in Figure 1. The scanning laser microscope is constructed around the basic frame of a Leitz Metalloplan optical microscope, mounted on optical breadboard along with other optical and mechanical components, as shown in Plate 1.

The various modes of operation of the SLM are as follows:

- *XY table scanning mode.* In the XY scan mode a sample is raster scanned beneath the laser spot via a Burleigh XY Worm Table, with a resolution of 4nm. The

Figure 1 Block diagram of SLM component parts

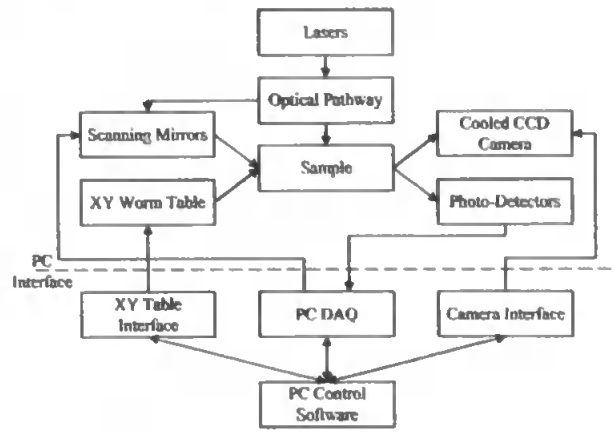

Plate 1 The scanning laser microscope system in the CRIST laboratory

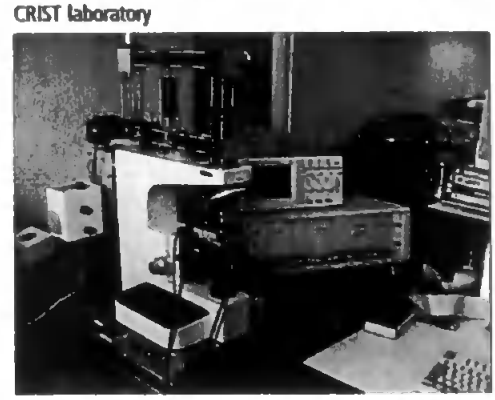

magnetic or intensity (pseudo-topographic) information is then extracted by sampling all the photo-detector outputs using the computer I/O board, then applying the required algorithm to the data. Plate 2 shows bubble memory magnetic domain patterns using the polar Kerr effect (scan area 32μm × 40μm). The reflected light intensity is a function of the sample magnetisation (domain orientation), and LabView enables the reflected intensity to be represented by a grey scale image. The change in intensity represented here is typically less than 1 per cent.

- *Galvanometer scanning mode.* In the galvanometer scan mode the sample is held stationary whilst the laser spot is raster scanned over it via the scanning mirrors. The galvanometer position is controlled using the computer I/O board voltage outputs. Again the computer processes magnetic or topographic information after it is sampled to create an image. Plate 3 shows a pseudo-topographic (reflected intensity) image of an integrated circuit layout (galvanometer scan area 100μm^2).
- *Dye pulse laser.* A further imaging mode of the SLM utilises a dye pulse laser. This requires the software to trigger a waveform generator, and at a set time period later trigger the laser. Finally, at some point in time after this, data are acquired from the photo-detectors. Each of these time periods must be accurately related to the others. The magnetic image is retrieved from the quadrant photo-detectors as for other modes of operation.
- *CCD camera image acquisition.* Another mode of image acquisition uses a super-cooled CCD camera, triggered after a pulse of light has illuminated a sample. The camera is supplied with a set of functions in the form of a Windows dynamic link library (DLL), also known as an application program interface (API). These functions cover all that is required to operate the camera.

Plate 2 Bubble memory magnetic domain patterns using Kerr effect static laser XY table scan 32μm × 40μm

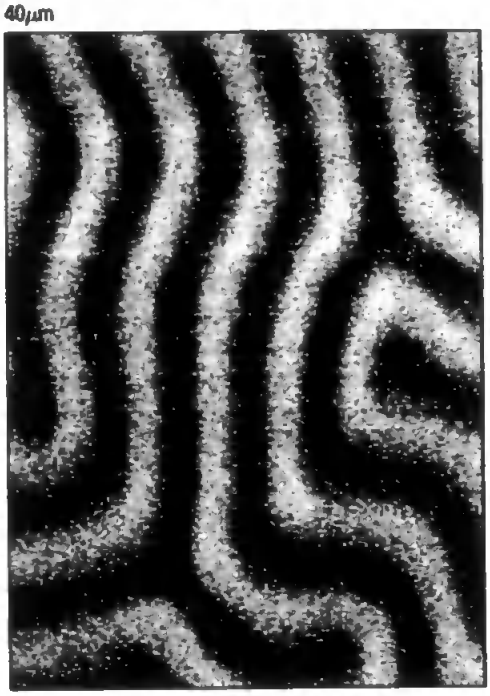

Plate 3 Integrated circuit layout pseudo-topography (intensity) using galvanometer scan – 100μm^2

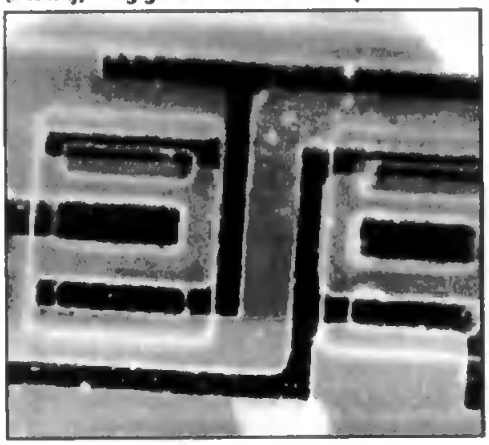

B. Magnetic force microscopy

The magnetic force microscope (MFM) is based on the atomic force microscope (AFM)[10]. In the AFM a small probe, a silicon cantilever with an atomically sharp tip, is brought into contact with a sample surface, and raster scanned across it. The resultant deflection of the tip is recorded and used to create an image of the surface topography. In magnetic force imaging the tip is coated in a ferromagnetic material, and moved away from the surface several tens of nanometres. It is then raster scanned, and the interaction between the magnetic field of the sample and the tip recorded to create an image of the magnetic forces.

The development of our MFM, shown in Plate 4, is based on a versatile, modular form,

Plate 4 The magnetic force microscope

enabling easy access to the specimen and easy change of tips/cantilevers[11]. It uses optical beam deflection to sense cantilever movement and is designed to operate in either topographic or magnetic force imaging modes. This system is also designed to work in low vacuum (or in a helium atmosphere). The benefits of vacuum (and helium) operation are significant, since the removal of much of the normal viscous air damping enables a significant increase in the cantilever's effective Q-value, as operation moves into the molecular damping region (independent collisions of non-interacting air molecules). This in turn results in better resolution of images produced by resonant techniques. Plate 5 shows an image of the topography of a hard disk surface (scan area $1\mu m \times 1\mu m$), showing granular structure of surface and diagonal grooves from texturing process.

Plate 5 Hard disk topography, $1\mu m \times 1\mu m$ surface scan, showing granular structure of surface and diagonal grooves from texturing process

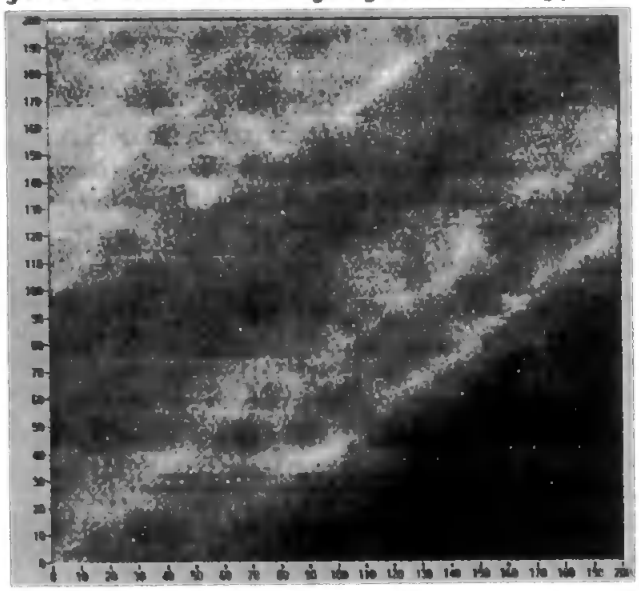

A variety of scanning modes exist for the MFM. The "static" scan, as described above, is the simplest; however, this requires samples with relatively powerful magnetic fields. Resonant scanning is a standard mode of operation, where the cantilever is resonated, and the effects of the sample's fields on that resonance are monitored in different ways to create an image. In recent years LiftMode™ has being recognised as a very useful mode of operation[12]. In this case the topography of the sample is mapped out with an initial scan, from which the data are used to control the height of the MFM probe, in resonant mode, to do a second magnetic scan. This results in removal of topographic effects from the resulting magnetic image.

The design and function of the probe used to interact with the stray fields from a magnetic sample are a major MFM research subject. The standard ferromagnetic design has several inherent problems. The tip magnetisation can suffer from hysteresis over time, together with wear and damage during its useful life. The magnetic properties of different samples, i.e. if the sample is magnetically "hard" or "soft", mean that a range of different designs and coatings need to be employed. Therefore, an instrument must be reconfigured each time a new type of sample is imaged. Furthermore, these imperfections may have serious consequences in the acquisition of useful, quantifiable data.

We are currently investigating a new type of MFM probe that uses an electromagnetically induced field as a replacement for the standard probe's stray field. Although electromagnetic MFM probes have been described before, this design is unique[13]. The field is induced around a micro-fabricated aperture using a controlled current. The aperture would be situated near the end of a standard cantilever that has been coated in a conductive material, e.g. gold. This design has the advantage that the specimen interaction is variable, giving controllable field intensity, and as such the results would be repeatable. The new probe has been theoretically simulated to create images of magnetic domain patterns, and it is anticipated that work on the fabrication of these new and innovative probes will begin soon. The practical issues of using the probe in our MFM instrument are also undergoing analysis.

C. Dual beam polarisation interferometry

Optical interferometry is a well established technique for precise and non-contact measurement. Various types of interferometry, such as heterodyne interferometry[14], sinusoidal phase modulating interferometry[15], and phase-shifting interferometry[16], have been developed to make high resolution measurement of small displacements. However, apart from the complexity of the system construction, these existing methods are generally feasible only for low-speed measurement applications. When a high-speed measurement is needed, it is difficult to find a suitable technique if the measurement accuracy requirement is high. The speed limitation in these displacement measurement interferometers is mainly due to the use of slow modulation or scanning techniques. In the CRIST laboratory, a dual beam polarisation interferometer has been constructed, which can be used for high-speed measurement of dynamic morphology/topography, and in our case for the complex measurement dynamic disk head flying height[17,18].

The polarisation interferometer configuration utilises two orthogonally-polarized light beams to remove the directional ambiguity of the displacement, and is shown schematically in Figure 2. The main part of the interferometer utilises a polarising beam splitter PBS1, two quarter-wave plates QW1 and QW2, two mirrors M1 and M2, and a non-polarising beam splitter NPBS1 as both a beam splitter and phase shifter.

Employing a polarising beam splitter PBS1 makes the best use of the laser beam and prevents the returning beam from feeding back into the laser diode. The mirror M2 is driven by a piezoelectric translator (PZT1), which can be used to perform system calibration. Mirror M3 is used as a reference plane when single point displacement is measured. When the system is used to measure the relative displacement of two adjacent points, such as the vertical movement of the hard-disk read/write head relative to the disk surface, M3 is removed and the reference beam is extracted by NPBS1 to the second measurement point. Mirror M2 can also be micro-positioned manually to adjust the spacing of the two measurement points. A 670nm wavelength laser diode is used as the light source. The laser beam passes through the polariser and enters the polarising beam splitter PBS1. Then the s-polarised component is coupled out and reflected by mirror M1 and focused on the measurement point on the sample. The p-polarised component passes through and is focused on to the reference mirror or another measurement point. The returning beam enters the interferometric receiver, which is used to measure the intensity and phase difference between the two polarised beams. The interferometric receiver consists of a non-polarising beam splitter NPBS2, two polarising beam splitters PBS2 and PBS3, a quarter-wave plate QW3 and four photo-detectors. The detected voltage signals are amplified and equalised, then sampled in by the computer through a 12-bit A/D converter board. The sampling rate of the A/D converter will determine the measurement speed of the system. The A/D converter board with a sampling rate of 20MS/s is commercially available at present. The computer, through a 12-bit D/A converter board and a high voltage (150V) amplifier also controls the piezoelectric translators.

We take the electric field of the two orthogonally polarised beams to be of the standard form:

$$E_p = A_p \exp(i(\omega t)) \quad (1)$$

$$E_s = A_s \exp(i(\omega t + \phi)) \quad (2)$$

where ω is the angular frequency of the radiation, A_p and A_s are the amplitudes of E_p and E_s respectively, and

$$\phi = 4\pi(d + \Delta d)/\lambda. \quad (3)$$

Figure 2 Dual-beam polarisation interferometer

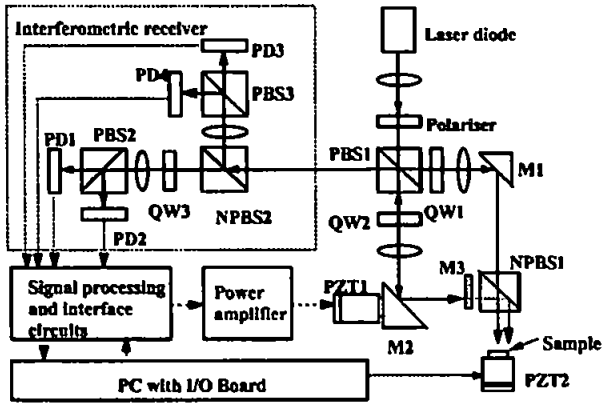

In equation (3), λ is the wavelength of the laser beam, d is the static optical path difference between the two polarised beams and Δd is the displacement to be measured. The wave intensity being received by each of the four photo-detectors (P_{PD1} to P_{PD4}) is proportional to the square of the electric field, and by simple signal conditioning and processing quadrature signals $P_{PD2} - P_{PD1}b_2/b_1$ and $P_{PD3} - P_{PD4}b_3/b_4$ are obtained. The computer samples these signals with two channels of the A/D converter board. The displacement Δd is then determined by phase evaluation and unwrapping[19].

To test the ability and effectiveness of this interferometer, several experiments have been conducted. A 12-bit D/A converter, with a 0-10V voltage output, drives another piezoelectric translator, PZT2, to move the sample. One of the measurement results is shown in Figure 3, in which PZT2 moves the sample in a saw-wave form with amplitude of about 8.5nm.

The dual beam polarisation laser interferometer can be used for accurate high-speed measurement of small displacements, vibration, and disk flying height. Theoretically, a 12-bit A/D converter can provide a measurement resolution higher than λ/4,096. However, because of the system noise, especially the electrical noise, the system in its present configuration has a general measurement resolution of about 0.5nm. The dual beam polarisation interferometer in its first version has been demonstrated to work effectively in our application. However, there are a number of issues to be addressed in order to realise its true potential. The interferometer will be developed from its present state to include a frequency stable He-Ne laser and the interferometer itself will be made to be compact and from thermally stable materials (invar as opposed to aluminium). These improvements will significantly improve the signal-to-noise ratio available, enabling more precise measurements of small displacements to be made. Choosing a higher sampling rate A/D board can also increase the system's measurement bandwidth.

D. CD-ROM optics

The interaction between the read-write head and the disc surface causes the flying height of the head above the surface to change, and so the dynamic morphology of the rotating disk(s) is extremely important. As the head moves outside its operating margin data-transfer becomes a problem, eventually leading to data-transfer error, as shown in Figure 4. As the disk (aluminium-magnesium, coated with a thin magnetic layer and thin lubrication layer) rotates at speeds of up to 10,000rpm the disk flexes radially and circumferentially and the CD-ROM optics will be utilised to measure these rotation-induced effects.

A CD-ROM drive utilises a laser with photodiodes to read data from the disk. The photo detector comprises four sensors and when the disk is perfectly focused the laser spot reflected off the disk will be centrally placed on the four sensors. The spot will then move either left or right to cover one pair of spots depending on the distance of the disk.

Figure 3 Measurement result for displacement amplitude of about 8.5nm

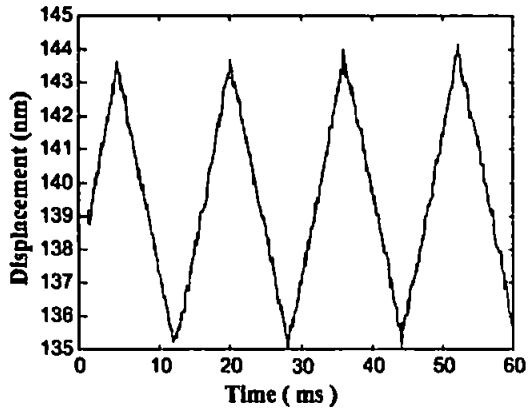

Figure 4 Effect of vibration on disk drive operations: 3.5" hard disk

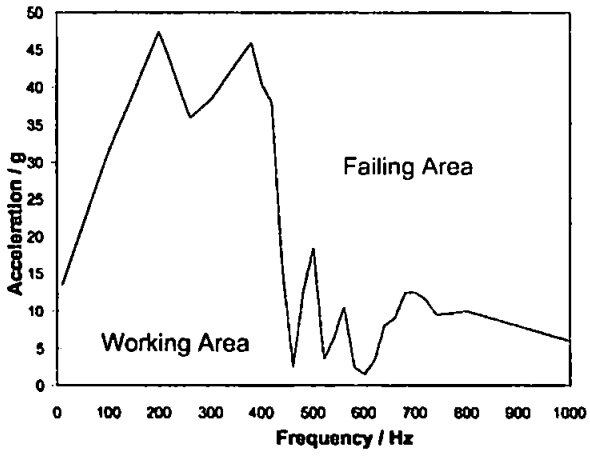

The CD head is mounted to a micrometer controlled sliding table and aligned so as to reflect off of a typical hard disk drive disk. In normal operation two of the segments are summed and the difference from the other two segments is compared, to yield a signal four times greater than that observed from just the one segment.

Using an oscilloscope to monitor the signal on one of the photodiodes it was recorded that a peak voltage of 30mV was measured when the lens was 2.80mm away from the disks' surface. The response from the detectors is linear with distance, with a change of ± 0.2mm yielding a change in output of ± 20mV, a response therefore of 0.1mV/μm. After signal conditioning, the response becomes 0.4mV/μm. Work in this area is part of ongoing research.

E. Piezoelectric sensors

An alternative means of characterising hard disk flutter is to use a thick film piezoelectric sensor, in this case polyvinylidene di-fluoride (PVdF). The sensor, in the form of a 110μm sheet, was used as a cantilever. When a piezoelectric material is deformed the potential difference across its electrodes is proportional to the average induced strain. The fixed end of the sensor was bonded to the drive's chassis such that the cantilever is pre-tensioned against the disk. Any movement of the disk would therefore bend the cantilever from its static position. Because the cantilever is pre-tensioned, when the disk is static there is always a DC voltage. If the disc causes the cantilever to move from its static position there will be a change in the cantilever's induced stress; the output voltage will increase as the strain increases and vice-versa. The end of the cantilever rests on the edge of the disk to sense maximum displacement. Figure 5 shows the results obtained using this sensor arrangement, for a 3.5" hard disk drive rotating at 4,500rpm. The first peak (at 75Hz) corresponds to disk rotation (disk clamping and spindle bearing), the second peak at around 500Hz corresponds to disk flutter, as predicted by finite element analysis, and the peaks at higher frequencies are attributed to disk-suspension arm interaction.

Figure 5 Response from piezoelectric sensor showing the effect of disk flutter. Inset shows the actual sensor at the edge of the disk

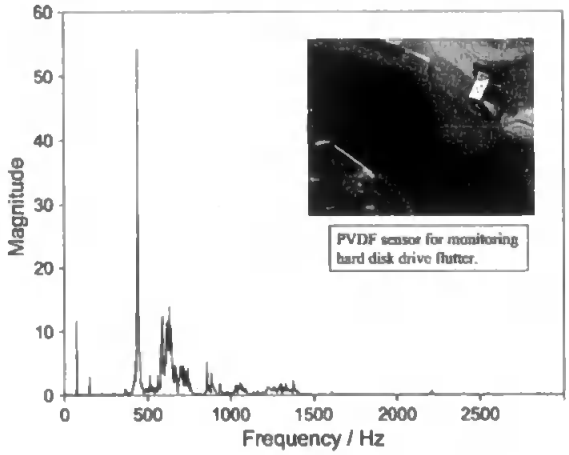

F. Hard disk drive control system

It is appropriate now to look at the control system that is being developed for active control of the read-write head for both track following and flying height[20]. Current hard disk drives utilise a voice coil motor for positioning the head with respect to the data tracks, and design the head suspension system such that air flow, due to the rapidly rotating disk, "lifts" the head to the desired height above the disk surface. The system developed in the CRIST laboratory will still use the voice coil motor for coarse track following, but fine positioning and flying height control will be affected using piezoelectric stack actuators, as shown in Plate 6. Stack actuators offer advantages of useful actuation at low voltage (< 3V) and wide bandwidth operation.

The attitude of the head is monitored using optical beam deflection (OBD), whereby a laser beam is deflected by a small mirror above "the head" on to a position sensing quadrant photodetector, capable of simultaneously measuring displacements in the horizontal and vertical planes. The output of the detector, which is linear for small displacements, and has spatial resolution comparable with interferometers (i.e. sub nm), is applied to the DSP implemented proportional integral and derivative (PID) controller for real time active control of the head suspension system. The suspension arm is set into resonance by applying bursts of band-limited white noise to the piezoelectric stacks and the resonant modes are sensed

Sensor Review
Volume 20 · Number 4 · 2000 · 307–315

Plate 6 Suspension arm incorporating stack actuators for simultaneous head positioning and flying height control

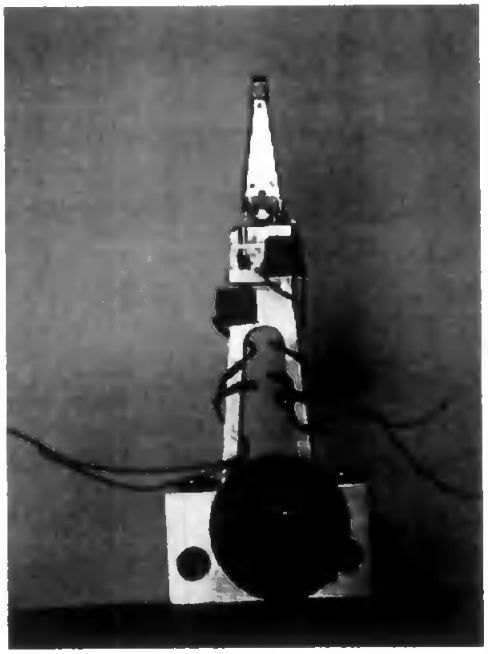

optically, for both data tracking and flying height control. However, actuation in one plane can induce resonance effects in the orthogonal plane, and vice versa.

Modified PID controllers have been implemented to control and position the suspension arm with adequate bandwidth and stability. Bode plots show that the PID servo system's control loop for the tracking stage can be closed with a 25.6kHz gain cross-over frequency and phase and gain margins of 54° and infinity respectively. The flying height control stage is closed with a gain cross-over frequency of 2.33kHz and phase and gain margins of 51° and infinity respectively. Figure 6 shows the experimental open loop response and the theoretical closed loop response for track following, with the response for the flying height control similar to that for track following.

In an actual hard disk drive, position sensing would be achieved via the read/write head for flying height and from the tracking servo for track positioning. If data are read back from the disk, then according to the Wallace spacing loss equation[21], the amplitude of the read-back signal will be modulated by the spacing variations between the head and the disk due to the surface irregularities of the disk. The read-back signal from the magnetic head reflects the surface

Figure 6 Open and closed loop response for track positioning

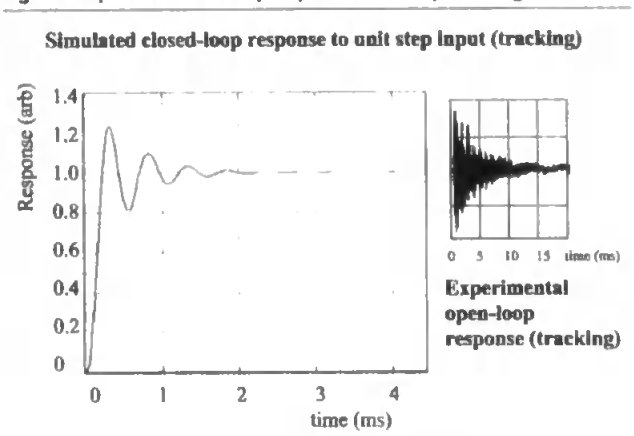

topography of the disk, and will provide a feedback signal for the control system.

Conclusion

In the CRIST laboratory a number of sensor systems have been developed for the characterisation of magnetic media and data storage systems. An SLM, with dynamic read-write capability, and an MFM have principally been developed for the characterisation of magnetic and magneto-optical thin films. By utilising the intensity imaging mode, the SLM is able to characterise the surface reflectivity with a spatial resolution of around 1μm. The MFM operates with the probe at constant height and so a prerequisite is that the surface topography is known. This is determined from a pre-imaging scan in AFM mode, whereby the probe tip is brought into contact with a sample surface, and raster scanned across it. The resultant deflection of the tip is recorded and used to create an image of the surface topography. The dual beam interferometer, for measuring head flying height, is so far able to measure dynamic surface topography of a rotating hard disk, with sub-nanometre resolution. Current instrument development is focused towards the simultaneous measurement of the head position, to realise the determination of its actual height above the disk surface in real time.

In parallel with this is work on the dynamic characterisation of disk drives for ruggedised operations, such as in seismic data logging. Two experimental systems have been

developed for this based on CD-ROM optics and thick film piezoelectric sensors to measure the topography of the rotating disk drive under hostile operating conditions. Measurements of data-transfer to and from the disk will be used to further the understanding of data-transfer failure mechanisms under hostile operating conditions.

Operation of hard disk drives relies on the head-to-disk flying height being maintained at a constant height. A sensor-controller-actuator system has been developed to enable both the flying height and the track position to be maintained. Optical sensing is used at present to determine the attitude of the head and the response used to drive two independent actuators via a DSP implemented PID controller. Future developments of this system will include the replacement of the optical sensor by a direct measurement of the head's position from the actual head readout signal itself. This will form the basis of a realisable system that will be developed commercially in partnership with our collaborators, the Data Storage Institute, Singapore.

References

1 Morrison, E., "The development of a prototype high-speed stylus profilometer and its application to rapid 3D surface measurement", *Nanotechnology*, Vol. 7 No. 1, 1996, pp. 37-42.
2 Zhang, J.-H. and Cai, L., "Profilometry using an optical stylus with interferometric readout", *Meas. Sci. Technol.*, Vol. 8 No. 5, 1997, pp. 546-9.
3 Jalocha, A. and Pieralli, C., "A scanning optical profilometer using the SNOM architecture", *Pure Appl. Opt.*, Vol. 3 No. 5, 1994, pp. 793-804.
4 Bowen, D.K., Chetwynd, D.G. and Schwarzenberger, D.R., "Sub-nanometre displacements calibration using X-ray interferometry", *Meas. Sci. Technol.*, Vol. 1 No. 2, 1990, pp. 107-19.
5 Cuthbert, L. and Huynh, V.M., "Statistical analysis of optical Fourier transform patterns for surface texture assessment", *Meas. Sci. Technol.*, Vol. 3 No. 8, 1992, pp. 740-45.
6 Carey, R.C., Jenkins, D.F.L., Newman, D.M. and Thomas, B.W.J., "Laser scanning at full objective aperture using 2-axis galvanometer mirrors", *Meas. Sci. and Technol.*, Vol. 4, 1993, pp. 488-91.
7 Clegg, W.W., He, L., Jenkins, D.F.L. and Windmill, J.F.C., "A magneto-optic scanning laser microscope to characterise static and dynamic behaviour in magnetic materials", poster presentation, CMMP 99 Conference, Leicester, 1999.
8 Clegg, W.W., He, L., Jenkins, D.F.L. and Windmill, J.F.C., "A magneto-optic scanning laser microscope facility for the time-resolved examination of domain dynamics", poster presentation at FOM 2000, Shirahama, Japan, April, 2000.
9 Clegg, W.W., He, L., Jenkins, D.F.L., Windmill, J.F.C. and Fry, N., "A scanning laser microscope system to observe static and dynamic magnetic somain behaviour", oral presentation at IMTC 2000, Baltimore, MA, submitted for *IEEE Trans. IMTC*, 2000.
10 Farley, V., "A high performance magnetic force microscope", *Meas, Sci. and Technol.*, Vol. 7, 1996, pp. 30-5.
11 Clegg, W.W. and Windmill, J.F.C., "A novel scanning force microscope head configuration compatible with vacuum operation", paper presented at CMMP Conference, UMIST, Manchester, 1998.
12 http://www.di.com (Digital Instruments).
13 Zhou, H. *et al.*, "Recent progress in the functionalization of atomic force microscope probes using electron-beam nanolithography", *J. Vac. Sci. Technol. A*, Vol. 17 No. 4, 1999, pp. 2233-9.
14 Dai, X. and Seta, K., "High-accuracy absolute distance measurement by means of wavelength scanning heterodyne interferometry", *Meas. Sci. Technol.*, No. 9, 1998, pp. 1031-5.
15 Wang, X., Sasaki, O., Takebayashi, Y., Suzuki, T. and Maruyama, T., "Sinusoidal phase-modulating Fizeau interferometer using self-pumped phase conjugator for surface profile measurements", *Optical Engineering*, Vol. 33, 1994, pp. 2670-74.
16 Creath, K., "Phase measurement interferometry techniques", *Progress in Optics*, Vol. 27, 1990, pp. 273-359.
17 Liu, X., Clegg, W., Jenkins, D. and Liu, B., "Polarization interferometer for measuring small displacement", IMTC/2000, Baltimore, MA, May 2000.
18 Clegg, W., Liu, X. and Liu, B., "Dual beam normal incidence polarization interferometry flying height testing", *IEEE International Conference on Magnetics*, Paper CP-04, Toronto, April 2000,.
19 Malacara, D., *Optical Shop Testing*, 2nd ed., John Wiley & Sons, New York, NY, 1992.
20 Chilumbu, C., Clegg, W.W., Jenkins, D.F.L. and Robinson, P., "A novel two-dimensional suspension arm for flying height control and high-bandwidth track following in advanced hard disk drives", oral presentation at IMTC/2000, Baltimore, MA, May 2000.
21 Wallace, R.L., "The reproduction of magnetically recorded signals", *The Bell Tech. J.*, 1951, pp. 1145-73.

Head-Media Interface Instability Under Hostile Operating Conditions

Glen Tunstall, *Senior Member, IEEE*, Warwick Clegg, David F. L. Jenkins, and Chibesa Chilumbu

***Abstract*—In the office environment, computers reliably transfer data to and from the hard disk drive and data transfer errors are extremely rare. However, when even "ruggedized" computers are operated in hostile conditions, valuable data can be lost as a result of read-write error due to either shock or vibration, seriously impairing drive performance. For this work, drives have been vibrated over large frequency ranges in order to characterize their data-transfer performance. In order to observe the cause of the problems, a drive has been modified with integral sensors to identify internal system failures and the results of these investigations are presented. These sensors have enabled the first unobtrusive tests of the drives' mechanical frequency response while the drive is in operation with sensors that can be easily and inexpensively embedded within a hard disk drive for use in a generic, smart, vibration resilient drive.**

***Index Terms*—Hard disk drive, PVdF, sensor, vibration.**

I. Introduction

HARD disk drives are an economical form of mass storage, widely used as secondary memory in virtually all computer systems. Conventional hard drives are very reliable under normal operating conditions, but they can suffer from mechanically induced failure when operated in hostile conditions. In areas where vibrations exist, hard disk drives can and do fail and no longer read or write data. At best, the data transfer rate becomes vastly inferior.

Environments such as the military and aerospace are synonymous with large shocks and vibrations. Ocean-going craft can also encounter difficulties with hard drives as the engine and waves transmit vibrations through the hull. Dennis [1] evaluated many proposed solutions, though mainly large vibration isolation cages and mountings that damped the vibrations. However, additional isolation mountings are not the ideal solution. The extra space and weight needed preclude this method from many key areas: adding both weight and bulk to a drive is hardly an improvement. Passive dampers, which are only effective over a limited bandwidth, are all that are used in current "ruggedized" laptops.

II. Disk Drive Fundamentals

It is important to understand precisely what is happening within the drive and which system areas are failing under conditions of vibration. When mechanical components are vibrated, they bend and distort and this is further compounded when vibrated at resonant frequencies.

There are two major mechanical components that, when excited at resonance, can result in data transfer failure. First, there is the suspension arm that pre-tensions the head against the disk to counterbalance its aerodynamic upthrust. This is designed to control the flying height of the head during normal operating conditions. If the flying height of the head is such that it is outside of its normal operating range, then the signal degrades and ultimately can lead to data transfer failure. In severe cases, the head will crash down onto the disk and cause irrecoverable damage. Second, there is the hard disk (the data storage medium) itself. The disk can be driven such that it flutters up and down, causing tracking (or mis-registration) problems [2]. The problem can be compounded by the fact that if the suspension arm is resonating, and, therefore, the head, the disk can be driven into oscillation due to the head pushing onto the disk and vice-versa [3], [4].

Hard disk drives predominantly use 3.5-in disks. These disks are all made to identical standards by a few different manufacturers. It is fair to say that there are negligible variations in their construction. Therefore, all modes excited by the disk are common to all drives using 0.8 mm thick, 3.5-in diameter disks.

III. Experimental

A test rig has been constructed to allow the hard drive to be vibrated at accelerations of up to 50 g [7]. The hard drive is rigidly clamped to a plate that is vibrated by an electro-dynamic shaker. In these experiments, the drive is mounted so that it is excited in the plane through its spindle. Vibrating the drive in this manner closely simulates vibrations experienced when the drive is in its normal operating environment. Excitations in this plane maximize any resonant effects of the disk and suspension arm. Vibrating the drive in other planes will still excite the same modes but to a lesser degree. If the drive were to be excited in another plane, different effects and resonant modes will also be experienced, like the lateral bending of the suspension arm. The test rig allows the drive to be mounted in distinct, different orientations.

A piezoelectric sensor mounted to the plate enables measurement of the vibrations experienced by the drive and provides a feedback signal for the signal amplifier. A PC is used to control the sweeps of vibration and acceleration that the drive receives. While the drive is being vibrated, the computer can write and read data to and from it, monitoring the time taken for the data to be correctly transferred. As the amplitude of vibration increases, the drive's transfer rate slows down, eventually leading to the drive completely failing to transfer data.

Manuscript received May 4, 2000; revised February 14, 2002. This work was presented at the 17th IEEE Instrumentation and Measurement Technology Conference, Baltimore, MD, 1–4 May 2000.

The authors are with the Centre for Research in Information Storage Technology, University of Plymouth, Plymouth, U.K.

Publisher Item Identifier S 0018-9456(02)04311-5.

0018-9456/02$17.00 © 2002 IEEE

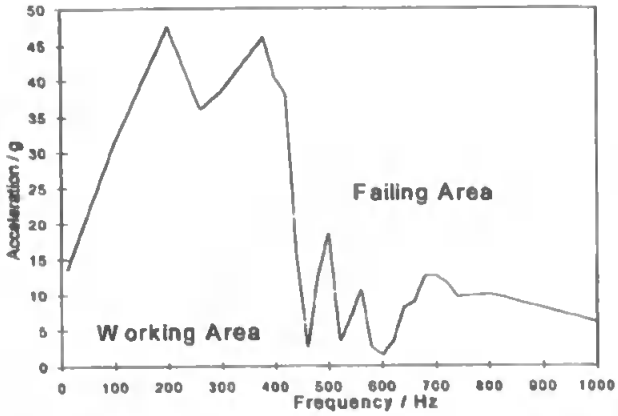

Fig. 1. Effect of vibration on 3.5" hard disk drive operations, showing particularly bad data transfer in the 450–600 Hz region.

Some interesting characteristics of a typical 3.5-in drive's performance are its inability to transfer data at vibration levels greater than 1 g at 450 Hz and 600 Hz and yet the drive is resilient to about 45 g of vibration below 400 Hz. These characteristics can be clearly seen in Fig. 1.

It was found that all 3.5-in hard disk drives tested, from a variety of manufacturers, showed poor performance under conditions of vibration at frequencies around 450 Hz to 700 Hz.

All systems, when subjected to vibration, can go into resonance. It is evident that hard disk drives suffer from this phenomenon. The fact that the drives operate poorly at certain frequencies is indicative of this. However, it is necessary to ascertain which component or system is failing.

To do this, sensors have been incorporated within the hard drive housing to try to gain an understanding of what is occurring. However, the environment that the drive operates in must at all times be undisturbed by the sensors. Hard disk drives are hermetically sealed to prevent dust contamination damage and this dictates that when applying sensors to a *working* hard drive a sealed environment must be retained. In addition to this, the sensors included are both inexpensive and integrated within the drive. This enables the opportunity to develop a drive that can actively detect vibration, resonant modes, and drive the suspension arm accordingly, via real-time feed back into a control system using piezo-electric actuators, to cancel such activity and create the "ruggedized" drive. While other measuring techniques, typically interferometers or laser Doppler vibrometers, exist that can measure the disk and arm motion, they require external components added to the system that are bulky, expensive, and complex. This is not wholly practical in, for example, a laptop.

To measure the bending of the suspension arm, a thin (28 μm) sheet of poly vinylidine flouride, PVdF, piezo material was bonded to the suspension arm to measure the average strain, as shown in Fig. 2. It is extremely important to use as fine a connecting wire and as thin a layer of cement as possible so as not to disturb the system. The coaxial wire, which was connected to the sensor, was bonded to the suspension arm, allowing it to pivot at the same point as the arm pivots. This prevents the problem of the voice coil motor not having enough power to allow the suspension arm to track correctly across the disk.

Fig. 2. Picture showing the inside of the modified hard disk drive. The piezo element bonded to the top surface of the suspension arm is an actuator (see text). On the lower side of the arm is the PVdF sensor.

Fig. 3. A PVdF thin-film sheet has been bonded to the drive in a manner such that it is pre-tensioned. Note that it is positioned at the outer edge of the disk.

Measuring the disk movement is rather more difficult since the rotating disk has many modes of resonance.

The purpose of measuring the disk displacement is to isolate disk and suspension arm movement to further our understanding about which is going into resonance and at what frequencies. The sensor on the suspension arm will be able to identify when the suspension arm is moving, but the suspension arm might be moving because the disk has gone into resonance and the arm is following it, as it is designed to. Therefore, a sensor needs only to measure the displacement of the disk in the region where the head is positioned above the disk. Using software that utilizes BIOS commands, it is possible for the head and suspension arm to read data from any chosen track on the disk. Therefore, the head was placed at the outer edge of the disk to provide the most sensitivity to disk fluctuations and easier disk measurement.

Another PVdF sensor was used to measure the disk's displacement. This time, the sensor used was a cantilever that only introduces subtle changes to the system, with one end rigidly bonded to the drive's chassis in a manner that pre-tensions the cantilever against the disk, as shown in Fig. 3. Any movement of the disk would, therefore, bend the cantilever from its static position. The cantilever is bonded to the chassis at its most rigid point, closest to where the drive is mounted in a PC cage or on the test rig. This virtually eliminates any possibility of the cantilever being falsely driven into resonance by its mounting. This

Free Disk /Hz	Disk completely clamped /Hz
277	440
298	742
512	1082
1097	1872

Fig. 4. Results from finite element analysis showing the lower, relevant, modes of the static disk when both clamped and free.

does not preclude the drive's chassis from flexing. This will be detected by the disk moving and hence recorded by the sensor. It is fair to say though that chassis and bearing flex is detrimental to flying height stability and as a result needs to be recorded, which this sensor does.

The magnitude of the signal level was predicted to be very small, so every attention to reducing noise had to be incorporated. The coaxial wires running from the sensors embedded within the drive were further shielded with a fine mesh sleeve.

To record the signals from the sensors, they were connected to a 12-bit data acquisition board, capable of sampling the signal at up to 200 kHz. The system resolution is more than adequate to observe arm and disk movement attributed to external disturbances.

IV. Finite Element Analysis

Finite element analysis software was undertaken using Pro Mechanica to model the resonant characteristics of the disk and the results are shown in Fig. 4. Models were created to determine the resonant modes for both free and clamped disks. To simplify the model the disk was assumed to be rectangular in cross section. The final model is outlined in Fig. 5. The disk cannot be modeled as completely circular, since the model is limited by the finite element mesh size. A reasonable number of points defining the radii were chosen. In this case, the disk was defined as having five inner rings and 24 dissecting lines, as shown in Fig. 6. Simulations were also made with a far greater number of points and the effects on the predicted resonant modes were minor. It was found that when clamped, the disk's first predicted mode of resonance is at 440 Hz and this was confirmed by practical tests.

It is known that the disk's resonant frequencies will be slightly changed due to the gyroscopic effect of the disk spinning. Further to this, it is also understood that due to the static position of the sensor and the nature of the disk's resonant undulations, a condition is created where the sensor detects two modes instead of the one static resonant frequency. These resonant peaks are detected at the static resonant frequency, modulated by the disk's rotational speed. The only mode that does not suffer from this effect is the "umbrella" mode, where the entire outer circumference diaphragms.

Finite element analysis clearly demonstrated the difference in resonant frequencies between a clamped and unclamped disk. Due to the mechanical nature of the disk's clamp, perfect clamping does not occur and this results in both clamped and unclamped modes being excited.

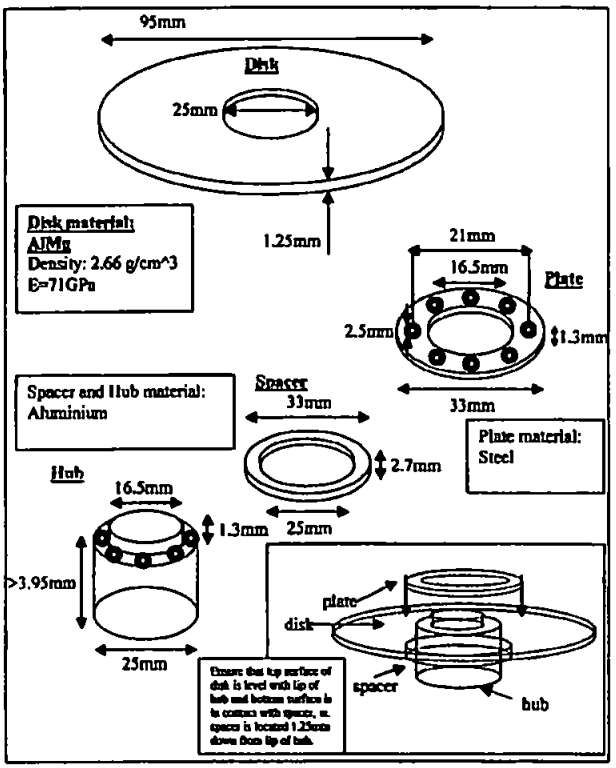

Fig. 5. Diagram outlining the key dimension and materials used when modeling the disk using Pro-Mechanica Finite Element Analysis software.

V. Results

Since we wish to extend this work to include active control of the head's flying height, a piezoelectric actuator was also mounted on the top of the suspension arm. Ultimately, an active arm will use the piezo actuator to drive the arm, counteracting any resonant modes and the sensor element is used to record overall response. Tests have shown that the piezo actuator makes only minor changes to the arm's mechanical characteristics.

In order to validate the system and enhance our understanding of the components being measured, tests were undertaken that could easily be related to other work [2], [4]–[6], but being fundamentally different in the respect that these tests are the first unobtrusive tests while the drive is in operation. These tests were designed to interpret the frequencies of resonance of the disk. The drive was run with its lid on so as to emulate its normal working condition. The disk was then excited through impulse shocks transmitted to it in the form of a mass dropped onto the chassis. The shocks were delivered repeatedly in such a way as to excite all of its prominent modes of resonance and the frequency response was calculated by FFT. Once built up, the results gave great insight into all the accessible modes of both the disk and suspension arm, confirming many of the modes observed in other papers, shown here in Figs. 7 and 8.

The peaks at 75 Hz, 150 Hz, and 225 Hz are due to disk warpage and uneven clamping. This creates a degree of disk runout and hence peaks at the disk speed and its harmonics are observed. In this cas, the disk is spinning at 75 Hz or 4500 rpm.

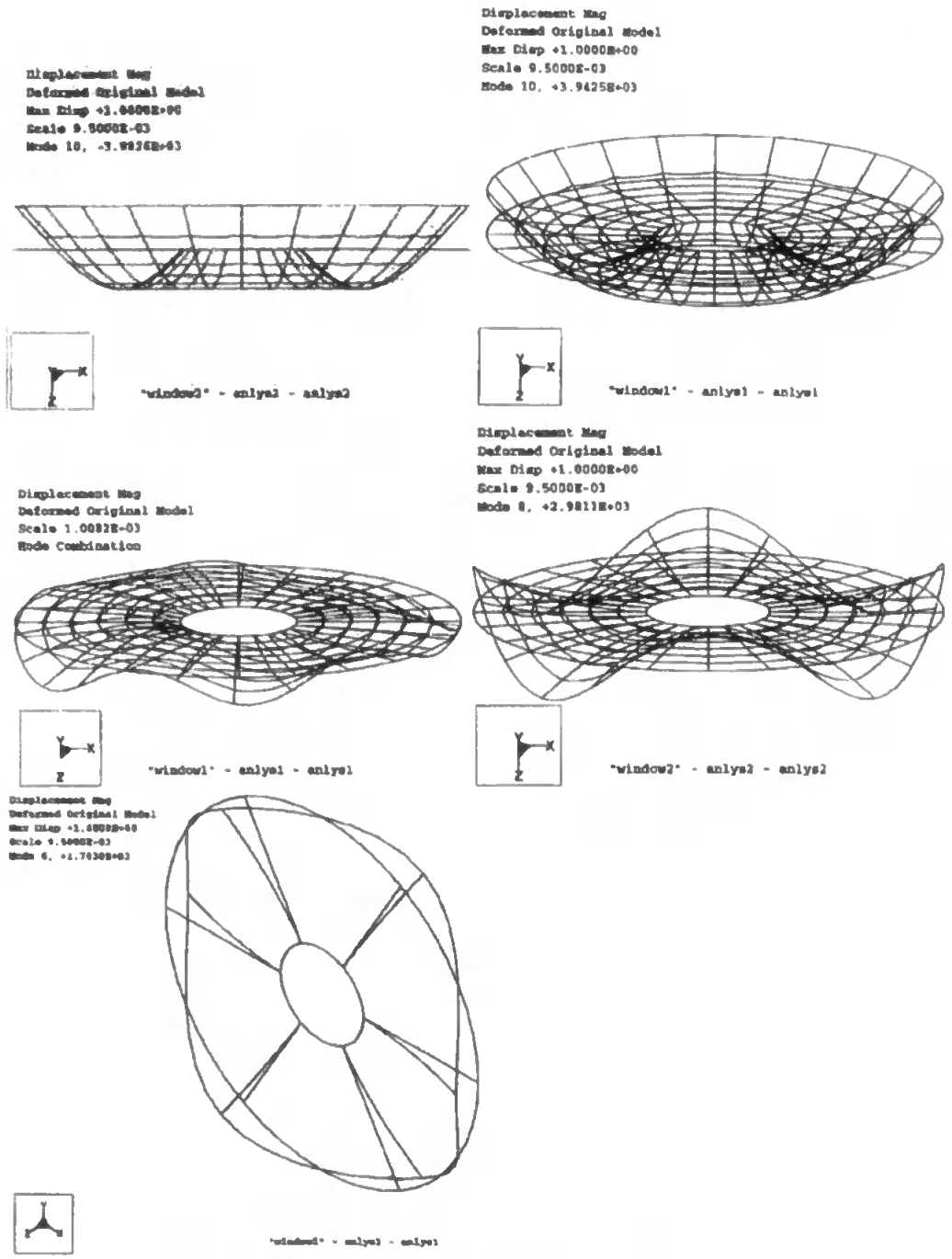

Fig. 6. Results from Pro-Mechanica showing the resonant modes: the upper two show the "umbrella" mode.

The suspension arm has major resonances at 1 kHz, 1.29 kHz, 1.45 kHz, 2 kHz, and 2.22 kHz. The suspension arm is observed to be bending at 440 Hz and between 590 and 855 Hz. This is because the disk is bending, seen as large peaks in Fig. 7, and the suspension arm is following the disk, maintaining the correct flying height for the head [3], [4]. It was also noticed that, in some cases, where the suspension arm went into resonance, the force of its movement was enough to bend the disk. For example, the suspension arm experiences modes at around 1.29 kHz and 1.45 kHz which are coupled and seen in Fig. 6, as movement in the disk at these frequencies. If this interaction were to become too great, it would be possible for the head to actually crash into the disk.

The modes measured unobtrusively with the PVdF sensors are in good agreement with those measured by others [2], [4]–[6]. There are, however, subtle differences attributed to the lid that acts as an air damper and so suppresses disk movement. The disk flexes up and down, the so-called "umbrella" mode, when the entirety of its circumference is in phase. The pocket of sealed air between the disk and lid limits its movement; the

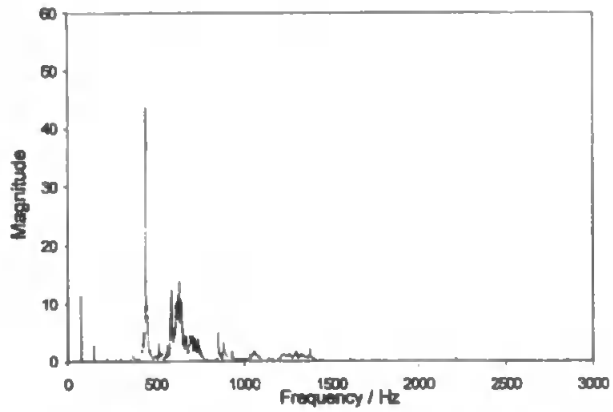

Fig. 7. This graph shows the frequency response of the disk alone when subjected to impulse excitation.

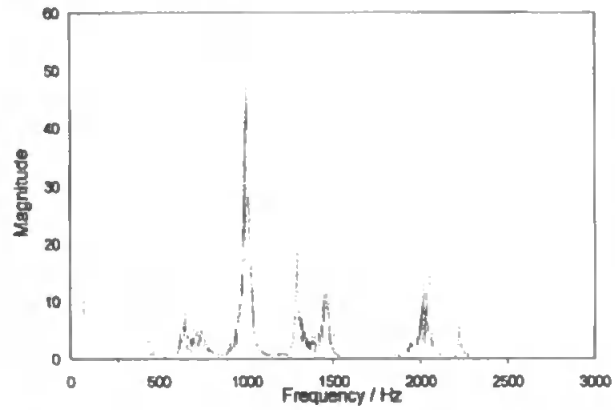

Fig. 8. Graph of the results for the same excitation but of the suspension arm flying on the disk.

lid in effect acts as a damper. The air bearing's performance is also slightly adjusted when operated with the lid on. The slider relies upon air flow created by the spinning disk. With the lid removed the local air velocity is going to be affected, hence affecting the air bearing's characteristics.

In order to reinforce our understanding of existing results, a measure of the tracking error was obtained. The drive was vibrated, from 50 Hz to 3 kHz, while the tracking servo signal was observed. The magnitude of this signal corresponds to the degree of track displacement, or how far the head has moved away from its desired position in the center of the data track. This is known as the tracking error. From Fig. 9 it can be seen that large radial displacements were observed around 1775 Hz and 1875 Hz. This is probably due to the suspension arm going into resonance and causing the tracking servo to compensate for this apparent misalignment. The peak observed at 575 Hz is attributed to disk resonance. Displacements, although comparatively small, were repeatedly observed around 2225 Hz. The two modes at around 1.9 kHz and 2.22 kHz correspond with the activity, detected by the PVdF sensor, of the arm at around 2 kHz and at 2.22 kHz.

VI. Conclusion

Data loss was found to be significant at frequencies between 450 and 700 Hz. The disk's first resonant mode was found ex-

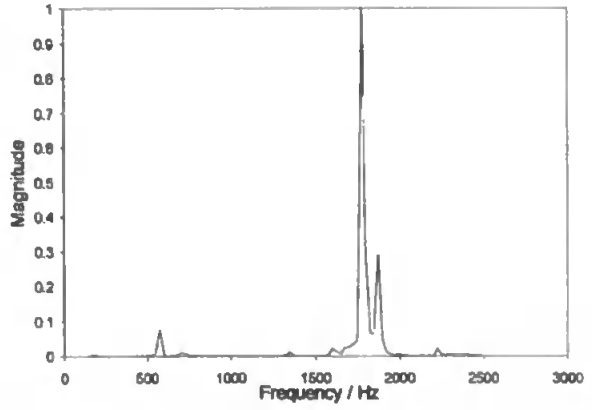

Fig. 9. Tracking error synchronous with applied drive vibration.

perimentally to be at 440 Hz and validated through finite element analysis simulations. It was found that when the disk goes into resonance, the movement was great enough for disk and suspension, coupled via the air bearing, to move synchronously together. This has been observed through modes being detected by both PVdF sensors at exactly the same frequencies. However, there is an initial phase lag between disk motion and arm motion, the exact nature of which has yet to be experimentally verified. This creates a variation in the flying height, a major contributing factor to data transfer errors.

Disk and arm movement has been found to increase tracking errors, seriously degrading the drive's performance to transfer data. This is particularly evident at frequencies where the arm and disk are coupled and suffering from a resonant force.

References

[1] N. Dennis, "Wideband passive mechanical mounting systems for disk drives on boats in rough seas," *IEEE Oceans*, Oct. 1997.

[2] J. S. McAllister, "Characterization of disk vibrations on aluminum and alternate substrates," *IEEE Trans. Magn.*, vol. 33, Jan. 1997.

[3] A. M. Allen and D. B. Bogy, "Effects of shock on the head-disk interface," *IEEE Trans. Magn.*, vol. 32, Sept. 1996.

[4] J. R. Edwards, "Finite element analysis of the shock response and head slap behavior of a hard disk drive," *IEEE Trans. Magn.*, vol. 35, Mar. 1999.

[5] H. Bittner and I. Y. Shen, "Taming disk/spindle vibrations through aerodynamic bearings and acoustically tuned-mass dampers," *IEEE Trans. Magn.*, vol. 35, pp. 827–832, Mar. 1999.

[6] I. Y. Shen and C. P. Roger Ku, "On the rocking motion of a rotating flexible-disk/rigid-shaft system," in *Advances in Information Storage and Processing Systems*. New York: ASME, 1995, vol. 1, ISPS, pp. 271–282.

[7] D. Jenkins, W. Clegg, C. Chilumbu, and G. Tunstall, "Actuators for tomorrow's ruggedised hard disk drives," in *Datatech*. London, U.K.: ICG, 1999, vol. 3, pp. 71–75.

Glen Tunstall (SM'95) received the B.Eng. degree in electronic engineering in 1998. Currently, he is pursuing the Ph.D. degree, researching hard disk drive performance under conditions of vibration and measuring internally and unobtrusively the systems which fail.

He is with CRIST, a research group at the University of Plymouth, U.K.

Warwick Clegg studied physics at the University of Liverpool, U.K., in the mid-1960s and then went on to receive the M.S. and Ph.D. degrees from the University of Manchester, U.K., for work on magnetic data stores.

He has recently moved to the University of Plymouth, U.K., where his current research includes instrumentation for optical and magnetic recording and micro-imaging using scanning laser and scanning probe techniques. Following his appointment as Research Professor, he is now Head of the Department of Communication and Electronic Engineering.

David F. L. Jenkins received the B.Sc. (physics), M.Sc. (lasers and their applications), and Ph.D. (photothermal deflection spectroscopy) degrees.

After completing Ph.D. research at the Royal Military College of Science, he became a post-doctoral Research Fellow at the Coventry University, U.K., in 1990, working on magneto-photo-acoustic spectroscopy. Between 1993 and 1997, he worked in the Information Storage Group, Division of Electrical Engineering, University of Manchester, U.K., researching into active vibration control of micromechanical structures. In 1997, he moved to the University of Plymouth, U.K., as Lecturer in the Centre for Research in Information Storage Technology, where he has continued his research into microactuators and microsensors. He has recently been appointed Senior Lecturer.

Chibesa Chilumbu received the B.Eng. (Hons) degree in electrical engineering from the University of Manchester, U.K., in 1996. He is currently pursuing the Ph.D. degree in information storage at the University of Plymouth, U.K. His Ph.D. research concerns head-positioning control methods in advanced hard disk drives. This work includes composite piezoelectric sensors and actuators, the development of hard disk drive suspension arms and control algorithms for optimizing the performance of these arms.

Actuators for Tomorrow's Ruggedised Hard Disk Drives

David F. L. Jenkins, Warwick W. Clegg, Chiesa Chilombo & Glen A. Tonstall, *University of Plymouth, Plymouth, UK*

Abstract

The areal storage density of magnetic hard disks is continually increasing. Typical available commercial storage densities at present are 3 Gbits/in^2 and it is predicted that densities in excess of 40 Gbits/in^2 will be possible before the year 2003. Along with this development is the requirement for the accuracy of head positioning to move beyond that provided by present technology, both in terms of x-y positioning for track/sector location and z-axis positioning for flying height control. The demands on head positioning control are even more demanding when the hard disk drive is operated under hostile conditions of shock and vibration. This paper considers the problem of read-write error associated with hard disk drives operating under adverse conditions and looks at how current actuator technology may be used to circumvent the problem.

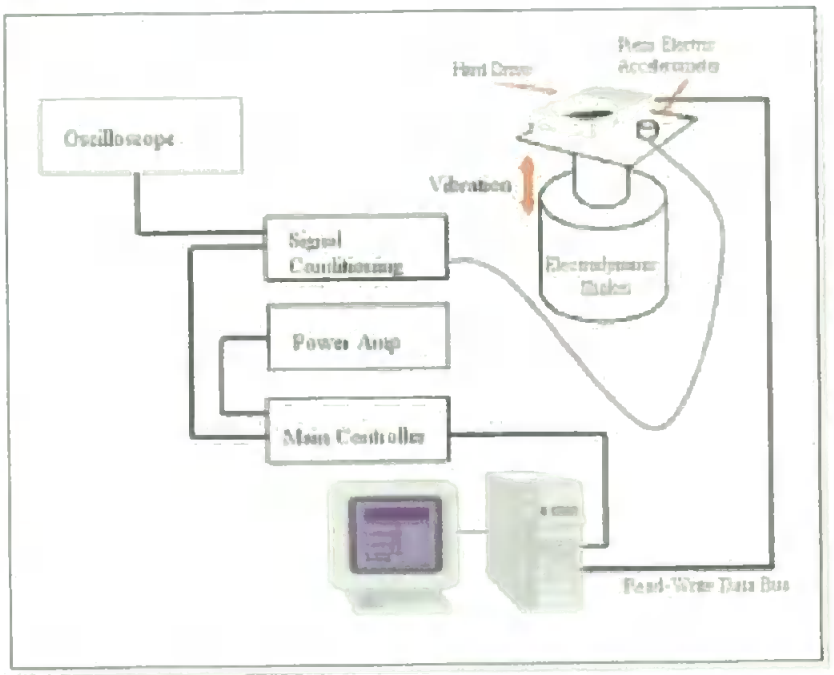

Figure 1
Schematic experimental arrangement for evaluating read-write data transfer as a function of frequency and acceleration

Introduction

As we move towards the new millennium we are faced with the increasing demands of hard disk drive technology. Data storage density continues to increase, which means that the head must fly even closer to the disk surface: state of the art flying heights are currently around 15 nm. This is coupled with the increasing demand for faster track access, which means that the disk drive is required to operate at increasingly higher speed. This represents a challenge for PCs operating in the office environment, but presents more serious difficulties for computers working in conditions where they are subjected to shock and vibration. This is of particular interest to military and aerospace applications; and to a lesser extent will also affect users of laptop computers.

The use of piezoelectric materials has received considerable attention because of their light weight, fast response, low cost, high stiffness and availability in different sizes. Piezoelectric materials are widely used as sensors and actuators in applications such as: active vibration control [1], noise reduction [2], shape control [3] and damage assessment [4]. Piezoelectric materials, such as lead zirconate titanate (PZT), are commonly available as bulk ceramics and in thick and thin film form. Recent advances in the design and manufacturing of aerospace and automotive systems have extended the use of piezoelectric fibre-reinforced composite materials, owing to their high stiffness-to-weight and strength-to-weight ratios. As a result, research efforts concerning the use of piezoelectric fibre-reinforced composite structures, both for continuous and distributed structures, have been on the increase. Chandrashekhara and Donthireddy [5] presented a mathematical model to demonstrate the dynamic response of piezo-composite beams. The independent behaviour of the sensor and actuator was investigated and numerical results were presented to demonstrate the ability of the closed loop system to actively control the vibration of laminated beams. The aim of the work presented in this paper is to show progress towards the fabrication of a stiff, light weight active composite 'smart' arm, fabricated from glass or carbon fibre-reinforced composites, which would be used in a dual-actuation mechanism in advanced computer hard disk drives. This would enable both positioning control of the head flying height (z-axis) above the disk and high resolution tracking (y-axis), capable of sub-nanometre positioning.

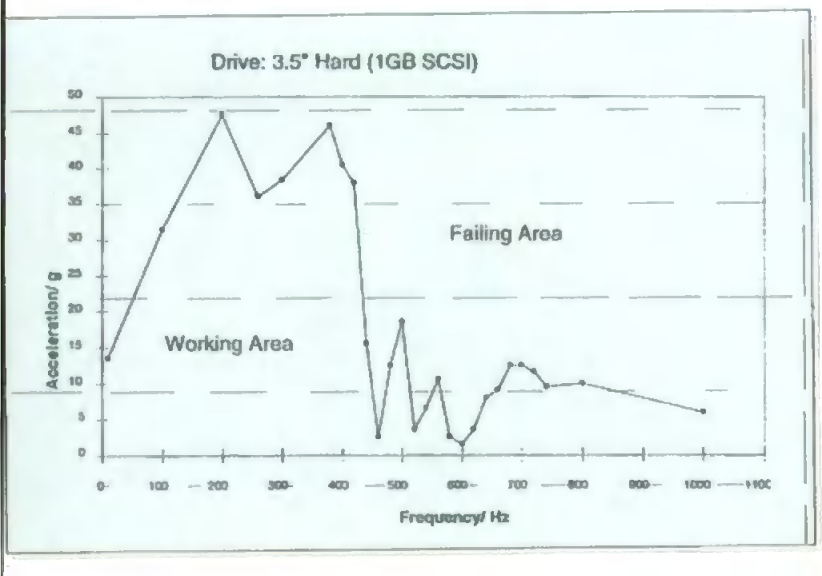

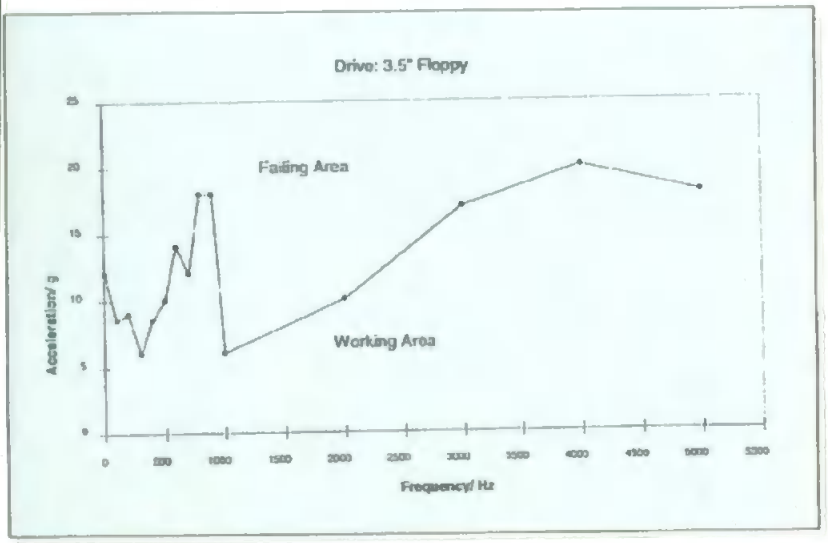

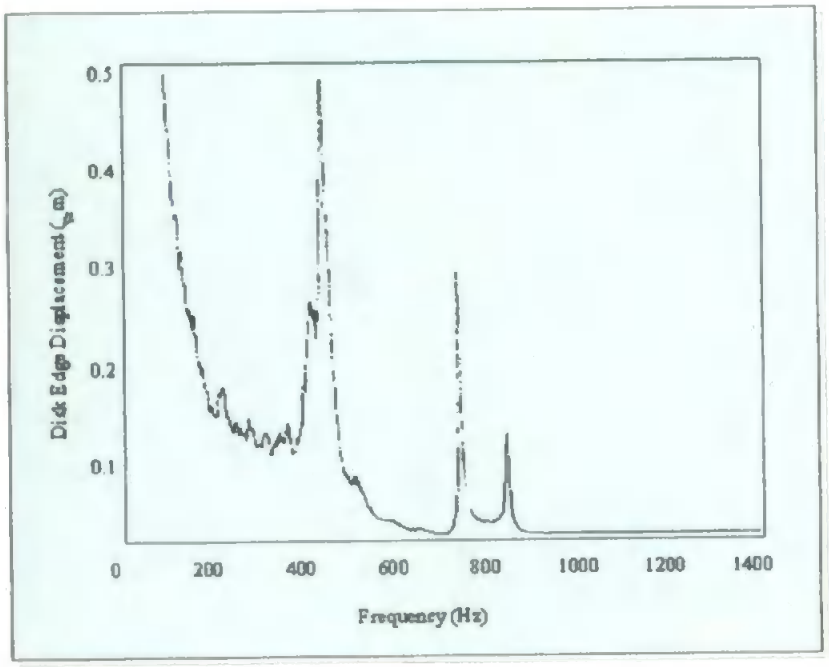

HARD DISK DRIVE CHARACTERISATION

A number of issues are being addressed in this work to characterise disk drive performance under conditions of shock and vibration:

- Read-write data transfer.
- Dynamic characterisation of the head.
- Dynamic characterisation of the disk.

A vibration test rig has been constructed to determine the conditions under which a given disk drive (hard or floppy) fails. The test system consists of an electrodynamic shaker driven via a power oscillator controlled by a PC-operated function generator. The software used is able to generate sinusoidal frequency sweeps or random frequency / amplitude tests. The disk drive under investigation is rigidly clamped to the top plate of the electrodynamic shaker and the disk is vibrated whilst data is being either read from or written to the disk. Data written to the disk can be either a 1 or 0, or a random mixture of both. The arrangement used is shown schematically in Figure 1. The data generated is interpreted to generate a plot of the Working Area and Failure Area as a function of frequency and acceleration. Figures 2 and 3 show typical results for a 1 GB hard disk and a 3½" floppy disk drive. These figures show the regions of correct operation and failure. It should be noted that all regions above the line correspond to failure, whereas at any point below the line read-write operation are possible, but performance degrades as the boundary is approached.

Looking at Figures 2 and 3 it can be seen that floppy disk drives are considerably worse at transferring data under conditions of vibration at 500 Hz or less compared to hard disk drives, and the situation reverses at higher frequencies. For hard disk drives we observe that the device is particularly susceptible to failure in the frequency region 400 Hz to 800 Hz, and this has been true for all hard drives tested in our laboratory.

HEAD-DISK INTERFACE CHARACTERISATION

In order to improve the data transfer of hard disk drives under adverse conditions, it is necessary to determine how the relative motion of the head and disk correlates with the conditions under which failure occurs. This work falls into a number of areas:

- Finite element analysis of the dynamic morphology of rotating disks.
- Disk vibration measurements using accelerometers.
- Experimental measurement of disk vibration characteristics.
- Head flying height measurements.

The modelling of the hard disk has been carried out using finite element analysis. The disk is modelled to determine the modal frequencies of vibration. This shows that the resonant frequencies are 470 Hz and 800 Hz. To check

Figure 2 (top)
Working and failure areas for a 1 GB hard disk drive

Figure 3 (middle)
Working and failure areas for a 3½" floppy disk drive

Figure 4 (bottom)
Resonant frequency of hard disk

experimentally, initial work has been undertaken using a miniature accelerometer attached to the perimeter of the disk. The displacement of the disk was recorded over a large frequency range, after an initial excitation. This shows that the fundamental frequency was 564 Hz and that the resonant frequency was 488 Hz. Higher modes, with correspondingly reduced amplitudes, at 800 Hz and 960 Hz, are also observed. These results are in agreement with McAllister [6] and Edwards [7]. Figures 4 and 5 show the natural and resonant response of a typical hard disk drive respectively.

ACTUATORS

The areal recording densities of magnetic hard disk drives (HDDs) have doubled every 18 months in recent years. Seagate recently set a new areal density benchmark of 16.3 GB/in2 [8]. Within this same development, a flying height of 15 nm has been set and a new benchmark for track density (43 000 tpi) has been established. The current prediction is that if this trend of growth continues, we should expect areal densities of hard drives to be around 40 GB/in^2 by the year 2002, and the head flying height to be around 10 nm. In order to achieve such high areal densities, very narrow data tracks will be required. With current technology, which uses a conventional voice-coil motor, it will become increasingly more difficult to position a magnetic head on top of a narrow data track with the high accuracy and precision required. This has been attributed partly to the hysteresis of the actuator's pivot bearing and the actuator's structural resonant modes, which limit the track-following servo's low-frequency error rejection attenuation and bandwidth [9]. One method that could circumvent this is the use of a dual-stage actuation mechanism. This involves the use of a fine high-bandwidth microactuator for very fine data tracking and head flying height control. Most research into dual-stage actuators has involved the use of the microactuator for data tracking only [9-12].

However, another need has also been identified to be able to control the head flying height. The microactuator, in conjunction with appropriate positioning control algorithms, will be able to control the suspension arm such that the flying height can be adjusted to maintain the head at the correct height above the rotating magnetic disk. Maintaining the correct flying height is becoming increasingly more important as flying heights are reduced even further to realise greater areal storage densities in magnetic disks. In this laboratory, three possible routes have been identified to develop actuators that would enable active flying height control to be achieved as well as providing fine data tracking.

- Bonded piezoelectric actuators
- Embedded piezoelectric actuators
- Composite piezoelectric arms.

BONDED PIEZOELECTRIC ACTUATORS

Piezoelectric bulk ceramic element such as lead zirconate titanate (PZT) can be attached close to the root of the load beam suspension arm to either position the arm up or down or to suppress induced motion within the arm at resonant frequencies [13]. When operated in this way, the actuator thickness should be as small as possible, but of comparable thickness to that of the cantilever. The two main reasons for this are: to optimise the cantilever actuation [14] and, to prevent the actuator from affecting the dynamic characteristics of the cantilever. This technique has been used previously for micro-positioning and active vibration control [15].

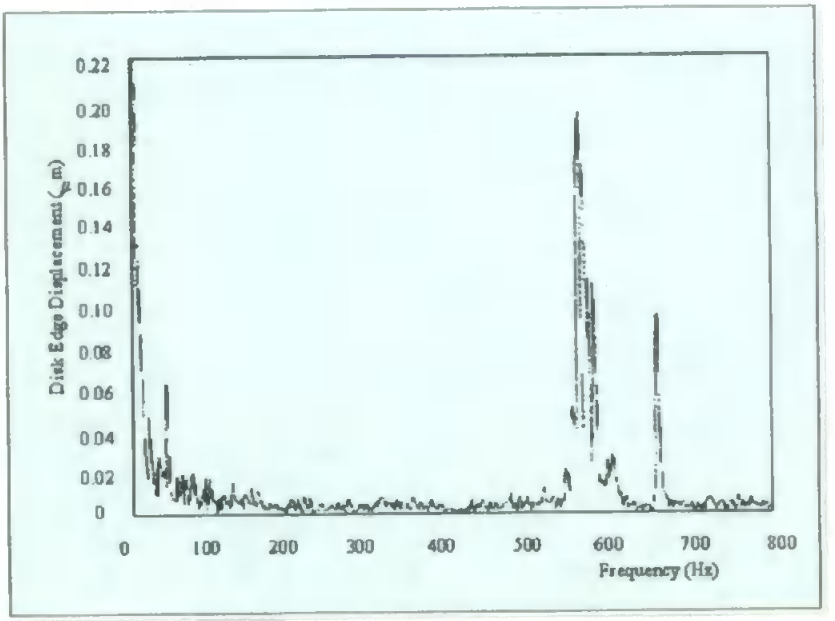

Figure 5
Natural frequency of hard disk

Another route involving bonded actuators is the use of composite piezoelectric materials. It is possible to make a piezoelectric thick film by combining piezoelectric powder and epoxy resin [16]. However, films produced using this method have a much lower piezoelectric activity compared to bulk ceramics and, because of the flexibility of the film, this activity cannot be coupled adequately to the underlying structure. In order to circumvent this problem, composite films have been reinforced using glass fibre and/or carbon fibre [17]. These films offer much improved rigidity, compared to standard composites, resulting in increased effective bending moments of the arm. Current work is being extended to improve the films by reinforcing the composite using PZT fibres. This will form what we will call 'an actively reinforced composite', which should offer improved actuation and rigidity.

EMBEDDED PIEZOELECTRIC ACTUATORS

The simplest method is to embed piezoelectric stacks into the head suspension system. While retaining the current stainless steel load beam suspension, the piezo-stacks are embedded at the end of the aluminium frame arm. One stack is embedded such that when actuated, it produces motion of the arm in the x-y plane (for fine data tracking). The other stack is embedded such that it produces motion in the z-axis. Since both piezoelectric stacks are embedded at the end of the aluminium frame, resonance effects within the aluminium arm do not affect the performance of the piezoelectric stacks. In addition, the location of the piezoelectric stacks ensures that increased servo bandwidth can be realised. This work is also currently in progress, and is of great commercial interest.

ACTIVE COMPOSITE

Current technology uses a sprung stainless steel cantilever, to which the head and gimbal assembly is attached at the end. As stated previously, a voice coil motor is used to position the head in the x-y plane for track selection, whereas the flying height (z-axis) is determined from the compliance of the arm, aerodynamic characteristics

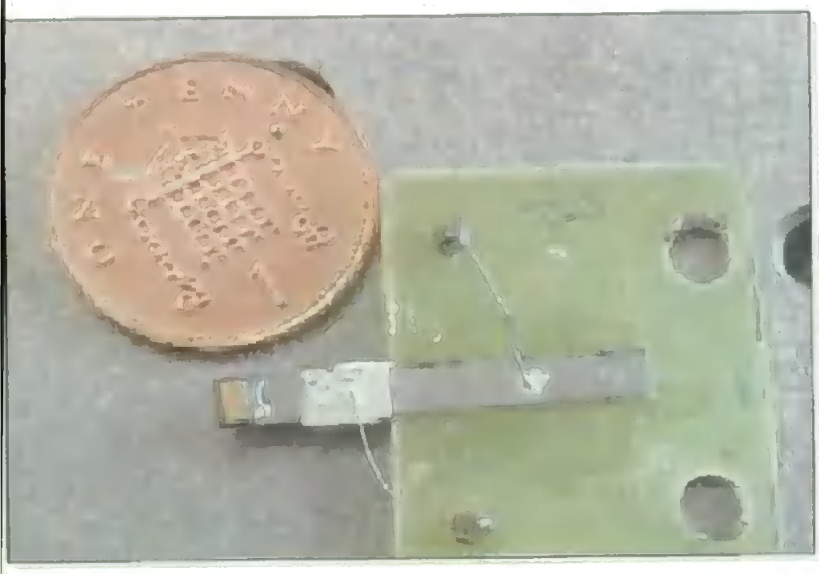

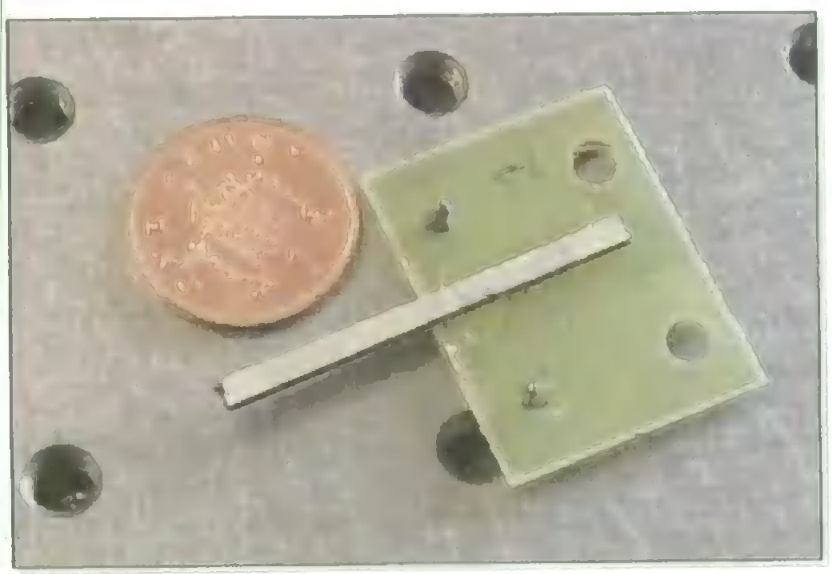

Figure 6 (top)
Composite piezoelectric film bonded to the root of the cantilever

Figure 7 (above)
Prototype of composite arm

of the air-bearing slider and the speed of rotation of the disk. The whole load suspension arm is fabricated from carbon and glass fibre, with PZT distributed within the composite framework to make it active. The composite arm would control the head flying height and the current aluminium frame would have a piezo-stack embedded within its frame to produce fine motion for data tracking, hence realising the dual-stage 2-dimensional actuation. However, the fabrication of such a composite arm is time-consuming and requires several stages of intricate work, and hence may be unattractive for commercial adoption in current disk drive mass-producing factories. A prototype of such a composite arm is shown in Figure 7.

CONCLUSION

A measurement system has been developed to determine the success rates of data transfer to and from the hard disk under conditions of vibration (and shock). In parallel with work, the dynamic morphology of hard disks has been investigated experimentally using accelerometers and modelled using finite element analysis. The results obtained have, not surprisingly, shown that data transfer is strongly affected by the dynamic behaviour of the disk itself.

In order to improve hard disk performance, in terms of reliable data transfer, it is a fundamental requirement that the read/write head is maintained at a constant height above the rotating disk. Our research has shown that disk flexure can severely affect data transfer under adverse conditions, but it should be possible to circumvent this limitation by developing appropriate sensor-actuator systems. A number of possible configurations have been investigated, based upon optical sensing and piezoelectric micro-actuators. The wide bandwidth of piezoelectric actuators has already been shown to enable resonant vibrations to be damped whilst simultaneously allowing the flying height to be controlled. Future work will continue the research and development into sensor-actuator systems in parallel with the characterisation and modelling of hard disk drives. In particular, we are interested in modelling laminate disks incorporating passive damping. These may give a significant improvement in ruggedised systems, even without active control of the head-suspension system.

REFERENCES

[1] M.J. Cunningham, D.F.L. Jenkins, W.W. Clegg and M.M. Bakush, Sensors and Actuators, A 50, 147 (1995).

[2] C.Q. Chen and Y.P. Shen, Smart Mater. Struct., 6, 403 (1997).

[3] K. Ghosh and R.C. Batra, SPIE Proc., 2427, 107 (1995).

[4] A.C. Okafor, K. Chandrashekhara and Y.P. Jiang, Smart Mater. Struct., 5, 338 (1996).

[5] K Chandrashekhara and P Donthireddy, Eur. J. Mech., A/Solids, 16, No. 4, 709 (1997).

[6] J.S. McAllister, IEEE Transactions on Magnetics, January 1997, Vol. 33, No. 1, 968-973.

[7] J.R. Edwards, IEEE Transactions on Magnetics, March 1999, Vol. 35, No. 2, 863-867.

[8] Technology update. Data storage magazine (page 10), March 1999.

[9] T. Hirano, L.S. Fan, W.Y. Lee, J. Hong, W. Imaino, S. Pattanaik, S. Chan, P. Webb, R. Horowitz, S. Aggarwal and D. Horsley, IEE/ASME Transactions on Mechatronics, September 1998, Vol. 3, No. 3, 156-165

[10] R. Evans, P. Carlson, W. Messner, Data Storage Magazine, April 1998, 43-44.

[11] T. Imamura, M. Katayama, Y. Ikengawa, T. Ohwe, R. Koishi and T. Koshikawa, IEE/ASME Transactions on Mechatronics, September 1998, Vol. 3, No. 3, 166-173.

[12] K. Mori, T. Munemoto, H. Otsuki, Y. Yamaguchi and K. Akagi, IEEE Transactions on Magnetics, November 1991, Vol. 27, No. 6, 5298-5300.

[13] M.J. Cunningham, D.F.L. Jenkins, W.W. Clegg and M.M. Bakush, Sensors and Actuators A – Micromechanics, Vol. A50, 1995, 147-50.

[14] M.J. Cunningham, D.F.L. Jenkins and M.M. Bakush, IEE Proceedings – Science, Measurement and Technology, 1997, Vol. 144, 45-48.

[15] D.F.L. Jenkins, M.J. Cunningham, G. Velu and D. Remiens, Presented at ISIF 1997, New Mexico, USA, March 1997. Integrated Ferroelectrics. Vol. 17, 1997, 309-318.

[16] W.W. Clegg, D.F.L. Jenkins and M.J. Cunningham, Sensors and Actuators A, A58, 1997, 173-177.

[17] C. Chilumbu, D.F.L. Jenkins and W.W. Clegg, Presented at Euroceramics VI, Montreux, Switzerland, August 1998. In print, Proc. Electroceramics VI, (Spring 1999).

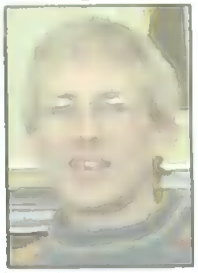

ABOUT THE AUTHORS

David F.L. Jenkins holds the degrees of B.Sc. (Physics), M.Sc. (Lasers and their Applications) and Ph.D. (Photothermal Deflection Spectroscopy). After completing his Ph.D. research at Royal Military College of Science he became a post-doctoral Research Fellow at Coventry University in 1990, working on Magneto-Photo-Acoustic Spectroscopy. Between 1993 and 1997 he worked in the Information Storage Group, Division of Electrical Engineering at University of Manchester, researching into active vibration control of micro-mechanical structures. In 1997 he moved to University of Plymouth to take up the position of Lecturer in the Centre for Research in Information Storage Technology, where he has continued his research into micro-actuators and micro-sensors.

Warwick Clegg studied Physics at the University of Liverpool in the mid-1960s, and then went on to gain Masters and Doctoral Degrees at the University of Manchester for work on magnetic data stores. He has recently moved to the University of Plymouth where his current research includes instrumentation for optical and magnetic recording, and micro-imaging using scanning laser and scanning probe techniques.

Chibesa Chilumbu obtained his B.Eng (Hons) degree in Electrical Engineering from University of Manchester in 1996. He is currently studying for the degree of Ph.D. in Information Storage at University of Plymouth. His PhD research concerns head-positioning control methods in advanced hard disk drives. This work includes composite piezoelectric sensors and actuators, the development of hard disk drive suspension arms and control algorithms for optimising the performance of these arms.

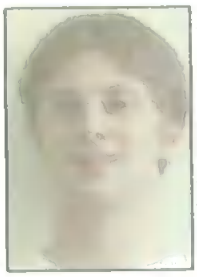

Glen Tunstall graduated with a B.Eng. (Hons) degree in Electronic Engineering in 1998 from the University of Plymouth and is currently studying for the degree of Ph.D. in Information Storage at University of Plymouth. He is researching into hard drive performance under conditions of vibration, and will be developing sensor/actuator systems to actively improve their performance. He is part of CRIST, a research group at the University of Plymouth.

IF YOU HAVE ANY ENQUIRIES REGARDING THE CONTENT OF THIS ARTICLE, PLEASE CONTACT:

David Jenkins
Centre for Research in Information Storage Technology (CRIST)
University of Plymouth
Drake Circus
Plymouth
PL4 8AA
UK

Tel: +44 (0)1752 232589
Fax: +44 (0)1752 232583
E-mail: djfenkins@plym.ac.uk
Web site: http://cr1.see.plym.ac.uk/research/djfenkins.html

Multi-layer bulk PZT actuators for flying height control in ruggedised hard disk drives

D. F L. Jenkins, C. Chilumbu, G. Tunstall, W. W. Clegg, and P. Robinson
Centre for Research in Information Storage Technology, University of Plymouth,
Drake Circus, Plymouth PL4 8AA, UK.

Abstract – When a hard disk drive is operated under hostile conditions fluctuations of the head flying height affect data-transfer, eventually leading to complete data-transfer failure. A test facility has been developed to enable data-transfer and their associated failure mechanisms to be characterised. In order to circumvent this problem and to obtain greater control of the head flying height a novel suspension arm has been developed which incorporates multi-layer bulk PZT actuators. This will enable real-time active adjustment of the head flying height with high precision and accuracy, while the disk drive is in operation. The arm developed is tested dynamically and characterised, and specialised closed-loop control algorithms developed to position and control the head above the disk surface.

INTRODUCTION

Hard disk drives are an economical form of mass storage, widely used as secondary memory in virtually all computer systems. Conventional hard drives are very reliable under normal operating conditions, but they can suffer from mechanically induced failure when operated in hostile conditions. In areas where vibrations exist hard disk drives can, and do fail, and no longer read or write data. At best the data-transfer rate becomes vastly inferior.

Environments such as military and aerospace are synonymous with large shocks and vibrations. Ocean going craft can also encounter difficulties with hard drives as the engine and waves transmit vibrations through the hull. Dennis [1] evaluated many proposed solutions, though mainly large vibration isolation cages and mountings that damped the vibrations. However, additional isolation mountings are not the ideal solution. The extra space and weight needed precludes this method from many key areas: adding both weight and bulk to a drive is hardly an improvement. Passive dampers, which are only effective over a limited bandwidth, are all that are used in current 'ruggedised' laptops.

The data-storage recording densities of magnetic hard disk drives (HDDs) have doubled every 18 months in recent years. IBM recently demonstrated a storage density of 35.3 GB/in^2 [2]. In order to realise high track and storage densities of 40 GB/in^2 or more, flying height will be reduced to around 5-10 nm. One approach that has been considered to achieve such low flying heights is the use of an extremely smooth disk surface to enhance the slider flying stability and reduce thermal noise created by friction. This approach may, however, require zone texturing, when the conventional contact-start-stop (CSS) is used, to avoid serious head-disk damage [3]. Although a load/unload process has been proposed to address this problem [4], the challenge is to be able to maintain the correct flying height in conditions of shock and vibration while the drive is in operation. This is especially useful in portable hard disk drives or dedicated drives being used in critical applications for military and medical purposes, or fieldwork such as mineral exploration, sporting activities or even space navigation.

In this paper, a novel feature that incorporates actively controlling the correct flying height while the HDD is in operation is presented. Through careful design and with the use of multi-layer bulk PZT actuators, the suspension arm is able to realise motion in two orthogonal axes. One corresponds to motion required to provide fine data tracking and the other, precision flying height control. In current commercial HDDs, the net loading force is approximately 35mN during normal operation [5]. An adjustment of $\pm$ 10mN of this loading force would result in a change in the flying height of about $\pm$ 20%, giving sufficient tolerance for active flying height control.

DISK DRIVE FUNDAMENTALS

It is important to understand precisely what is happening within the drive, and which systems areas are failing under conditions of vibration. There are two major mechanical components that, when excited at resonance, can result in data-transfer failure. Firstly, there is the suspension arm that pre-tensions the head against the disc. This is designed to control the flying height of the head during normal operating conditions. If the flying height of the head is such that it is outside of its normal operating range, then the signal degrades, and ultimately can lead to data-transfer failure. In severe cases, the head will crash down onto the disk and cause irrecoverable damage. Secondly, there is the hard disk itself. The disk can be driven such that it flutters up and down, causing tracking (or mis-registration) problems [6]. The problem can be compounded by the fact that if the suspension arm is resonating, and therefore the head, the disk can be driven into oscillation due to the head pushing onto the disc and vice-versa [7, 8].

0-7803-5940-2/01/$10.00 2001 IEEE.

DISK DRIVE CHARACTERISATION

A test facility has been constructed to allow the hard drive to be vibrated at accelerations of up to 50g over a 10 kHz bandwidth. The hard drive is rigidly clamped to a plate that is vibrated by an electro-dynamic shaker, driven by computer controlled frequency sweeps. Mounted to the plate is a piezoelectric accelerometer to monitor vibrations that the drive experiences.

The first set of experiments were conducted to assess the data-transfer performance of the drive whilst undergoing induced external vibration. Certain trends have been observed for all the drives tested. Consistent transfer data failure has been observed between 400Hz and 600Hz, as displayed in Figure 1.

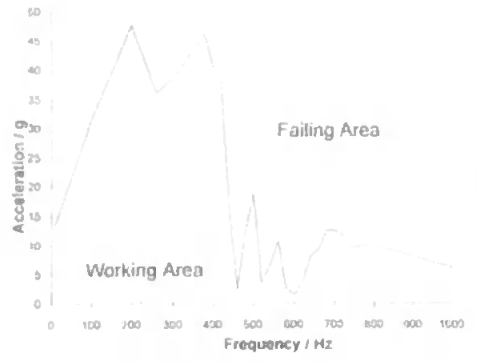

Fig. 1 Data-transfer as a function of frequency of vibration and acceleration, showing that principle data-transfer failure occurs between 400 and 700 Hz.

The next tests were designed to measure the movement of the suspension arm using a piezoelectric strain sensor (PVdF). The strain, assumed to be proportional to suspension end displacement, was measured as a function of excitation frequency, as shown in Figure 2. Results obtained using CR-ROM optics, currently under development, show good correlation with this data.

DATA LOSS PREVENTION

Ultimately, to prevent performance degradation, an actively controlled suspension arm will be fitted to a hard drive. The suspension arm will be built such that, ultimately, actuators will be able to control the head in two orthogonal planes. This will allow freedom to change the flying height, and also enable sensitive tracking adjustments. With an appropriate control system this will allow the head to carefully follow the disk surface and make sensitive tracking corrections.

SUSPENSION ARM DESIGN

A prototype of the suspension arm described above has been built as shown in Figure 3. It comprises a duralumin frame within which piezoelectric actuator stacks (type (alloy of two major materials, aluminium and copper)

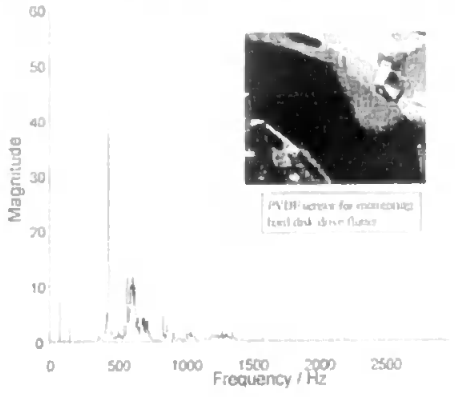

Fig. 2 Frequency response of rotating disk drive obtained using piezoelectric sensor (inset).

711/2/05051, Morgan-Matroc, UK) are embedded. One actuator maintains the desired flying height of the head above a rotating disk whereas the other ensures high-bandwidth precision and accurate track following. A stainless steel loading beam is glued to the framework of the suspension arm but instead of the slider-head arrangement attached at its end, it has a small mirror attached to facilitate the characterisation of the arm when using the optical beam deflection technique [9, 10].

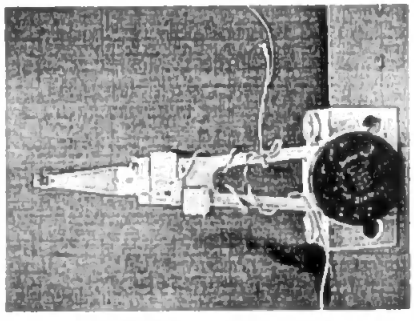

Fig. 3 Prototype suspension arm incorporating multi-layer bulk PZT actuators

SUSPENSION ARM CHARACTERISATION

The suspension arm is tested dynamically by investigating the amount of end-deflection possible at voltages comparable to those used in a hard disk drive environment. Also, resonance modes of the arm are investigated in order to help develop a suitable closed-loop servo controller. The arm is set into resonance by applying bursts of band-limited white noise to the piezoelectric stack and the resonant modes sensed optically. However, actuation in one plane can induce

resonance effects in the orthogonal plane, and vice-versa. The results are shown in Figure 4 and it can be seen that the fundamental resonance is at 140 Hz, although because of its complex mechanical structure there are other resonances at higher frequencies. It is important to remember that due to the complex nature of the arm, resonance in one stage of motion does induce resonances in other stage of motion (used for track following).

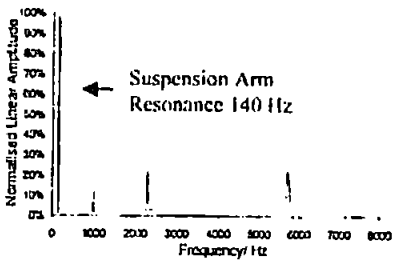

Fig. 4 Frequency response of suspension arm to a broadband white noise. Fundamental arm resonance is at 140 Hz.

SUSPENSION ARM CONTROLLER DESIGN

Proportional integral and derivative (PID) controllers have been implemented to control and position the suspension arm with adequate bandwidth and stability [11].

The transfer functions of the flying height control stage, is approximated to be of second order and is of the form:

$$G(s) = \frac{\omega_n^{\ 2}}{s^2 + 2\rho\omega_n s + \omega_n^{\ 2}} \qquad (1)$$

Where ω_n is the natural frequency of the individual stage of motion of the suspension arm and ρ is the damping factor. Both these parameters are calculated from the values of the time constant (τ) and the resonant frequency (f_r) of each individual stage of the suspension arm.

The transfer function of the plant $G_{PFH}(s)$ for the flying height control motion stage includes the transfer function of the suspension arm (flying height motion) $G_{FH}(s)$ plus the gain parameter of the OBD sensor k_{FH}.

Hence the transfer function of the plant $G_{PFH}(s)$ is given as:

$$G_{PFH}(s) = G_{FH}(s) \cdot k_{FH} = \frac{0.774 \cdot 10^6 \cdot 0.4265}{s^2 + 1.7964 \cdot s + 0.774 \cdot 10^6} \qquad (2)$$

Where $\omega_n^{\ 2} = 0.774 \cdot 10^6$, $2 \cdot \rho \cdot \omega_n = 1.7964$ and $k_f = 0.4265$.

The PID compensator developed has a transfer function of the form:

$$G_c(s) = K_p + \frac{K_i}{s} + K_D \cdot s \qquad (3)$$

Where K_i is the integral gain, K_D is the derivative gain and K_P is the proportional gain term. All these three parameters of the controller must to be determined. The transfer function $G_{CFH}(s)$ of the PID controller developed for the flying height control stage is:

$$G_{CFH}(s) = \frac{299 \cdot 10^{-3}}{s} \cdot \left(s^2 + 754 \cdot s + 6.02 \cdot 10^5\right) \qquad (4)$$

The closed-loop transfer function $CLTF_{FH}(s)$ of the system for the flying height control motion, also showing the location of the poles and zeros, is calculated as:

$$CLTF_T = \frac{(s + 377 - 678j)(s + 377 + 678j)}{(s + 193 + 1081j)(s + 193 - 1081j)(s + 384)} \qquad (5)$$

The closed-loop system bandwidth of the flying height control motion stage is calculated from its Bode plot. The system bandwidth realised is about 4.8 kHz. The flying height control stage is closed with a gain crossover frequency of 1.34 kHz and phase and gain margins of 50° and infinity respectively. This implies that the control system is very stable.

Modified proportional integral and derivative (PID) controllers have been implemented to control and position the suspension arm with adequate bandwidth and stability. Bode plots show that the PID servo system's control loop for the tracking stage can be closed with a 25.6 kHz gain crossover frequency and phase and gain margins of 54° and infinity respectively. The flying height control stage is closed with a gain crossover frequency of 2.33 kHz and phase and gain margins of 51° and infinity respectively. Figure 5 shows the experimental open loop response and the theoretical closed loop response for flying height control respectively. This shows that a considerable improvement is possible with closed loop operation. The settling time is reduced from around 1.5 s to 10 ms. Control system refinement may yield improvements over this.

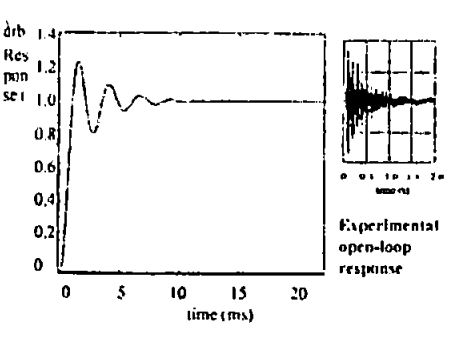

Fig. 5 Simulated closed response for flying height control, with inset showing the open loop response to a step input.

In an actual hard disk drive, position sensing would be achieved via the read/write head for flying height and from the tracking servo for track positioning. If data is read back from the disk, then according to the Wallace spacing loss equation [12], the amplitude of the read-back signal will be modulated by the spacing variations between the head and the disk due to the surface irregularities of the disk. The read-back signal from the magnetic head reflects the surface topography of the disk, and will ultimately provide a feedback signal for the control system.

CONCLUSIONS AND DISCUSSION

A test facility has been developed for the characterisation of hard disk drive performance under hostile operating conditions. The electrodynamic vibration system is enables failure mechanisms to be characterised in terms of vibration frequency and acceleration. Analysis of the data-transfer frequency response, and the CD-ROM optics and piezoelectric sensor systems, indicate that disk-flutter is a major factor in data-transfer error. Finite element analysis of a rotating drive, carried out in our laboratory, suggest that the use of a disk , laminated with a visco-elastic layer, will assist by passively damping the disk. However, this does not alleviate the requirement for active control of the suspension arm. The combined active-passive system should offer improved response times.

A novel suspension arm has been developed, with actuation enabled by the use of embedded multi-layer bulk PZT actuators. When this suspension arm is fully integrated into the HDD environment, it will enable real-time flying height adjustments to be made. This will improve data-transfer and also avoid, or reduce, head stiction and wear. Closed-loop positioning algorithms have been developed to enable the high-frequency positioning process of the arm to be achieved. After implementation of the control system in hardware the experimental closed loop performance will be confirmed. This work will be presented for future publication. Further work is also being undertaken to show that enough force is generated by the piezoelectric actuator to actively control the flying height of the head amidst the air bearing above the rotating magnetic disk.

REFERENCES

[1] N Dennis. *IEEE Oceans* 1997.

[2] IBM Storage press releases. IBM sets another disk drive world record, October 4, 1999

[3] P Gao and S M Swei. *Meas. Sci. Technol.*, Vol. 11, (2000), pp.89-94

[4] Q H Zeng and D B Bogy. *IEEE Transactions on Magnetics*, January 2000, Vol. 36, No. 1, pp.140-147

[5] B. Bhushan. "Tribology and mechanics of magnetic storage devices". Springer, IEEE Press, ISBN 0-7803-3406-X

[6] J. S. McAllister. *IEEE Transactions on Magnetics*, Vol. 33, No.1, January 1997.

[7] Miller Allen and D B. Bogy. *IEEE Transactions on Magnetics*, Vol. 32, No.5, September 1996.

[8] J R. Edwards. *IEEE Transactions on Magnetics*, Vol.35, No.2, March 1999.

[9] B J Nelson, Y Zhou and B Vikramaditya, *Proceedings of the SPIE* – The International Society for Optical Engineering, Vol. 3202, (1998), pp.30-41

[10] Tuli, A B Bhattacharyya, B C Forget and D Fournier. *Sensors and Actuators A [Physical]*, Vol. A64, Iss. 3, (1998), pp.203-7

[11] C. L. Phillips and R. D. Harbor, "Feedback control systems", Prentice Hall, ISBN 0-13-371691-0

[12] R. L. Wallace. The Bell Tech. J., 1951 pp.1145-1173.